This book is written for engineers involved in the operation, control, and planning of electric power systems. In addition, the book provides information and tools for researchers working in the fields of power system security and stability. It consists of two volumes. The first volume provides traditional techniques for the stability analysis of large scale power systems. In addition, an overview of the main drivers and requirements for modernization of the traditional methods for online applications are discussed. The second volume provides techniques for online security assessment and corrective action studies. In addition, the impact of variable generation on the security of power systems is considered in the second volume. The first volume may be considered as a background builder while the second volume is intended for the coverage of edge techniques and methods for online dynamic security studies.
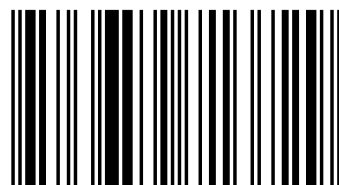
Power System Dynamic Security - Volume 1
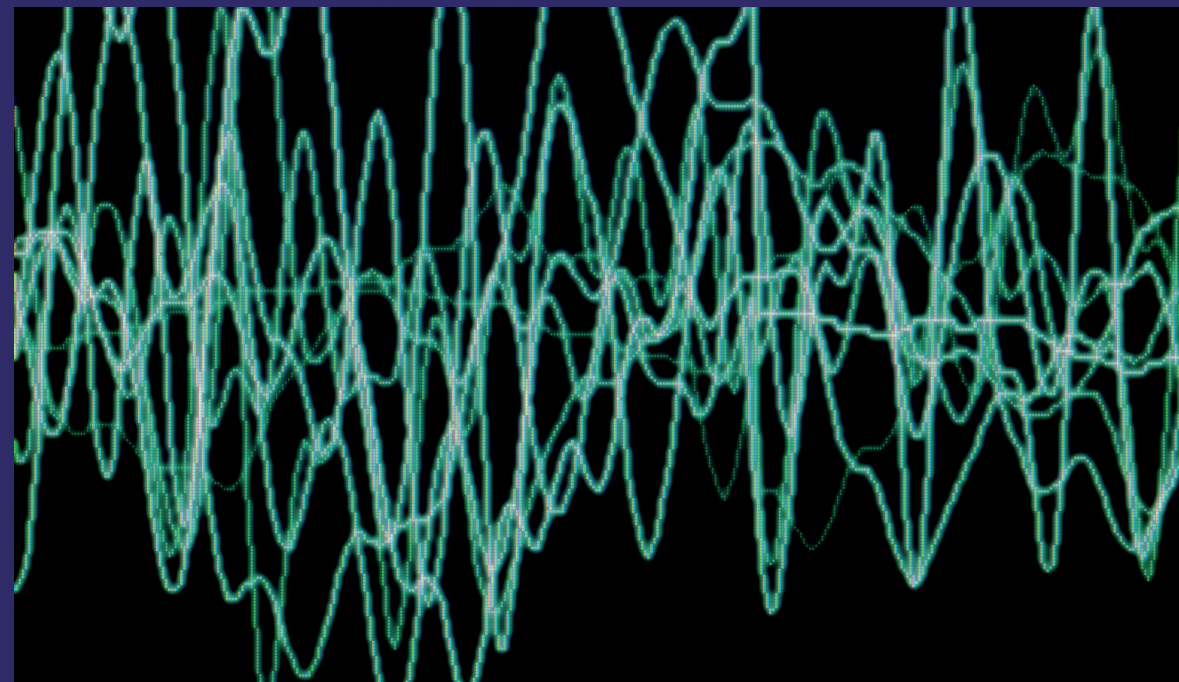
Mohamed EL-Shimy

Dr. M. EL-Shimy is currently an Assoc. Prof. in the department of Electrical Power and Machines – Ain Shams University. He is also an electromechanical specialist, and a freelance trainer. He is a technical reviewer for some major journals and conferences. He teaches several courses, published many researches, and supervised several dissertations.

Dynamic Security of Interconnected Electric Power Systems – Volume 1

EL-Shimy

Mohamed EL-Shimy

Dynamic Security of Interconnected Electric Power Systems – Volume 1

Mohamed EL-Shimy

Dynamic Security of Interconnected Electric Power Systems – Volume 1

LAP LAMBERT Academic Publishing

Mohamed EL-Shimy

Ain Shams University - Egypt

Dynamic Security of Interconnected Electric Power Systems – Volume 1/2

PREFACE

This book is written for engineers involved in the operation, control, and planning of electric power systems. In addition, the book provides information and tools for researchers working in the fields of power system security and stability. The book consists of two volumes. The first volume provides traditional techniques for the stability analysis of large scale power systems. In addition, an overview of the main drivers and requirements for modernization of the traditional methods for online applications are discussed. The second volume provides techniques for online security assessment and corrective action studies. In addition, the impact of variable generation on the security of power systems is considered in the second volume. The first volume may be considered as a background builder while the second volume is intended for the coverage of edge techniques and methods for online dynamic security studies.

The book covers some essential aspects related to the fast and online assessment of the dynamic security and stability of large-scale interconnected power systems. In addition, the impact of grid-connected variable renewable energy sources on the transient stability of power systems. Corrective actions for transient stability preservation and restoration are also presented with a focus on the load shedding for restoring and enforcement of power system stability. For these targets, the minimization of load shedding is considered as a techno-economical solution for solving stability problems associated with a sudden drop in the power generation. These sudden drops may be caused by several reasons such as forced outage of generating units, or the intense reductions in the renewable resources. The load shedding minimization for dynamic security preservation is also considered in this book.

One of the major problems associated with the fast and online studies of power system transient stability and dynamic security is the massive dynamic order of the models of large-scale interconnected systems. Therefore, dynamic model reduction is considered as a vital tool for facilitating a fast and efficient platform for power system studies especially for online applications. The most commonly used practical technique by power utilities to derive reduced electromechanical models of large interconnected power systems is based on the concept of coherency and dynamic aggregation. Therefore, this technique is adopted in this book. In addition, the concept of remote areas is introduced for the maximization of the model reduction considering the dissipation effect.

Two methods are presented for the construction of the coherency-based electromechanical equivalence. The first method is presented in the first volume and it uses the data sets of the system database for the construction of the electromechanical equivalents. The second method is presented in the second volume and it solely uses online measurement instead of the traditional data sets. The latter method can be

effectively executed online and this becomes possible due to the availability of WAMS and PMUs. The WAMS and PMUs are recently introduced in power systems for time-synchronized measurements, telemetry, and recording of critical quantities (such as state variables, and status of components). Consequently, accurate online analysis and management of large-scale power systems becomes possible. An overview of the functionality and characteristics of these systems are summarized in the first volume of the book.

The first volume consists of three chapters and starts with a detailed overview of the operational requirement of recent and future power systems considering the integration of variable generation resources into the electricity grid (chapter 1). The fundamentals and advances of power system security requirements are also presented in chapter 1. An overview of the electromechanical equivalence techniques is presented in chapter 2. An improved coherency-based equivalence technique is presented in this volume (chapter 3). The presented technique uses the traditional data sets for the construction of the equivalence. In addition, the concept of remote areas is introduced for the maximization of the dynamic model reduction of very large-scale systems. Several case studies are presented for the evaluation, validation, and analysis of the presented theories and models.

M. EL-Shimy, May, 2015

CONTENTS

CHAPTER 1
INTRODUCTION

1.1 ELECTRICAL ENERGY SOURCES AND THEIR OPERATIONAL CHARACTERISTICS

Generally, electrical energy is produced through energy conversion processes. In these processes, the naturally available energy resources such as fossil fuels or wind resources are converted into electrical energy. The conversion processes are handled by man-made energy production technologies such as steam-turbine generators (STGs) or wind turbine generators (WTGs). The main functions of an energy production technology are to capture the primary energy resource, converting it to electrical energy, and controlling the produced energy to fulfil the load or grid-interconnection requirements. An electrical grid also contains technologies for other functions such as protection, control, energy transport to load, monitoring, communication, and energy storage devices. Although each energy resource is of a unique type, there are many energy production technologies that convert that energy resource to a useful energy (such as electricity or heat). Fig. 1.1 illustrates some example of the primary energy resources and their methods of conversion to electricity.
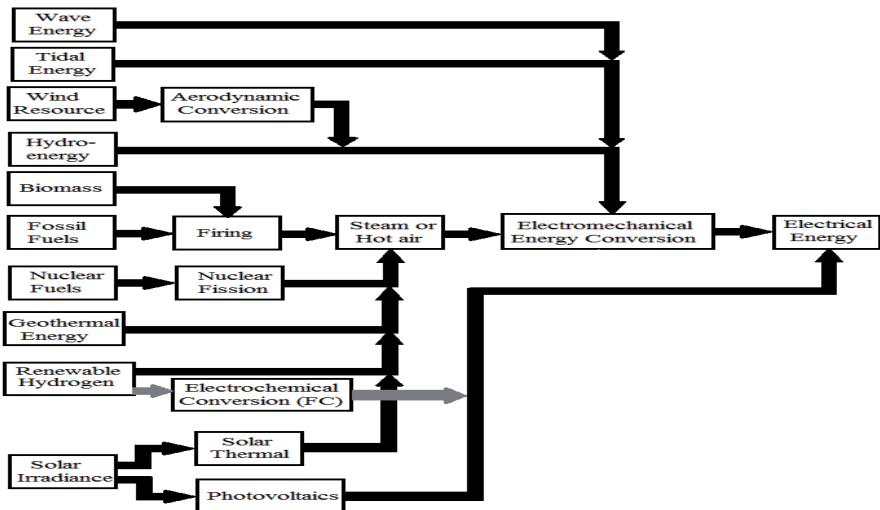
Fig. 1.1: Conversion of primary energy resources to electrical energy

From operational points of view, energy sources can be characterized by several indices [1]. These indices include the intermittency, variability, dispatchability (or manoeuvrability), resource predictability, controllability, and capacity factors. The intermittency describes the extent to which an energy source unintentionally unavailable. The variability describes the extent to which the output of an energy source is changed in an uncontrollable and undesired way. The predictability describes the extent to which a correct prediction or forecast of an energy resource is possible. The dispatchability describes the capability of an energy source to change its output on demand. The dispatchability level of an energy source is highly dependent on the nature of the primary energy resource and the energy storage possibility. Resources of low intermittency and low variability and high predictability results in high dispatchability of the energy source. Generally, the dispatchability of storable energy resources such as fossil fuels is very high in comparison with non-storable energy resources such as wind and solar. The quickens of on-demand output changes of a dispatchable energy source is highly dependent on the adopted energy conversion processes, the controllability, and the capacity of the energy source. For example, large nuclear power plants do not provide fast manoeuvrability in comparison with small STGs; the MW/s rate limit of small STGs is very high in comparison with nuclear power plants. Therefore, the appropriate energy mix should be managed for supplying the power system demand.

Fig. 1.2 illustrates a generic load curve and a suggested energy mix [2]. The figure shows three distinct zones of the load curve. These zones are the base load, the mid-range load, and the load peaking. The main difference between these zones is the rate of change of the load. The base load is characterized by an almost constant load while moderate rate of change of the load is available in the mid-range zone. Highest rate of change of the load and smallest duration characterize the load peaking zone. According to the characteristics of various loading zones, appropriate energy sources are selected to supply each zone. The selection is mainly based on the MW/s rate limit capability of the generating units.

The primary energy resources can be classified according their capability of replenishment into two broad categories; non-renewable (or conventional) and renewable energy resources [3, 4]. The renewable energy resources can be classified according to their variability; resources such as wind, solar, and tidal energies are highly variable while resources such as biomass, and hydro energies are of low variability. The differences in the variability level of various energy resources significantly affect the dispatchability of the energy sources. In addition, variations of

the output power of a given energy source decreases with the decrease in the energy resource variability, and intermittency. The unexpected chances of significant changes in the power output of a given resource are reduced with the improvement in the resource predictability.
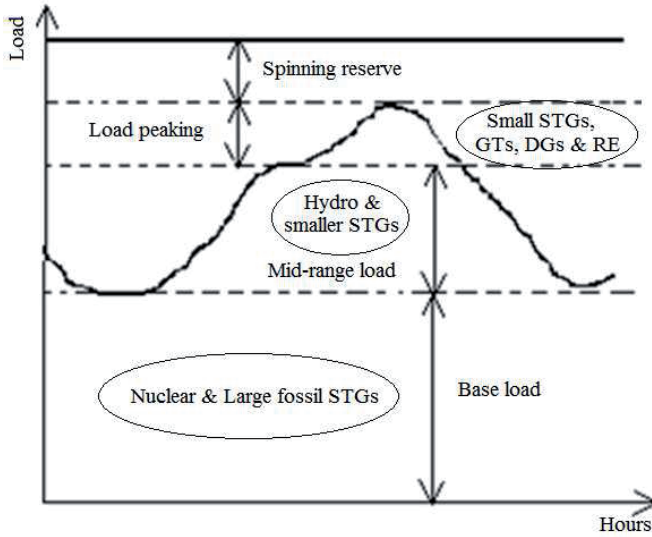
Fig. 1.2: Daily load fluctuations and energy mix

Sudden or large reductions in the energy production in power systems can be attributed to three main causes. These causes are shortage or sudden reduction of the primary energy resources, and forced outage of generating units. These issues are not only highly possible in variable renewable energy sources, but also possible in conventional energy sources, especially when the primary energy source is limited and not continuously available. Large changes or swings in the power production affects the security, reliability, power quality, and stability of power systems. Therefore, contingency analysis as well as corrective actions should be made for keeping the system operationally intact [5].

Although conventional energy sources provide better operational characteristics in comparison with renewable energy sources, their use causes drain of the international fossil resources as well as severe ecological impacts. Conventional energy resources are distributed in an uneven way throughout the world. In addition, their global reserve is continuously reduced. This causes a major worldwide energy

security threats. In addition, the excessive use of fossil fuels significantly contributes in many critical international problems such as global warming, acid rains, and health degradation of living creatures. Therefore, there is a global trend using renewable resources as power sources instead of fossil fuels; however, integration of large amounts variable renewable sources into power systems is expected to cause some critical problems due to their inherent variability as described earlier. Recent and current researches are struggling in finding ways for reducing the variability of renewable energy sources [1]. Suggested ways include geographical diversity, storage, renewable hydrogen-based systems, and interconnections. In addition, energy use reduction and energy efficiency enhancement are among the salient approaches for energy consumption minimization [6 - 9].

From a technological point of view, renewable energy sources should provide specific minimum requirements to be integrated with power grids [10 - 17]. These requirements are usually called grid-codes. A grid code is "a technical and operational specification which defines the parameters a facility connected to a public electric network has to meet to ensure safe, secure, and economic operation as well as proper functioning of the power grid". Generally, a facility is any component connected to the grid. This includes generating plants, load equipment, transmission and distribution (T&D) facilities, and other networks. There are several grid codes that should be considered when integrating facilities to power grids. These codes include planning codes, operation codes, connection codes, data communication codes, and balancing codes [11]. Regardless the natural variability of most renewable energy resources, technological advances in renewable energy approaches a level at which new wind energy and solar energy technologies fulfil most of the grid codes. In addition, the recent technologies provide operational capabilities close to the conventional generators. From economical point of view, renewable energy sources specially wind and solar energy systems are currently with competitive lifetime costs in comparison with conventional energy costs [18 - 25].

The placement criteria of energy sources in a power grid is dependent on the energy source type. Conventional energy sources are usually placed as close as possible to the load centers. On the other side, the placement of renewable sources is mainly dependent on the availability of the renewable resource. On many occasions, locations with rich renewable resources are remotely located with respect to load centers. In these cases, renewable sources are usually connected to the grid via long transmission systems that presents weak links [14, 26, 27]. Generally, a transmission

link interconnecting two areas (or systems) is said to be weak if its capacity less than the capacity of the smaller area (or system) by about 15 – 20% [28].

1.2 POWER SYSTEM SECURITY: CONTINGENCY ANALYSIS AND CORRECTIVE ACTIONS

Power system security [5, 29 - 34] may be defined as the continuous ability of the power system to keep all the system limits not violated with minimum interruption to the supplied loads. The main target of the power system security is to keep the system intact under normal and disturbed conditions. Therefore, the successful security system should minimize the impact of disturbances on the operation, economics, and power quality of power systems. In addition, an acceptable system security level guarantees the immunity of power system to disturbances and makes the system defensive. Therefore, secure operation of power systems requires the integration of all practices designed for keeping acceptable system operation when components fail.

Power system security covers both static and dynamic phenomena. Therefore, the security analysis is usually categorized to static (or adequacy) and dynamic security [5, 31]. The static security considers the impact of static or slow changes in the system limits while the dynamic security considers the impact of disturbances (or contingencies) on the system. The core definition of the dynamic security and stability is the same, but the security is a wider term than stability [29]. The stability is defined as [36] "the ability of an electric power system, for a given initial operating condition, to regain a state of operating equilibrium after being subjected to a physical disturbance, with most system variables bounded so that practically the entire system remains intact"; however, "Security not only includes stability, but also encompasses the integrity of a power system and assessment of the equilibrium state from the point of view of overloads, under- or overvoltages and underfrequency" [29].

The system limits define the normal operation of power systems. These limits or constraints can be classified into two categories; the equality and inequality constraints. In addition, the system limits may be classified according to their origin into intrinsic and operating range limits. The equality constraints basically represent the load flow equations while the inequality constraints represent the allowable range of acceptable operation of various components in the system. In fact, the intrinsic and operating range limits elaborates the inequality constraints associated with a specific component. The intrinsic limits of an equipment are determined basically from the

design and characteristics of the equipment. The operating range limits are generally less than the intrinsic limits and they are limited by the fulfilment of the overall operational requirements of the system. For example, consider a simple hypothetical system where an off-grid generating plant supplies a load center via a short transmission line with negligible impedance.The generator is capable of producing a voltage magnitude at its terminal in the range 85% - 115% while the load requires a voltage magnitude in the range 95% - 105%. In this case, the generator voltage limits present the intrinsic limits of the generator and they are mostly related to its design. Successful operation requires that the voltage magnitude at the load bus should not be violated. Therefore, the operating range limits of the generator bus-voltage magnitude becomes equal to the load requirements (i.e. 95% - 105%). It is worthy to be mentioned that the 95% - 105% voltage limits present an intrinsic limit as viewed from the load perspective. It is also important to know that the operating range limits should not violate the intrinsic limits of any component within a system. Otherwise, the system will be incapable of fulfilling the operational requirements. Both intrinsic and operating range limits are not absolute constants. The intrinsic capability limits usually decline with time due to degradation of the equipment. For example, the annual output degradation rate of PV systems is about 0.7% [35]. The degradation may be attributed to the aging, operational stresses, and maintenance quality. The operating range limits are also variable. For example, the ampacity (or ampere capacity or current limits) of a cable are highly dependent on the temperature of its surroundings. The ampacity limits are usually increased during the winter and decreased during the summer. This is for avoiding over-temperature of the cable insulation.

Recalling that in the normal operation of a power system, all the inequality and equality constraints of the system are satisfied. In addition, the system security requires a minimum available, reserve margin [5] (see Fig. 1.2). Power system security may also be defined as the ability of the system to withstand credible contingencies without violating the normal operation limits. A system operating under normal conditions is also said to operate in the *normal state*. The security strength of the system is usually defined by the maximum number of time-independent, and simultaneous disconnection of major system components (such as generators, transformers, and line) without affecting the normal operation of the system. Defining N as the minimum number of components required to supply the system peak load (see Fig. 1.2). A system with an N-k security criterion is a system in which k components may be simultaneously disconnected and the system will be able to fulfil the normal state requirements in the post-contingencies time. Due to investment

constraints, power systems are usually designed according to the N-1 security criterion [32]. The normal state is a secure state and a system operating in the normal state is said to be intact.

Deviations from the normal state requirements cause the system operation to move to insecure operating states. These deviations are mainly caused by contingencies which are stochastic and unexpected events; however, the rate of contingencies may be reduced for example by proper maintenance of components. Four insecure operating states can be realized [29 – 35, 37]. These states are the alert, emergency, extreme (or collapse), and restoration states. Fig. 1.3 illustrates the main operational characteristics of these states, and the interrelations between them. This figure is usually called the state transition diagram. Table 1.1 summarizes the characteristics of various states, some causes of state transitions, and examples of the corrective actions for each state. The nomenclature used in the table is illustrated in Fig. 1.3.
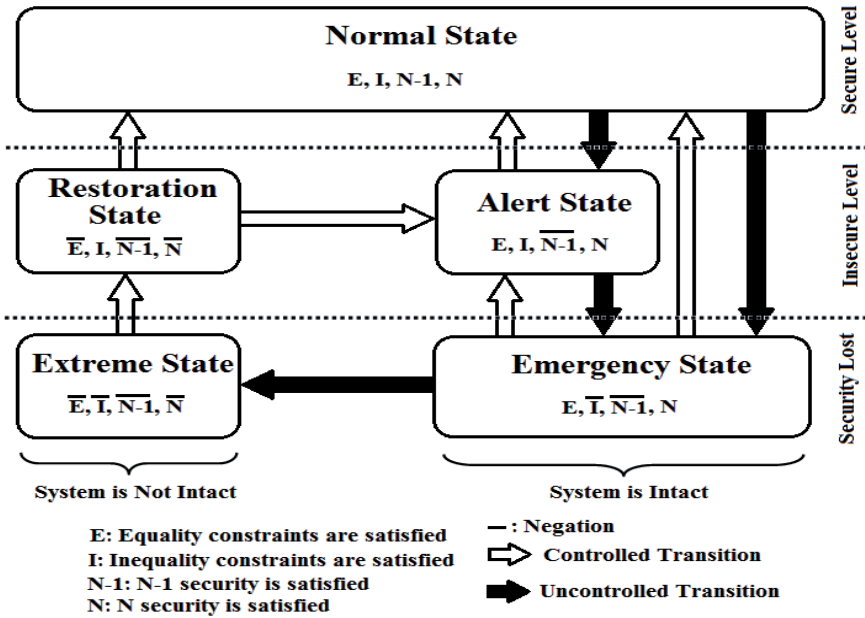
Fig. 1.3: State transition diagram

Details about various states are available at [29 – 35, 37]; however, it is worthy to be mentioned here that an intact system is capable of providing power balance. If the

power balance could not be achieved, then the system becomes not intact. Consequently, the synchronization of generators upsets. Therefore, the system frequency protection devices will split the system into parts or islands; the situation is called islanding and it is within the extreme state. The frequency and power balance conditions in each island are different and abnormal. Therefore, system blackout or unintentional brownout is usually detected. Delay is activating the possible corrective actions while the system is in the emergency state may be the main cause of the transition to the extreme state.

Table 1.1: Summary of operating states and state transitions

State	E	I	N-1	N	Intact system	Causes of transition from normal state	Corrective actions
Normal	√	√	√	√	Yes	-	-
Alert	√	√	x	√	Yes	Constraints are near their limits. Examples, reduction in the reserve margin or bus voltage close to the limits.	Preventive control. Examples, startup of non-spinning reserve or switching on compensators respectively.
Emergency	√	x	x	x	Yes	Severe disturbances. Example, short-circuit faults or cascaded ouages.	Emergency control actions (heroic measures). Example: fast fault isolation or operation of reclosers.
Extreme	x	x	x	x	No	Delayed or unsuccessful emergency control actions. Severe power imbalance.	Heroic and remedial actions such as load shedding, generator trip, or intentional islanding for keeping power balance.
Restoration	x	√	x	x	No	Attempt of restoring the system to the normal state or at least to the alert state.	Manual or automated reinsersion of generators and loads. The inequality constraints should be kept satisified during the entire restoration process.

Generally, delayed or unsuccessful corrective actions during the operation in any state may lead to severe consequences. Therefore, any security programme includes a contingency analysis block. The contingency analysis is an investigative simulation of hypothesized contingency for evaluating their impact on the system security. On the other hand, the corrective action analysis is the process of figuring the possible actions that may be taken for overcoming the consequences of security upsetting contingencies. The corrective action analysis works in two distinct modes. The first mode operates for solving the problems found by the contingency analysis. Therefore, this mode is offline while the second mode operates in real time operation for securing the system during its real-time operation. The contingency analysis and the corrective action analysis require the simulation of the system. Therefore, an accurate system model should be available. In addition, the results obtained from these analyses are highly dependent on the accuracy of the system model. Real-time models of a power system require centralized real-time data collection available from local measuring and monitoring devices at each system component. Therefore, telemetry is required for communication within the system and for estimating its state. The next section discussions about local and centralized measurements and telemetry will be given. Modelling levels and simulation for contingency analysis and simple numerical examples, including corrective actions are available at [5].

1.3 SYSTEM MONITORING

The main challenge in performing a meaningful real-time analysis of power system is to have a real-time model. System monitoring may be considered as the backbone of system security [10, 31, 38, 39]. In addition, real-time modelling of power system is essentially dependent on the system monitoring. This is because the monitoring provides up-to-date real time information about the operating conditions of power systems [5]. The term real-time model may be defined as a snapshot of the system. This snapshot includes the redundant measurements of critical quantities, estimated system topology, and estimated variables and parameters. The quality of a model is determined by its accuracy of simulating the physical system. In addition, the value of the studies and the conclusions derived from a model is essentially dependent on the quality of the model.

Generally, the term *electrical power system* describes a collection of devices that integrated together for providing a system that generate, transmit, distribute, and utilize electrical power. The term *instrumentation and control (I&C)* refers to a collection of devices for monitoring, control, and protection of power systems [38,

39]. *Innovative Electronic Devices* (IEDs) perform I&C functions, monitoring, data storage, and data analysis for a specific equipment, These IEDs are usually integrated with *Human Machine Interfaces* (HMIs) that provide PC-based software tools that communicate with the IEDs. The HMIs also provide additional data analysis and storage as well as facilitate the data to the operators. The monitoring and analysis of an integrated IED system comprise six data types [38]. These data types are illustrated in Fig. 1.4.

Instrumented Data
- They are periodically collected parameters and status from physically monitoring instruments such as potential and current transformers.

Settings Data
- These data include IED operational settings, thresholds of events, SER report trigger conditions, data interpretation settings, and archiving parameters.
- These data are created separately by expert engineers and expert analysis tools then they are transmitted to the IEDs.

Change-of-State (COS) Data
- These are the data describing what, when, and in what sequence changes happened. It is also called sequential events recorder (SER) or sequence-of-events (SOE).

Data Types in IED Systems

Derived Data
- IEDs calculate these data for providing a snapshot of the instantaneous state of the power system. These data may include power, energy, and peak load.

Historical Data
- These data provides a time series of events and system reactions.

Diagnostic Data
- These data includes the quality of the power system and the I&C system. IEDs provide immediate indication or alert of the failure or operation degradation of various components and the system.
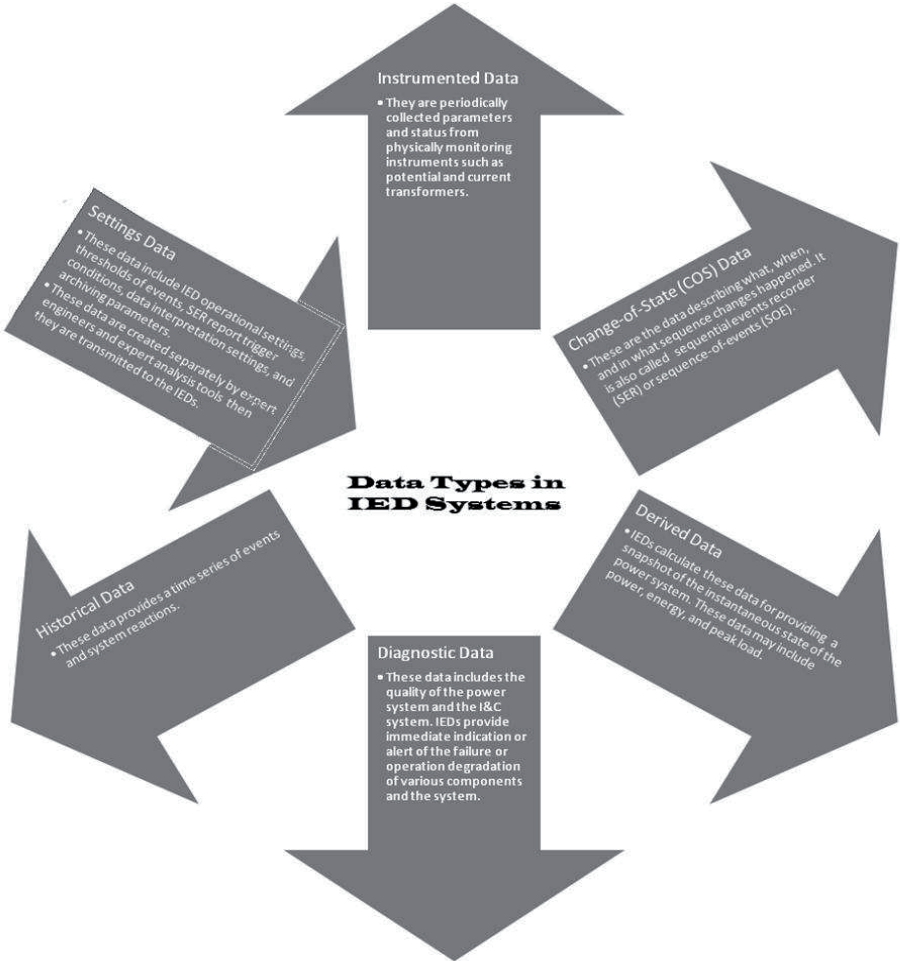
Fig. 1.4: Data types of IED systems

Regardless of its size and geographical extent, power systems must contain *telemetry systems*. These systems comprise a collection of devices for monitoring critical quantities and simultaneously transmitting these quantities to a central location. These quantities may include voltages, currents, power flows, status of circuit breakers, frequency, generator unit output, and tap positions of transformers. Old substations are usually equipped with *Remote Terminal Units* (RTUs). These units perform two functions; collecting the infield measured data and transmitting them to the control centers. Due to their relative capabilities and costs, the IEDs has recently replaced the RTUs. It is possible to find in the same substation RTUs and IEDs mixture connected to a Local Area Network (LAN) and a SCADA system for performing the data communication with the control center's SCADA computer(s) [40]. The communication links may be achieved by fibre optic cables, satellites, and microwave channels.

Integrating IEDs provide a powerful I&C system for the power system. These integrated IED systems are capable of performing and supporting many functions such as power system protection, automation, control, monitoring, analysis, and security. A *time synchronization command* from a centralized source allows all IED devices in the system to use the same clock value for timestamp purposes. Some system values are captured and archived periodically to enable trending analysis. Operation control centers usually include computers for gathering the collected telemetry data, processing them, checking them against restored operational and intrinsic limits. These computers also facilitate these data to the operators and notify them in the event of violation of any limits or events such as overloads, over voltage, and outage of lines. The central computers also use the collected data in conjunction with *a state estimation process* for building a system model that nearly represents the real-time physical power system. These models are available for system analysis studies such as contingency analysis, and stability analysis as well as system operation and control enhancement and system planning.

The state estimation is a process by which a value is assigned to an unknown quantity. The state estimation is based on the available system measurements. These measurements may be limited and suffers from errors. Therefore, the main objectives of a state estimator are to filter measurement noise, detect gross errors, estimate unknown quantities, and provide the best estimate of the system state variables. Building a power system model requires at least the availability of all system state variables which are the bus voltage magnitudes and relative bus voltage phase angles with respect to the reference bus. Economical constraints limit the installation of

monitoring devices at all buses. In addition, measured quantities are imperfect and suffers from measuring errors. Therefore, the state estimation provides a mathematical tool for estimating the best estimate of system state variables. The best estimate is usually determined based on optimized statistical criteria such as minimization of the sum of the squares of the differences between the estimated and measured values of a function [5, 40].

The direct measueremt of bus voltage magnitudes is considered as a traditional task while measuring relative phase angles required some challenges. The main challenge is the accurate synchronization between phase measuring devices for providing a real-time valid relative phase angles. This synchronizations are recently achieved through the use of *Phase Measurement Units* (PMUs) (also called *synchrophasor devices*) which are devices that distinguished for providing synchnoized measurement of relative phase angles of bus voltages [41]. A Phasor Measurement Unit (PMU) has been defined by the IEEE as "a device that produces synchronized phasor, frequency, and rate of change of frequency estimates from voltage and/or current signals and a time synchronizing signal". As shown in Fig. 1.5, the needed high speed synchronization sampling is achieved by a phase-lock oscillator along with a Global Positioning System (GPS) reference source. This provides a synchronization accuracy of at least one microsecond. PMUs can measure the AC power frequency (i.e. 50 Hz or 60 Hz) voltage and current waveforms at typical rate of 48 samples per cycle i.e. 2400 samples per second for 50 Hz systems and 2880 samples per second for 60Hz systems. To do so, the analogue waveforms are digitized by analogue to digital (A/D) converters for each phase. The resultant time tagged phasors can be transmitted to a local or remote receiver at rates up to 60 samples per second. Fig. 1.5 illustrates the PMU operating concept and functional block diagram of PMUs. By the time synchronized phasor measurements, synchronized *Wide Area Measurement* (WAM) is now possible. It is important to be mentioned here that the quality of the synchrophasor data are highly dependent on the accuracy of the input and output power, timing, and communication signals of PMUs. Therefore the IEEE Std. 1344-1995 [42] is prepared in the early stages of the use of PMUs. The objectives of this standard include settings the requirements that ensure consistent phasor measurements and communications.

The Wide Area Measurement System (WAMS) technologies use the PMUs to record and export dynamic power system synchronized high-sampling data. Although the realization of PMU technology is relatively recent (in 1988 by Dr. Arun G. Phadke and Dr. James S. Thorp at Virginia Tech), these technologies fill a large gap in

improving the accuracy of real-time monitoring and analysis of power systems. The applications of PMUs in power systems are extensive [43]. In addition, the United States–Canada Task Force on the 14 August 2003 blackout [44] recommends the use of time-synchronized data recorders to all utilities for enhancing the security of power systems. There are many fields of applications of PMUs in power systems [46 – 76].

(a)

(b)
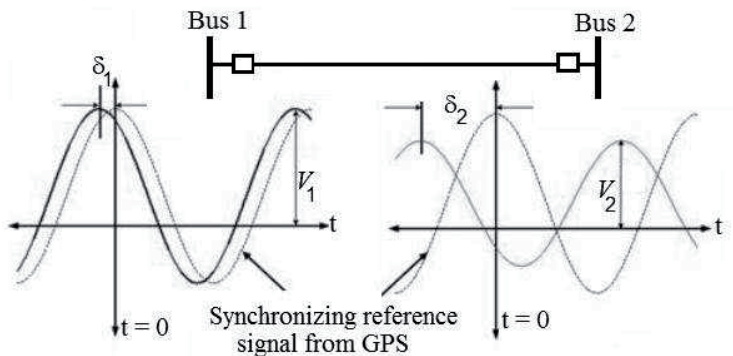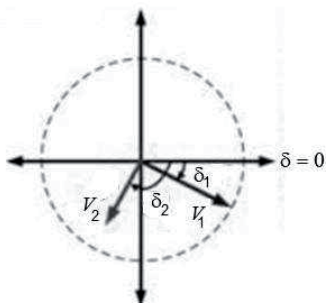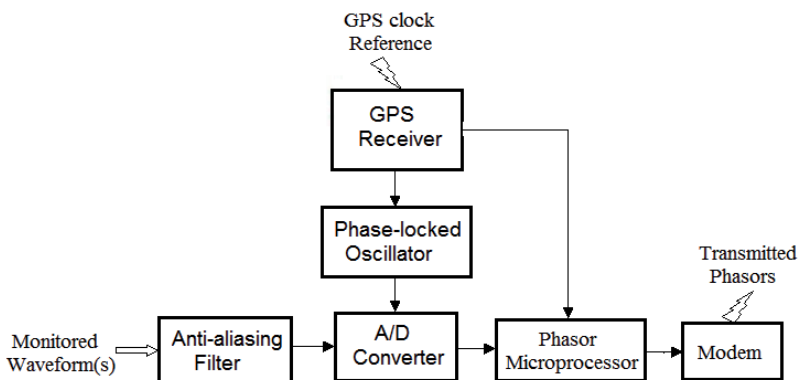
Fig. 1.5: PMUs; (a) Phasor measurement concept; (b) Phasor representation; (c) PMU functional block diagram

The key feature of the use of PMUs in these applications is the online execution in high accuracy as well as high speed. References [43, 75, 76] provide extensive details about these applications. The applications of PMUs include, but not limited to:

1. System monitoring [45, 46],
2. Observability, state estimation, and model validation [47 - 51],
3. Security assessment [52 -54, 76],
4. Real-time stability monitoring and analysis [55 – 60, 74 -76],
5. Protection and adaptive protection [61 - 65],
6. Fault location [66],
7. Islandind detection [67],
8. Online control [68 – 73 - 76],
9. Real-time dynamic equivalence [60, 74],
10. Real-time load shedding minimization [60],
11. Restoration [75, 76],
12. Postdistrubance analysis [60, 74 - 76].

1.4 REQUIREMENTS AND CONCEPTS FOR REAL-TIME STABILITY ANALYSIS

The classical dynamic security analysis involves off-line simulation of the stability of power systems as subjected to hypothetical set of contingencies. This kind of analysis is repeated for various possible topologies and operating conditions of the power system. Topologies can be changed, for example, when some components are taken out of service for performing maintenance (i.e. scheduled outages) or outage of some components due to faults (i.e. forced outages).The operating conditions changed, for example, due to changes in the systems loading or transactions between interconnected systems. For this scope and purpose, time-domain simulation of power systems using most of the available soft-tools such provide an efficient tool for performing the dynamic security analysis regardless of the relatively long time needed for the simulation and analysis of the results.

In real-time applications, dynamic security analysis becomes a complex task due to several reasons. These reasons include the time-domain based simulation time, which may be longer than the real-time dynamic changes and their real-time consequences especially in large-scale interconnected power systems. The extraction of the useful results from time-domain simulations and their interpretation as well as the follow up by the system operators adds also to the complications of the real-time dynamic security assessment. Another big challenge is the accuracy of the dynamic models used in the simulation as well as the inherent uncertainty of these models even if excellent state estimators are adopted. Construction of extensive dynamic models containing significant uncertainty makes the outcomes of the time-domain simulation with doubtful reliability.

Another critical point to be considered is the corrective and preventive actions that should be taken in real-time operation for keeping the system in a secure state; for example the normal or alert states shown in Fig. 1.3. The time here is very precious as cascaded outages or even blackouts are probable if the system operating conditions are vulnerable to instability conditions. Therefore, consuming much time in the assessment of the dynamic security makes the entire assessment process valueless; the assessment of a potential even may develop system instability before taking feasible corrective actions of even completing the security assessment. Therefore, the security assessment and consequently the risk of instabilities must be predicted fast enough for providing and implementing feasible corrective actions for preventing instabilities. In comparison with the time-domain based dynamic security assessment methods, faster methods for *prediction* and *prevention* of instability of power systems are urgently needed for preventing blackouts. A good approach for handling the security assessment task is the use of dynamic equivalence of power systems. The equivalence provides significantly reduced order models for the power systems in comparison with its detailed representation. Therefore, the equivalency can contribute in reducing the time needed for the time-domain simulation of power systems. If an SMDE of an interconnected power can be constructed such that its accuracy is high and its construction time is very low in comparison with the timeframe of the transient stability of power systems (less than several seconds), then the energy function based methods such as the EAC can be used. The use of the EAC in the dynamic security assessment and in prediction of instability risks is expected to significantly reduce the security assessment duration and enhance the overall security of the systems. In this book, two methods for dynamic equivalency for fast stability assessment of power system are presented. The first method is the traditional coherency-based dynamic

21

equivalence while the second method is the measurement-based dynamic equivalence method. The second method is also based on the coherency of generators; however, unlike the traditional method, the coherency is solely determined from measurements instead of data sets and simulations in the traditional methods. The latter method depends on the availability of WAMs and PMUs at selected locations in an interconnected power system. The SMDE model will also be extracted from an interconnected power system.

CHAPTER 2
ELECTROMECHANICAL EQUIVALENCE FOR FAST AND REAL-TIME TRANSIENT STABILITY ASSESSMENT – OVERVIEW

2.1 OBJECTIVES AND SCOPE

Although the power system security has two categories; static and dynamic. The survival of the system requires simultaneous secure operation from the static and dynamic aspects. Usually the time needed for the static contingency analysis is small enough for considering it as a real-time function; however, the dynamic security (or stability) analysis requires multiple order of the time needed for the static security assessment [76]. This longer time is mainly due to excessive computation time, especially in large-interconnected power systems even if supercomputers are used. There are complications associated with the dynamic modelling of power systems for real-time stability assessment. This is because time-domain simulation of detailed power systems requires extensive models that are mostly non-linear and differential equations. The solution of such models results also in a huge amount of data that adds to the complication of real-time stability assessment from the point of view of points of interpretation of the results. Energy based function models such as the Equal Area Criterion (EAC) [28, 81] provide a fast and accurate method for assessing the transient stability of power systems; however, these methods are useful for the analysis of a system with one or two machines. Therefore, their use in real systems is restricted.

This book presents some methods for significantly reducing the time of the dynamic security assessment process. Dynamic equivalency of power systems is considered as the main method for reducing the time needed for the stability assessment of power systems [74, 76 - 80]. In chapter 3, modelling and application examples are presented for performing the traditional coherency-based equivalence of power systems. In addition, an improved dynamic equivalency method is presented in the second volume of the book. In this method the coherency identification and the equivalency are mainly based on WAMs measurements that are available in most modern utility power systems. Recent technologies for power generation, such as wind and solar based power generators makes the standard equivalency methods face a challenge due to several reasons. These reasons include the estimation of the inertia of

these technologies and their impact of the overall equivalent inertia. The proposed method [60] overcomes the challenges of the equivalency of power systems that include any mix of generating technologies. This is achieved by estimating the equivalent inertia based only on measurements. At a selected bus, the methods are capable of determining the equivalent dynamic model provided that the generators within that part are suffienlty coherent. The coherency constraint is required for ensuring the accuracy of the determined dynamic equivalent models. In the second volume of this book, a fast method for the transient stability assessment of power systems is presented. The method is based on the EAC which provide very fast assessment of the transient stability of power systems; however, this method is applicable to the Single-Machine Infinite-Bus (SMIB) system model. This simple and accurate method is extended to cover large interconnected power system by the use of the proposed equivalency method. Therefore, the proposed method avoids the problems associated with the time-domain based methods and bypasses the restrictions placed on the EEA method. It will be also clarified that the presented method surpasses and overcomes the drawbacks associated with the Extended Equal Area Criterion (EEAC) method [82 - 87]. In addition, the proposed equivalency method will be presented in the second volume of the book to provide an accurate Single Machine Dynamic Equivalent (SMDE) of a power system for use in real-time transient stability assessment of power systems.

2.2 THE NEED OF AND METHODS FOR EQUIVALENCY

The modelling of large interconnected power systems for realtime or even faster transient stability simulation and dynamic security assessment arises for a number of reasons including:

(i)   Limitations on the size of computer memory,

(ii)   The excessive required computation time required,

(iii) Parts of the system that are far away from the disturbance have a little effect on the system dynamics and it is therefore unnecessary to model them with great accuracy,

(iv)   Often parts of large interconnected systems belong to different utilities, each having their control centers, which treat the other parts of the system as external subsystems,

(v)   Even assuming that the full system data is available, maintaining the relevant databases of the data sets would be very difficult and expensive. In addition,

the topology of power systems is not fixed; however, the topology changes with time. These changes may be due scheduled outage of components for repair and maintenance or due to forced outages due to failures. Therefore, tracking the topology changes is a very complicated matter, especially for online simulation.

These problems can be signficently reduced by considering a part of the system, called the internal subsystem. This part is modelled in details. Simple models referred to as the equivalent system or simply the equivalent present the remainder part of the interconnected system; called external subsystem. The equivalent model must represent the linear network components (e.g. transmission lines and transformers) as well as nonlinear components (such as synchronous generators and loads) in the original external subsystem. Model reduction methods can be divided into three groups [29, 30]:

(i) *Physical reduction*: which consists of choosing the simplest appropriate models for the system components. The selection of the models depends on the level of influence an individual element contributes in determining the system response to a particular disturbance or a set of disturbances. Generally, components that are electrically close to the disturbance are modelled more accurately in comparison with electrically far components. The justification of this method is based on the dissipation effect which defines the extent or spreading of a distustance in power systems. The dissipation level depends on the topology of power system, parameters of its components, the geographical distance between components, the operating conditions, and the strength of the disturbance.

(ii) *Topological reduction*: which consists of either eliminating or aggregating selected nodes in order to reduce the size of the equivalent network and the number of generating units to be modelled.

(iii) *Modal reduction*: which use linearized or highly simplified models of the external subsystem. This is usually based on eliminating or neglecting the unexcited modes of oscillations for a given disturbance.

Based on the type of considered study, power system equivalence can be divided into the three main categories [33, 88, 89]. These categories are described in the following.

(i) *Equivalence for Short-Circuit Studies*. Most actual short-circuit studies consists of determining the initial symmetrical values of short-circuit currents, then employing approximate methods to interrupt the results for different purposes such as determining relay setting or circuit breaker duties. Hence, for short circuit studies, the transient performance of synchronous generators is usually neglected. Therefore, the resulted equivalence is completely linear and the development of equivalents concentrates on the passive elements.

(ii) *Equivalent for Power-Flow Studies or static equivalence*. The principal information obtained from power-flow studies are the steady-state power flow and voltage conditions. These are vital information for operation, static security assessment, and planning of power networks. A typical situation in which power-flow equivalent may be desired where a detailed study of different operating conditions and of proposed system changes is to be made in one section of a large power network while an adjoining section is to remain essentially fixed. As power system networks does not conform with the characteristics of idealized linear networks, a true equivalent that would work for different operating conditions does not exist. However, for a given operating condition (base-case) a linearized equivalent can be found around this operating point. Currently, the power flow analysis, even for very large interconnected systems can be performed at a time that is sufficient for realtime applications. Therefore, the power flow equivalents are not currently adopted as a method of analysis of power systems.

(iii) *Equivalent for Transient Stability Studies or electromechanical equivalence*. In transient stability studies, the introduction of the electromechanical transient characteristics of the machines complicates the problem of simplifying the system. Nonlinear models of machines are considered in the dynamic equivalent of the power system. This kind of equivalence is essential for online analysis of power systems. Therefore, the main focus of this chapter is on this type of equivalence. Many methods are available for developing dynamic equivalent for transient stability studies, a brief description of most of these methods with their limitations of application will be listed in the following.

Historically, Ward-type equivalent [90] based on distribution factors that was commonly used in building power flow equivalents of the power systems on DC

calculating boards. Later, this method was extended for dynamic studies. In this type of equivalent there is only one possible external area and the system within this area was aggregated at interface bus by direct application of Ward type equivalent. The method is very simple to be applied, but due to representing a wide range of different dynamic characteristics, the response of the equivalent is greatly disagreeing with the actual system response. Improvements of Lyapunov-type energy-function stability method [91] was used to construct a single-machine infinite-bus equivalents of power systems and the power system transient stability was measured by calculating stability indices. The method proves its capability to predict the transient stability of small-scale power systems, but due to the used high approximating assumptions, the method appears to be limited.

Modal-based dynamic equivalent techniques [92 - 95], involves a three stage procedure:

1) *Constructing linearized-state-space model representing the external systems*,
2) *Separation of the natural modes by transformation of the comprehensive equations into canonical form*, and
3) *Reduction of the order of the canonical form equations*.

This method of equivalents suffers from many problems such as:

a) The equations of the resulting equivalent can not be interpreted as representing models of physical devices.
b) The resulting equivalent model is not compatible with the existing transient stability software tools.
c) The determination of the system eigenvalues requires large computational time and high computer memory. Moreover, the modal-based reduction methods suffers from many problems, the resulting equivalent obtained needs to be computed once for certain load flow and network configuration.

On-line measurements based dynamic equivalent methods [60, 74, 96] are based on identifying dynamic equivalents of a portion of a power system from measurements made only within a restricted area without intentional perturbations of the system. Therefore, the method is based on system measurements during various natural disturbances. The external area in this case is modelled as black-box and its electromechanical equivalence is determined solely from measurements at the

interface buses at the internal area. These features facilitate the high-speed construction of electromechanical equivalence that mimic the real power system, regardless of the knowledge of the details of the topology or the parameters or the operating conditions of the original system. The availability and the techno economic feasibility of WAM systems and PMUs make this method of equivalence a vital tool for online transient stability and dynamic security of power systems.

CHAPTER 3
TRADITIONAL COHERENCY-BASED ELECTROMECHANICAL EQUIVALENCE

3.1 OVERVIEW OF THE TECHNIQUE

The traditional coherency-based electromechanical equivalence method is mainly based on known power flow and data sets of parameters rather than measueremts. Therefore, this electromechanical equivalence method is mainly suitable for offline analysis of power systems such as dynamic security analysis; however, as will be shown, the method provides an accurate tool for the electromechanical equivalence of power systems [74, 78 – 80, 97, 98]. Therefore, the coherency based equivalents technique is the 'the practical method most commonly used by power utilities to derive reduced models of large power systems is based on the concept of coherency and aggregation [74]'. Coherency is attributed and identified by the dynamic performance of generators. A group of generators that exhibit similar rotor angle swings after being subjected to a disturbance are said to be coherent. These machines can be aggregated or represented by a single machine.

Coherency based dynamic equivalent involves a three-stage procedure (Fig. 3.1): (i) *Identification of coherent groups of generators*, (ii) *Network reduction*, and (iii) *Dynamic aggregation of generating unit model*s.
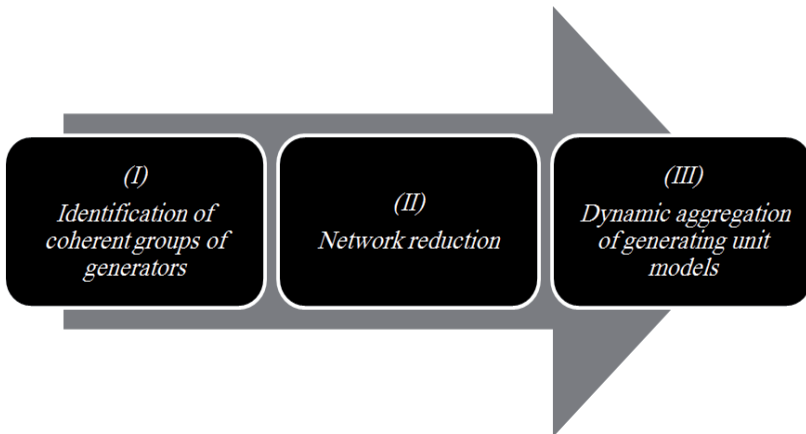

Fig. 3.1: Stages of coherency-based electromechanical equivalence

A coherent group of generating units can also be defined as a group of generators oscillating with the same angular speed and terminal voltages in a constant complex ratio for a set of disturbances. Thus, all the units in a coherent group can be attached to a common bus. Identification of coherent groups of generators can be based on heuristics or utilizing simplified and linearized power system models. In addition, the coherent groups can be identified using linear simulation for specific disturbances. The following assumptions are considered in the coherency identification. These assumptions will be verified in this chapter through several case studies.

i. *The coherency grouping of generators is independent of the size of the disturbance. Therefore, linearized system models can be used in identification phase,*

ii. *The coherency grouping is independent of the amount of detail in the generator model. Therefore, a classical synchronous machine model can be used in identification phase.*

The coherency-based dynamic reduction of power systems overcomes the numerical difficulties (and may be impossibilities especially with extra large systems) caused by modal-based dynamic reduction techniques.

The network reduction stage is generally based on replacing the terminal buses of a coherent group with a single equivalent bus. The parameters of the new lines are determined under the constraint that the power transferred from each bus of the boundary buses is the same in the original and reduced network. This constraint is essential for ensuring the correctness and the accuracy of the network equivalence. The dynamic aggregation of generating unit models stage is based on estimating the parameters of a single equivalent generating unit that exhibits the same speed, voltage, and total mechanical and electrical power as its detailed coherent group of generators during any perturbation.

3.2 IDENTIFICATION OF COHERENT GENERATORS (STAGE I)

The identification of coherent generators is the first stage in the coherency-based equivalency technique. The presented coherency algorithm is based on the correlation between linearized absolute-angle response of all generators in the power system. The linearized power system model is valid to simulate many types of power system disturbances along with low computer memory requirements and fast simulation. The solution of the proposed linearized model is based on the recursive

convolution using trapezoidal rule of integration [99,100]. For evaluating the proposed identification technique, comparisons between the coherency identification using the proposed model and the nonlinear solution of the system differential equations are carried out. In addition, the effect of fault severity, fault location within the study area, the details in generators modelling and their controls are studied to validate the proposed coherency algorithm. The nomenclature is listed in the *Appendix*.

3.2.1 PRELIMINARY CALCULATIONS

Using prefault base-case load flow, the p.u transient emf of all generators in the power system can be determined by:

$$\underline{E}'_i = \underline{V}_{gi} + (r_i + jX'_{di})\underline{I}_{gi} = \underline{V}_{gi} + (r_i + jX'_{di})\sum_{j=1}^{n}\underline{Y}_{ij}\underline{V}_j \quad (3.1)$$

where, i is an index for generator number i.

Loads are represented by their constant impedance static characteristics which is adequate for stability studies of large power systems. This is because the different characteristics of static load models tend to compensate each other, resulting in a composite effect of approximately a constant impedance load [101, 102]. In addition, the constant impedance load model is commonly used to represent loads in transient stability studies as they can be easily represented as a part of the network equations. Constant impedance loads exhibit the following voltage dependent model,

$$\left. \begin{array}{l} P_L = P_o \left(V_L / V_{Lo} \right)^2 \\ Q_L = Q_o \left(V_L / V_{Lo} \right)^2 \end{array} \right\} \quad (3.2)$$

The equivalent constant admittance to ground of loads are calculated by,

$$y_{jo} = g_{jo} - jb_{jo}$$
$$= \left(P_{Lj} / V_{Lj}^2 \right) - j\left(Q_{Lj} / V_{Lj}^2 \right) \quad (3.3)$$

where, j is an index for the load bus number j.

The proper diagonal elements of the bus admittance matrix Y_{BUS} are modified to include the equivalent constant admittance to the ground representing the system loads and the transient impedance of $(r + j\,X_d^{'})$ of each generator. The resulting modified bus admittance matrix Y^{MOD} can be arranged in the form

$$\begin{bmatrix} I_G \\ I_L \end{bmatrix} = \begin{bmatrix} Y_{GG} & Y_{GL} \\ Y_{LG} & Y_{LL} \end{bmatrix} \begin{bmatrix} E^{'} \\ V_L \end{bmatrix} \left.\begin{matrix} \\ \\ \\ \\ \end{matrix}\right\}$$
$$\text{i.e. } Y^{MOD} = \begin{bmatrix} Y_{GG} & Y_{GL} \\ Y_{LG} & Y_{LL} \end{bmatrix} \qquad (3.4)$$

All load buses are eliminated from the modified bus admittance matrix Y^{MOD} by setting $I_L = [0]$ in (3.4), then the load bus voltage vector takes the form

$$[V_L] = -[Y_{LL}]^{-1}[Y_{LG}][E^{'}] \qquad (3.5)$$

Eliminating $[V_L]$ from the first row in (3.4) using (3.5) results in the reduced bus admittance matrix Y^{RED} which represents the equivalent interconnections between all generators internal nodes and the equivalent interconnections to ground at each generator internal nodes.

$$\left[Y^{RED}\right] = \left[Y_{GG}\right] - \left[Y_{GL}\right]\left[Y_{LL}\right]^{-1}\left[Y_{LG}\right] \qquad (3.6)$$

3.2.2 Construction of the Linearized System Model

The construction of the power system linearized model consists of two basic steps (i) construction of power system linearized network model and (ii) construction of generator rotors linearized dynamic model. Proposed formation of both models will be derived as follows.

(i) Power System Linearized Network Model

The changes in the complex voltages and power injections at the network generator and load buses may be expressed using the Jacobian matrix form as:

$$
\begin{bmatrix} \Delta P_G \\ \Delta P_L \\ \Delta Q_G \\ \Delta Q_L \end{bmatrix} = \begin{bmatrix} \partial P_G / \partial \delta & \partial P_G / \partial \theta & \partial P_G / \partial E^{'} & \partial P_G / \partial V_L \\ \partial P_L / \partial \delta & \partial P_L / \partial \theta & \partial P_L / \partial E^{'} & \partial P_L / \partial V_L \\ \partial Q_G / \partial \delta & \partial Q_G / \partial \theta & \partial Q_G / \partial E^{'} & \partial Q_G / \partial V_L \\ \partial Q_L / \partial \delta & \partial Q_L / \partial \theta & \partial Q_L / \partial E^{'} & \partial Q_L / V_L \end{bmatrix} \begin{bmatrix} \Delta \delta \\ \Delta \theta \\ \Delta E^{'} \\ \Delta V_L \end{bmatrix} \quad (3.7)
$$

Equation (3.7) can be simplified based on the following approximations: (i) the power residuals ΔP_L and ΔQ_L are normally zero, and (ii) with high X/R ratios of transmission system the active and reactive flows can be decoupled. Based on these approximations, (3.7) can be reduced to the decoupled form

$$
\left[\Delta P_G \right] = \left[\partial P_G / \partial \delta \right] \left[\Delta \delta \right] \qquad (3.8)
$$

$$
\left[\Delta Q_G \right] = \left[\partial Q_G / \partial E^{'} \right] \left[\Delta E^{'} \right] \quad (3.9)
$$

The changes of power injections at the network generator buses are included in the system represented by the reduced bus admittance matrix Y^{RED}. Equation (3.8) can be written in series form

$$
\Delta P_{gi} = \sum_{j=1}^{n} J_{ij} \Delta \delta_j \qquad (3.10)
$$

$$
J_{ij} = \partial P_{gi} / \partial \delta_j \qquad (3.11)
$$

The Jacobian elements J_{ij} are calculated at prefault steady state conditions obtained from prefault load flow. The electrical power output of generator i is given by

$$
P_{gi} = E_i^{'2} G_{ii} + \sum_{\substack{j=1 \\ j \neq i}}^{ng} E_i^{'} E_j^{'} \left[B_{ij} \sin(\delta_i - \delta_j) + G_{ij} \cos(\delta_i - \delta_j) \right] \quad (3.12)
$$

Where B_{ij} and G_{ij} are real and imaginary parts of element (i, j) in the reduced admittance matrix Y^{RED}. A linearized form of (3.12) takes the form

$$\Delta P_{gi} = J_{ii}\Delta\delta_i + \sum_{\substack{j=1 \\ j\neq i}}^{ng} J_{ij}\Delta\delta_j \quad (3.13)$$

where

$$J_{ii} = -\sum_{\substack{j=1 \\ j\neq i}}^{ng} E_i E_j \alpha_{ij} \qquad (3.14)$$

$$J_{ij} = E_i E_j \; \alpha_{ij} \qquad\qquad (3.15)$$

$$\alpha_{ij} = G_{ij}\sin(\delta_i^o - \delta_j^o) - B_{ij}\cos(\delta_i^o - \delta_j^o) \qquad (3.16)$$

Equation (3.13) to (3.16) represents the linearized network model.

(ii) Generator Rotors Linearized Dynamic Model

The linearized model representing the dynamics of a generator rotor can be written in the form

$$M_i \frac{\partial \Delta\omega_i}{\partial t} = \Delta P_{mi} - \Delta P_{gi} - D_i\Delta\omega_i \quad (3.17)$$

$$\frac{\partial \Delta\delta_i}{\partial t} = 2\pi f_o \Delta\omega_i \qquad\qquad (3.18)$$

For constant mechanical power input, ΔP_{mi} is zero. In general, ΔP_{mi} can be used to simulate sudden changes in mechanical input power disturbances. The change in electrical power is defined in (3.13).

3.2.3 Solution of the proposed linearized model

Solution of the system linearized model represented by equations (3.13) to (3.18) will be carried out by the method of recursive convolution based on the trapezoidal rule of integration that require low computer memory. The method provides fast solution, and it is numerically stable for a large integration time step. Solution time step of about 0.1 sec or higher is quite efficient to secure accurate solution as typical natural frequencies of the rotor angle oscillation ranges from 0.25 to 2.0 Hz. Applying the trapezoidal rule to equation (3.17)

$$\int_{t-\Delta t}^{t} M_i \, \Delta\omega_i\,(t) = \int_{t-\Delta t}^{t} (\Delta P_{mi} - \Delta P_{gi} - D_i \Delta\omega_i\,(t))\partial t \quad (3.19)$$

Thus,

$$M_i\,(\Delta\omega_i\,(t) - \Delta\omega_i\,(t - \Delta t) = \frac{\Delta t}{2}(\Delta P_{mi}\,(t) + \Delta P_{mi}\,(t - \Delta t))$$

$$-\frac{\Delta t}{2}(\Delta P_{gi}\,(t) + \Delta P_{gi}\,(t - \Delta t)) - \frac{D_i \Delta t}{2}(\Delta\omega_i\,(t) + \Delta\omega_i\,(t - \Delta t)) \quad (3.20)$$

Rearranging (3.20) results in

$$(1 + \frac{\Delta t}{2}\frac{D_i}{M_i})\Delta\omega_i\,(t) - \frac{\Delta t}{2M_i}\Delta P_{mi}\,(t) + \frac{\Delta t}{2M_i}\Delta P_{gi}\,(t) = A_i\,(t - \Delta t) \quad (3.21)$$

where:

$$A_i\,(t - \Delta t) = (1 - \frac{\Delta t}{2}\frac{D_i}{M_i})\,\Delta\omega_i\,(t - \Delta t) + \frac{\Delta t}{2M_i}\Delta P_{mi}\,(t-\Delta t) - \frac{\Delta t\,(t)}{2M_i}\Delta P_{gi}\,(t - \Delta t) \quad (3.22)$$

Applying the trapezoidal rule to equation (2.18) and rearranging results in

$$\Delta\delta_i\,(t) - \pi f_o \Delta t\Delta\omega_i\,(t) = B_i\,(t - \Delta t) \quad (3.23)$$

where:

$$B_i\,(t - \Delta t) = \Delta\delta_i\,(t - \Delta t) + \pi f_o \Delta t\Delta\omega(t - \Delta t) \quad (3.24)$$

Solving (2.23) for $\Delta\omega_i(t)$

$$\Delta\omega_i(t) = \frac{1}{\pi f_o \Delta t}(\Delta\delta_i(t) - B_i(t - \Delta t)) \qquad (3.25)$$

Substituting (3.25) in (3.21) and rearranging results in

$$\frac{1}{\pi f_o \Delta t}(1 + \frac{D_i \Delta t}{2M_i})\Delta\delta_i(t) - \frac{\Delta t}{2M_i}\Delta P_{mi}(t) + \frac{\Delta t}{2M_i}\Delta P_{gi}(t) =$$

$$A_i(t - \Delta t) + \frac{1}{\pi f_o \Delta t}(1 + \frac{D_i \Delta t}{2M_i})B_i(t - \Delta t) \quad (3.26)$$

Solving (3.26) the resulted equation for $\Delta P_{gi}(t)$ takes the form

$$\Delta P_{gi}(t) = \frac{-2M_i}{\Delta t^2 \pi f_o}(1 + \frac{\Delta t}{2}\frac{D_i}{M_i})\Delta\delta_i(t) + \Delta P_{mi}(t) + C_i(t - \Delta t) \quad (3.27)$$

where:

$$C_i(t - \Delta t) = \frac{2M_i}{\Delta t^2 \pi f_o}(1 + \frac{\Delta t}{2}\frac{D_i}{M_i})B_i(t - \Delta t) + \frac{2M_i}{\Delta t}A_i(t - \Delta t) \quad (3.28)$$

Equation (3.27) can be written in matrix form as

$$[\Delta P_G(t)] = [K][\Delta\delta(t)] + [\Delta P_m] + [C(t - \Delta t)] \quad (3.29)$$

where: [K] is a (n_g by n_g) diagonal matrix with $K_{ii} = \dfrac{-2M_i}{\pi f_o \Delta t^2}(1 + \dfrac{\Delta t}{2}\dfrac{D_i}{M_i})$

Also rewriting (3.13) in matrix form becomes

$$[\Delta P_G(t)] = [J(t)][\Delta\delta(t)] \qquad (3.30)$$

Eliminating $[\Delta P_G(t)]$ from (3.29) using (3.30) and solving for $[\Delta\delta(t)]$ results in the final form *for the solution of the system linearized model as*

$$\left[\Delta\delta(t)\right]=\left[\left[J(t)\right]-\left[K\right]\right]^{-1}\left[\Delta P_m\right]+\left[\left[J(t)\right]-\left[K\right]\right]^{-1}\left[C\left(t-\Delta t\right)\right] \quad (3.31)$$

Speed deviation in p.u of all generators can be calculated using (3.25). The absolute angle $\delta(t)$ of each machine can be calculated using

$$\left[\delta(t)\right]=\left[\delta\left(t-\Delta t\right)\right]+\Delta t.\left[\Delta\delta\left(t-\Delta t\right)\right] \quad (3.32)$$

3.2.4 SIMULATION OF VARIOUS DISTURBANCES

Many types of disturbances can be simulated using the proposed linearized model. These disturbances include fault, line outage or fault clearing, line reclosing, and sudden change in input mechanical power disturbances. The power system under consideration is divided into study area and external area connected by several interface-buses as shown in Fig. 3.2. For coherency identification purpose, a disturbance is simulated within the study area and the absolute angle responses of all generators in the entire power system are determined using the proposed power system linearized model. The following describes the methods of simulating various disturbances using the presented linearized model.
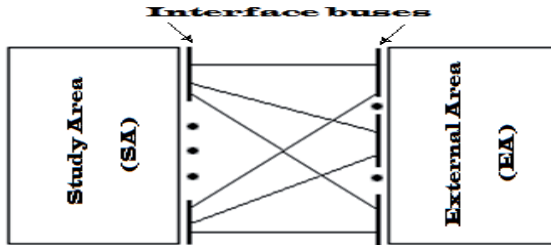

Fig. 3.2: Study and external areas

A *three-phase fault at a bus* can be simulated by adding a very high load at that bus in the full system data and reconstructing the fault reduced admittance matrix Y^{RED_F}. Simulation of either line outage or fault clearing can be carried out by representing that line by very high series impedance in the full system data and

reconstructing the post-fault reduced admittance matrix Y^{RED_PF}. The modified form of (3.16) can simulate the time changes in the linearized network model as

$$\alpha_{ij}(t) = G_{ij}(t)\sin(\delta_i^o - \delta_j^o) - B_{ij}(t)\cos(\delta_i^o - \delta_j^o) \quad (3.33)$$

In such way, the changes in the system reduced admittance matrix at specific times such as applying fault time and line-clearing time can be reflected as changes in the power injection at each generator bus.

The solution algorithm of the linearized model for fault and line-clearing simulation is summarized in the following steps:

(1)   Perform prefault load flow and calculate $E_i^{'}$ and $\delta_i(0)$ for all generators using equation (3.1).

(2)   Setup disturbances times, as functions of step size, and construct the prefault, fault, and post-fault reduced admittance matrices using the procedure described above in the form of equation (3.6).

(3)   Set $\Delta P_{mi} = 0$, calculate $A_i(t-\Delta t)$, $B_i(t-\Delta t)$, and $C_i(t-\Delta t)$.

(4)   Calculate $[\Delta \delta(t)]$ and $[\delta(t)]$ using (3.31) and (3.32).

(5)   Similarly calculate new generator power ΔP_{gi} using (3.29).

(6)   Continue until the desired simulation time expires.

The presented linearized model can also be used in simulating a *sudden change in the mechanical power input to generators*. For this type of simulation the reduced bus admittance matrix will not suffer time-dependent changes. The solution algorithm of the linearized model for the simulation of mechanical power input change is summarized in the following steps.

(1) Perform prefault load flow and calculate $E_i^{'}$ and $\delta_i(0)$ for all generators using (3.1).

(2) Setup disturbances times, as a function of step size, and construct the function $\Delta P_{mi}(t)$.

(3) Calculate $A_i(t-\Delta t)$, $B_i(t-\Delta t)$, and $C_i(t-\Delta t)$.

(4) Calculate $[\Delta \delta(t)]$ and $[\delta(t)]$ using (3.31) and (3.32).

(5) Similarly calculate new generator power ΔP_{gi} using (3.29).

(6) Continue until the desired simulation time expires.

3.2.5 Coherency Identification Criteria

The identification of coherent generators is based on correlation between absolute angle responses of all generators. The correlation factor ρ_{ij} between generator i and generator j responses is calculated using the soundly proved mathematical criterion in comparison with the criterion of [97] which does not observe the coherency requirements.

$$\rho_{ij} = \text{cov}(\delta_i(t), \delta_j(t))/(\sigma_i.\sigma_j) \qquad (3.34)$$

where: cov $(\delta_i(t),\ \delta_j(t))$ is the covariance between $\delta_i(t)$ and $\delta_j(t)$. σ_i and σ_j are the standard deviation of $\delta_i(t)$ and $\delta_j(t)$ respectively.

Calculation procedures of the covariance and standard deviation are detailed in [100]. Stronger coherency is secured as ρ_{ij} approaches unity. Therefore, accurate identification of coherent groups requires correlation factors (between the absolute angle response of coherent generators) of values close to unity. For example a minimum correlation factor of 0.999 may be selected as a criterion for identifying coherent groups of generators. This is equivalent to an identification accuracy of at least 99.9%. Sometimes, low number of coherent groups of generators are desired for signficently reducing the model of the external subsystem. In this case, the threshold value of the minimum correlation for coherency identification may be reduced, for example, to 0.99 i.e. accepting identification accuracy of 99%. Significantly reduced run times can be obtained knowing that if generator A is coherent with generator C, and generator A is coherent with generator B, then generator B is coherent with generator C (*see* Table 3.1).

3.2.6 COHERENCY IDENTIFICATION AND EVALUATION – CASE STUDY 1

The presented model coherency identification is applied for identifying the coherent groups of generators in the NPCC system [30, 103] as a case study. The system single-line diagram is shown in Fig. 3.3; the system is formed of 39 buses, 10 generators, 46 lines. The system parameters and load flow data are shown in Tables 3.1 to 3.3. The load flow results are shown in Table 3.4.
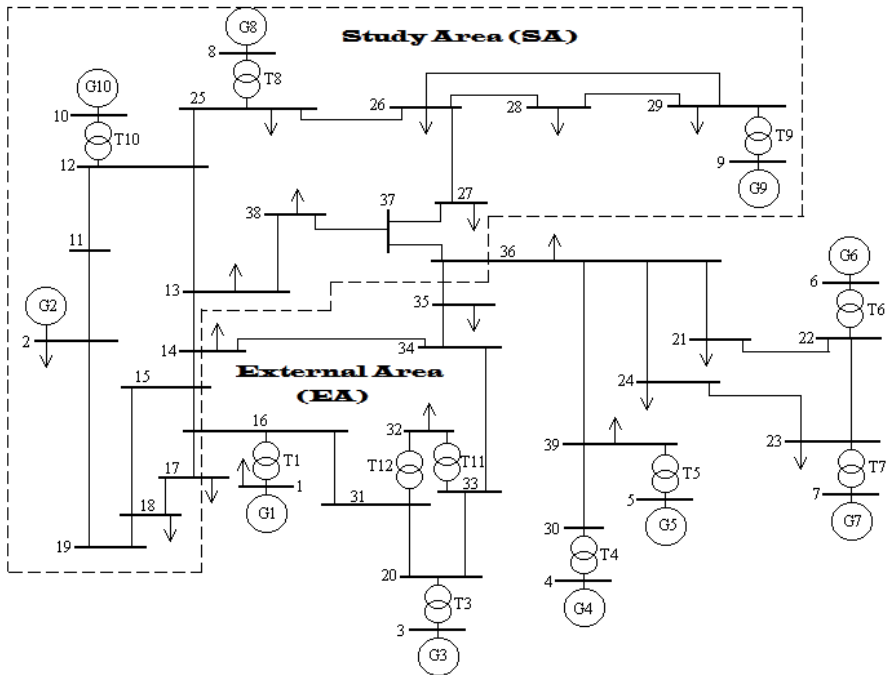
Fig. 3.3: NPCC system

Table 3.1: NPCC - Machine Data on 100 MVA base

Gen #	R_a	X_d	X'_d	X_q	X'_q	H	T'_{do}	T'_{qo}	D
1	0.0	0.2950	0.0647	0.2820	0.0647	30.3	6.56	1.5	0.0
2	0.0	0.0200	0.0060	0.0190	0.0060	500.0	6.0	0.7	0.0
3	0.0	0.2495	0.0531	0.2370	0.0531	35.8	5.7	1.5	0.0
4	0.0	0.3300	0.0660	0.3100	0.0660	26.0	5.4	0.44	0.0
5	0.0	0.2620	0.0436	0.2580	0.0436	28.6	5.69	1.5	0.0
6	0.0	0.2540	0.0500	0.2410	0.0500	34.8	7.3	0.4	0.0
7	0.0	0.2950	0.0490	0.2920	0.0490	26.4	5.66	1.5	0.0
8	0.0	0.2900	0.0570	0.2800	0.0570	24.3	6.7	0.41	0.0
9	0.0	0.2106	0.0570	0.2050	0.0570	34.5	4.79	1.96	0.0
10	0.0	0.2000	0.0040	0.1960	0.0040	42.0	5.7	0.50	0.0

Table 3.2: NPCC - Line Data on 100 MVA base

Bus #		R	X	B
From	To			
39	30	0.0007	0.0173	0.0000
37	27	0.0013	0.0173	0.3216
37	38	0.0007	0.0082	0.1319
36	24	0.0003	0.0059	0.0680
36	21	0.0008	0.0135	0.2548
36	39	0.0016	0.0195	0.3040
36	37	0.0007	0.0089	0.1342
35	36	0.0009	0.0094	0.1710
34	35	0.0018	0.2017	0.3660
33	34	0.0009	0.0101	0.1723
28	29	0.0014	0.0151	0.2490
26	29	0.0057	0.0625	1.0290
26	28	0.0043	0.0474	0.7802
26	27	0.0014	0.0147	0.2396
25	26	0.0032	0.0323	0.5130
23	24	0.0022	0.0350	0.3610
22	23	0.0006	0.0096	0.1846
21	22	0.0008	0.0135	0.2548
20	33	0.0004	0.0043	0.0729
20	31	0.0004	0.0043	0.0729
19	2	0.0010	0.0250	1.2000
18	19	0.0023	0.0363	0.3804
17	18	0.0004	0.0046	0.0780
16	31	0.0007	0.0084	0.1389
16	17	0.0006	0.0092	0.1130
15	18	0.0008	0.0112	0.1476
15	16	0.0002	0.0026	0.0434
14	34	0.0008	0.0129	0.1382
14	15	0.0008	0.0128	0.1342
13	38	0.0011	0.0133	0.2138
13	14	0.0013	0.0213	0.2214
12	25	0.0070	0.0086	0.1460
12	13	0.0013	0.0151	0.2572
11	12	0.0035	0.0411	0.6987
11	2	0.0010	0.0250	0.7500

Table 3.3: NPCC- Transformer Data on 100 MVA base

Bus #		R_T	X_T	Tap
From	To			
39	5	0.0007	0.0142	1.0
32	33	0.0016	0.0435	1.0
32	31	0.0016	0.0435	1.0
30	4	0.0009	0.0180	1.0
29	9	0.0008	0.0156	1.0
25	8	0.0006	0.0232	1.0
23	7	0.0005	0.0272	1.0
22	6	0.0000	0.0143	1.0
20	3	0.0000	0.0200	1.0
16	1	0.0000	0.0250	1.0
12	10	0.0000	0.0181	1.0

Table 3.4: Load Flow of the NPCC system on 100 MVA base

Bus #	V	θ	P_G	Q_G	P_L	Q_L
1	0.98200	0.00000	5.04509	1.36036	0.0920	0.04600
2	1.03000	-9.55016	10.00000	1.95746	11.04000	2.5000
3	0.98310	3.20174	6.5000	1.29104	0.00000	0.00000
4	1.01230	4.61664	5.08000	1.58151	0.00000	0.00000
5	0.99720	5.57217	6.32000	0.95582	0.00000	0.00000
6	1.04930	6.62654	6.5000	2.76414	0.00000	0.00000
7	1.06350	9.46958	5.60000	2.35485	0.00000	0.00000
8	1.02780	3.16537	5.4000	0.63019	0.00000	0.00000
9	1.02650	9.04654	8.3000	0.84790	0.00000	0.00000
10	1.04750	-2.47597	2.5000	1.46483	0.00000	0.00000
11	1.03829	-7.79710	0.00000	0.00000	0.00000	0.00000
12	1.02310	-4.89487	0.00000	0.00000	0.00000	0.00000
13	0.99576	-8.07759	0.00000	0.00000	3.22000	0.02400
14	0.95894	-9.35310	0.00000	0.00000	5.00000	1.84000
15	0.95660	-8.29471	0.00000	0.00000	0.00000	0.00000
16	0.95688	-7.56925	0.00000	0.00000	0.00000	0.00000
17	0.95140	-9.97400	0.00000	0.00000	2.33800	0.84000
18	0.95276	-10.5017	0.00000	0.00000	5.22000	1.76000
19	1.01028	-9.92054	0.00000	0.00000	0.00000	0.00000
20	0.95988	-4.71314	0.00000	0.00000	0.00000	0.00000
21	0.99046	-2.98024	0.00000	0.00000	2.74000	1.1500
22	1.01550	1.62430	0.00000	0.00000	0.00000	0.00000
23	1.01344	1.134841	0.00000	0.00000	2.74500	0.84660
24	0.98179	-5.45955	0.00000	0.00000	3.08600	0.92200
25	1.02088	-3.68918	0.00000	0.00000	2.24000	0.47200
26	1.01822	-4.76321	0.00000	0.00000	1.39000	0.17000
27	1.00150	-6.92554	0.00000	0.00000	2.81000	0.75500
28	1.02204	-0.95906	0.00000	0.00000	2.06000	0.27600
29	1.02143	1.95588	0.00000	0.00000	2.83500	0.26900
30	0.98832	-0.62515	0.00000	0.00000	6.28000	1.03000
31	0.95760	-5.69316	0.00000	0.00000	0.00000	0.00000
32	0.93795	-5.68713	0.00000	0.00000	0.07500	0.88000
33	0.95912	-5.47342	0.00000	0.00000	0.00000	0.00000
34	0.96168	-7.20767	0.00000	0.00000	0.00000	0.00000
35	0.96683	-7.32475	0.00000	0.00000	3.20000	1.53000
36	0.98196	-5.55956	0.00000	0.00000	3.29400	0.32300
37	0.99086	-6.73437	0.00000	0.00000	0.00000	0.00000
38	0.99197	-7.71437	0.00000	0.00000	1.58000	0.30000
39	0.98770	0.34648	0.00000	0.00000	0.00000	0.00000

A three phase-fault is simulated for indentifying the coherent groups of generators using the presented linearized model. The fault is applied to bus 2 and cleared after 3 cycles by removing line 2-19. The change in absolute angle and the absolute angles, calculated using (3.32), of all generators are shown in Fig. 3.4 and Fig. 3.5 respectively. Based on the abosulte angles shown in Fig. 3.5, the system is stable. For more details about the identification of the stability of generators from the patterns of the absolute and relative angle responses, the *Anderson and Fouad textbook* is recommended [104].
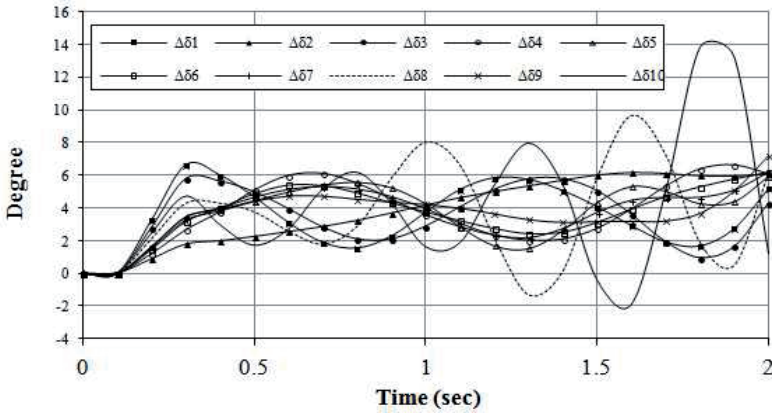

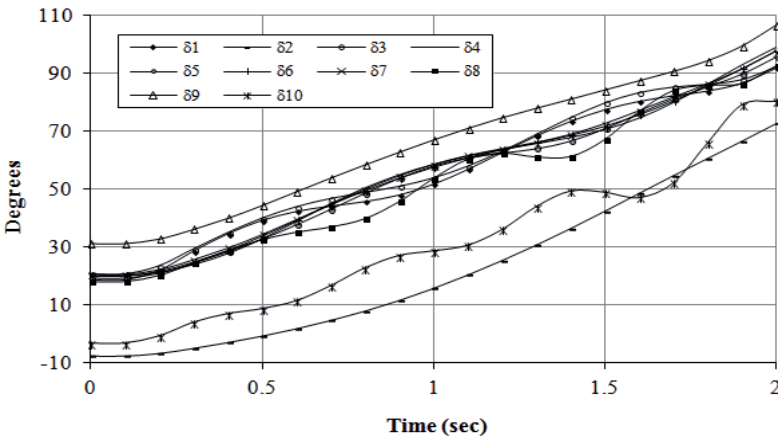Fig. 3.4: Linearized changes of the abosulte angles of the NPCC system for 3 cycles fault

Fig. 3.5: Linearized the abosulte angles of the NPCC system for 3 cycles fault

In this manuscript, a group of generators is said to be coherent if the correlation factor (ρ_{ij}) between the transient response of their absolute angles is greater than or equal to 0.999; a value that ensure high coherency between the generators. Based on this criterion, two groups of coherent generators are identified as shown in Table 3.5. The first group consists of generators 4, 5, 6, and 7, and the second group consists of generators 1 and 3. This is can also be easily identified from Fig. 3.5. Two proposed external areas are then selected (named EA1 and EA2).

Table 3.5: Correlation factors between linearized absolute angle responses of the NPCC system*

	$\delta 2$ (SA)	$\delta 3$	$\delta 4$	$\delta 5$	$\delta 6$	$\delta 7$	$\delta 8$ (SA)	$\delta 9$ (SA)	$\delta 10$ (SA)
$\delta 1$	0.9715	**0.9992**	0.9801	0.9848	0.9857	0.9864	0.984	0.9908	0.9729
$\delta 2$	-	0.9707	0.9703	0.9728	0.9736	0.9736	0.9805	0.9751	0.9832
$\delta 3$	-	-	0.9805	0.9859	0.9861	0.9871	0.9836	0.9907	0.9702
$\delta 4$	-	-	-	**0.9988**	**0.9995**	**0.9991**	0.9875	0.9968	0.9855
$\delta 5$	-	-	-	-	**0.9994**	**0.9998**	0.9923	0.998	0.9819
$\delta 6$	-	-	-	-	-	**0.9998**	0.9902	0.9986	0.9858
$\delta 7$	-	-	-	-	-	-	0.9914	0.9987	0.9842
$\delta 8$	-	-	-	-	-	-	-	0.9907	0.9729
$\delta 9$	-	-	-	-	-	-	-	-	0.9841

* Note: $\rho_{ij} = \rho_{ji}$

As shown in Fig. 3.6, these external areas include the first and second groups of coherent generators respectively. The linearized absolute angle response of each coherent group of generators is shown in Fig. 3.7 and Fig. 3.8. The study area (SA) is the subsystem outside EA1 and EA2. The results indicate the strong coherency between the generators comprising each coherent group.
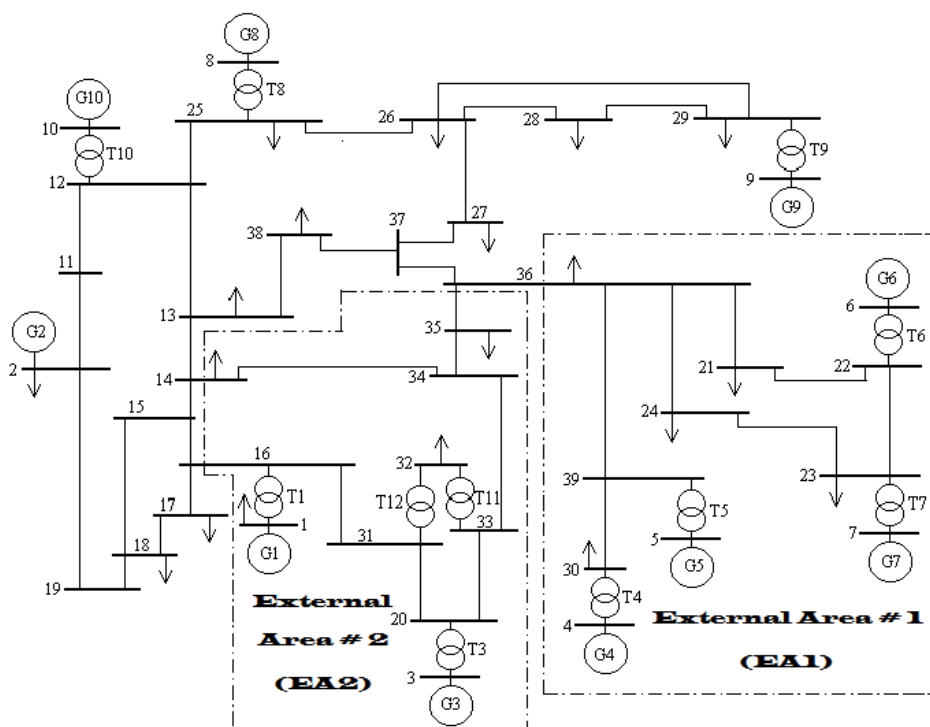
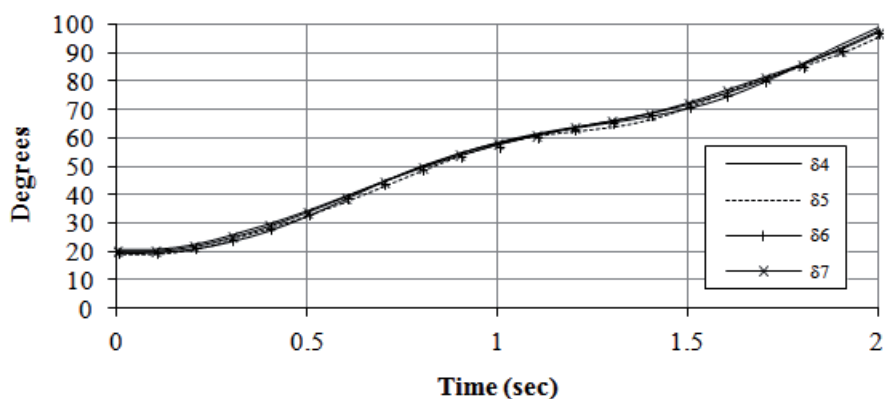Fig. 3.6: Coherent groups of generators in the NPCC system

Fig. 3.7: Linearized response of the first coherent group in the NPCC system
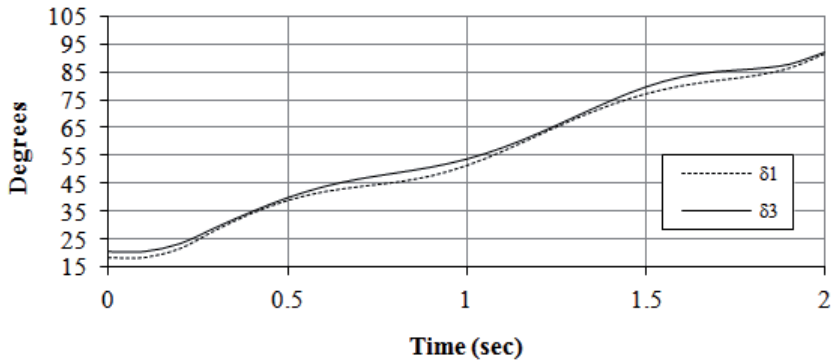
Fig. 3.8: Linearized response of the second coherent group in the NPCC system

It can easily be seen from Table 3.5 that the identification of coherent groups is highly sensitive to a threshold value of the correlation factor for coherency. For example, if the minimum correlation for coherency is selected to be 0.98 instead of 0.999, then all generators in the external subsystem will be considered as one coherent group; however, the coherency identification is reduced to 98% instead of 99.9%. Since each coherent group of generators will be reduced to one equivalent generator. Then, reducing the number of coherent groups significantly reduce the order of the external subsystem equivalent model. A situation which may be desired for a large scale interconnected system where the speed of simulating the equivalent system is of major importance for online simulation.

The results and consequently the presented linearized model and identification criterion are evaluated by different methods. These evaluation methods include: (i) Comparison between the linearized and nonlinear responses; (ii) Effect of fault severity on coherency grouping; (iii) Effect of fault location on coherency grouping; and (iv) Effect of details of generator model on coherency grouping. These results will be presented in the following.

(i) The *Effect of generator model non-linearity on the coherency grouping*. The absolute angle response of all generators is calculated with generators represented by nonlinear E'-constant classical model and the results are shown in Fig. 3.9. It is found that although the magnitude of absolute movement of rotor angles increased with the nonlinear model, the phase shift between generators is almost unchanged with respect to linearized model. Hence, conclusion upon coherency grouping is invariable. Fig. 3.10 and Fig. 3.11 show

46

the nonlinear E'-constant absolute angle responses of the first and second groups of coherent generators. These results ensure the accuracy of the presented linearized model in identifying coherent groups of generators.
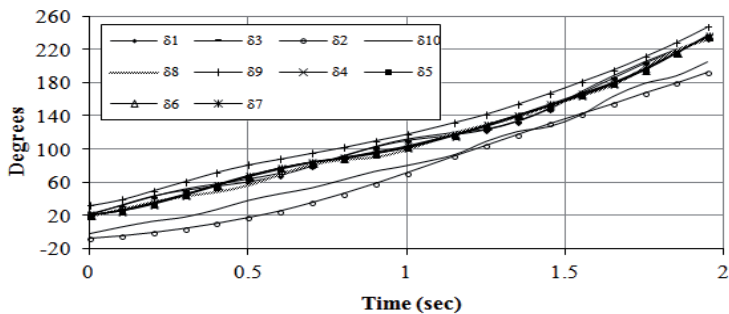

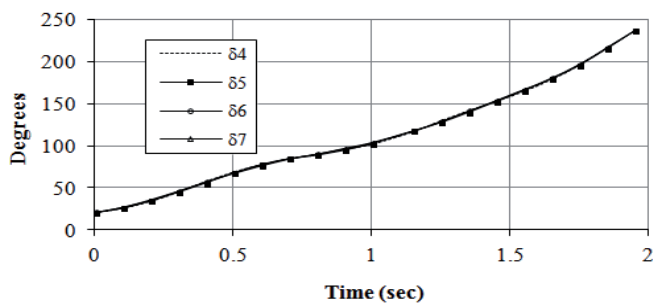Fig. 3.9: Nonlinear (E'-const.) response of the NPCC system

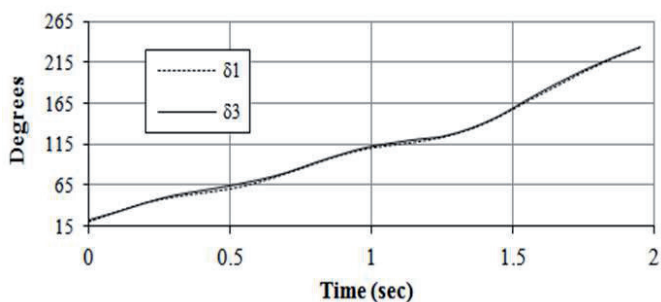Fig. 3.10: Nonlinear (E'-const.) response of the first coherent group

Fig. 3.11: Nonlinear (E'-const.) response of the second coherent group

(ii) The *effect of fault severity on the coherency grouping* will be now considered. For this purpose, the linearized change in absolute angle responses of NPCC system is determined for a considered fault i.e. a three-phase fault bus 2 cleared by removing line 2-19 after 3 cycles (Fig. 3.4 and Fig. 3.5). In this analysis the same fault is cleared after 10 cycles. The results are shown in Fig. 3.12 and Fig. 3.13.
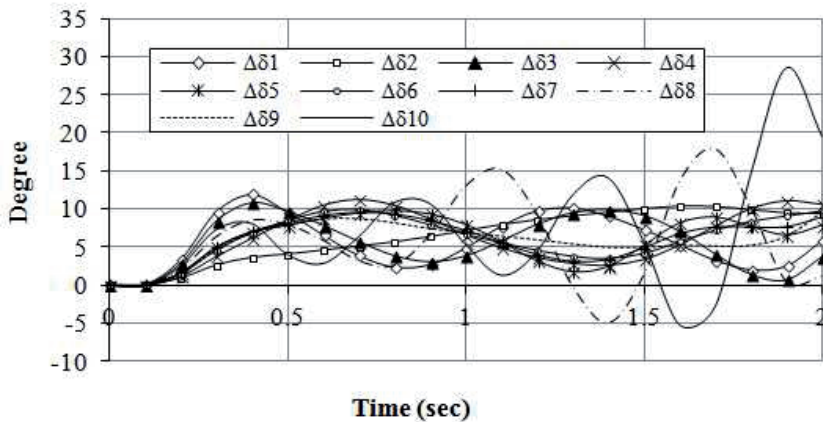

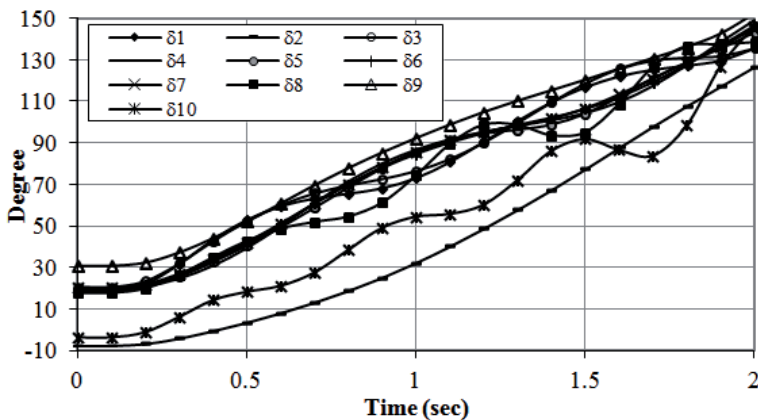Fig. 3.12: Linearized changes of the abosulte angles of the NPCC system for 10 cycles fault

Fig. 3.13: Linearized abosulte angles of the NPCC system for 10 cycles fault

Inspection of these results shows clearly that the coherency grouping remains unchanged with the severity of the fault. This is illustrated by showing the responses of the coherent groups of generators; Fig. 3.14 and Fig. 3.15.
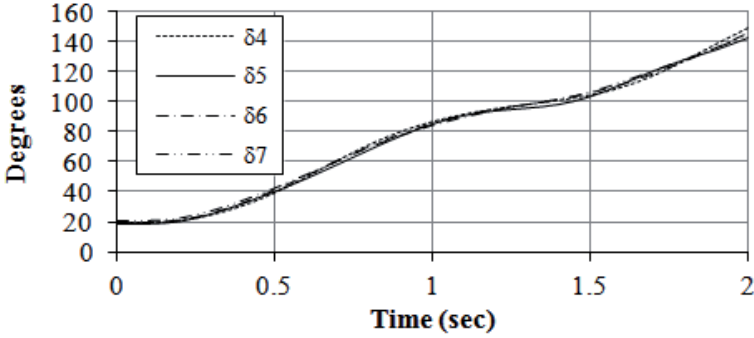
Fig. 3.14: Linearized response of the first coherent group in the NPCC system (10 cycles fault)
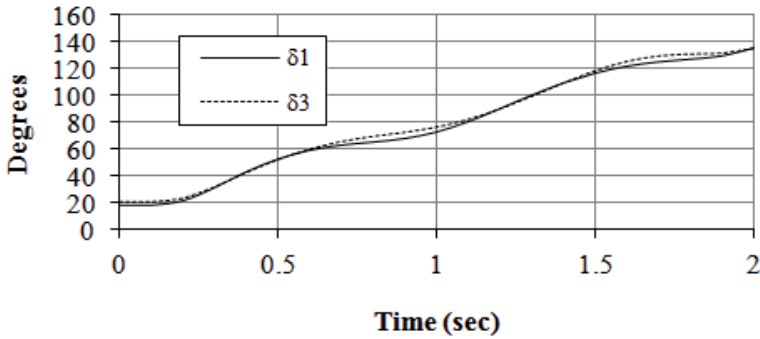
Fig. 3.15: Linearized response of the second coherent group in the NPCC system (10 cycles fault)

(iii)   The *effect of fault location on the coherency grouping* is considered in this section. For this purpose, two faults are considered.

    a. Fault at bus 29 cleared after 3 cycles by removing line 28-29. This location is electrically far from the fault at bus 2 used previously in the coherency identification and grouping of generators. The Linearized absolute angle responses are shown in Fig. 3.16.

b. Fault at bus 25 cleared after 3 cycles by removing line 25-26. This
location is electrically closer to the fault at bus 2 used previously in the
identification and grouping of generators. The Linearized absolute angle
responses are shown in Fig. 3.17.
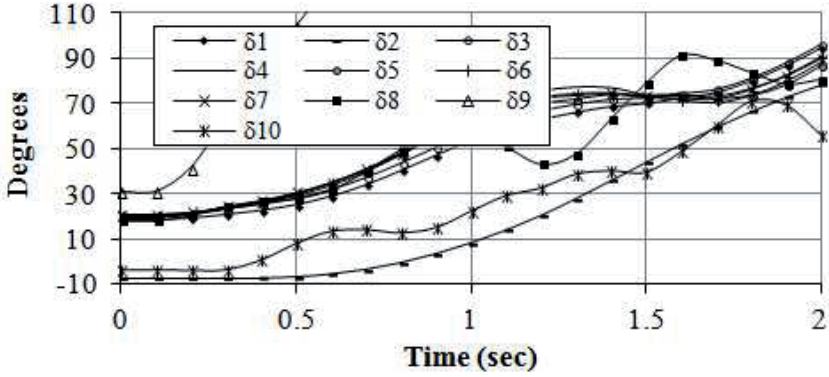
Fig. 3.16: Linearized response for a fault at bus 29
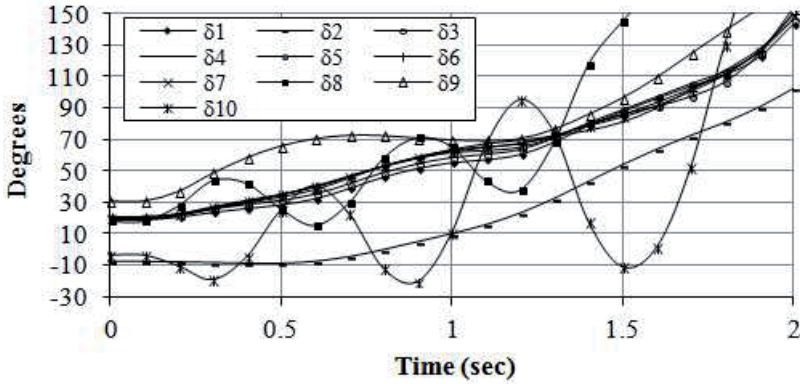
Fig. 3.17: Linearized response for a fault at bus 25

The correlation factor analysis of both faults revealed that the fault location is
also ineffective on the coherency grouping. Therefore, the coherency grouping
is valid for various disturbances irrespective of the fault location, the fault
severity, and nonlinearities of the models of generators. The following analysis
also illustrates that generator model details as well as generator controllers will

not affect the coherency grouping. Therefore, the coherency grouping is a system characteristic and also the electromechanical equivalence of the coherent groups as will be illustrated in the upcoming sections.

(iv)   The *effect of generator model details and generator controllers on the coherency grouping*. It was shown that the nonlinear classical E'-constant model gives the same coherent groups obtained with the linearized E'-constant presented generators model. Now, the effect of detailing the generator model will be considered. The nonlinear response of the NPCC system with generators represented by the transient model (E_d'-E_q' model) is simulated for this purpose. The nonlinear absolute angle response of the NPCC system for fault at bus 2 cleared after 3 cycles by removing line 2-19 with generators represented by transient model is shown in Fig. 3.18. The impact of the generator excitation control is considered by equipping all generators with a simple Automatic Voltage Regulator (AVR) model shown in Fig. 3.19. The parameters of the AVR are K_A=25, T_A = 0.025, V_{RMAX} = 10, and V_{RMIN} = -10. (All on 100 MVA base). The nonlinear absolute angle response of the NPCC system for fault at bus 2 cleared after 3 cycles by removing line 2-19 with generators equipped with the proposed AVR and represented by transient model is shown in Fig. 3.20. The correlation factor analysis of the results shown in Fig. 3.18 and Fig. 3.20 are shown in Tables 3.6 and 3.7.
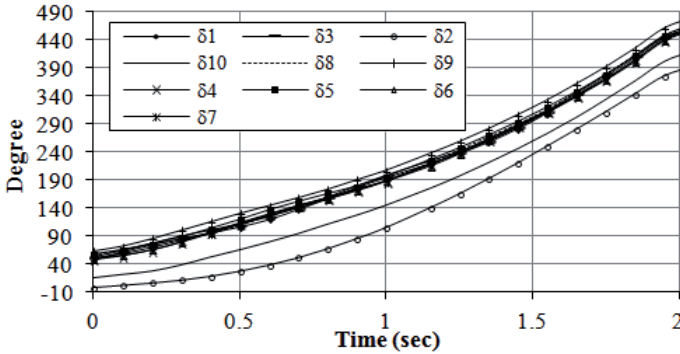

Fig. 3.18: Nonlinear response of NPCC system with generators represented by the transient model
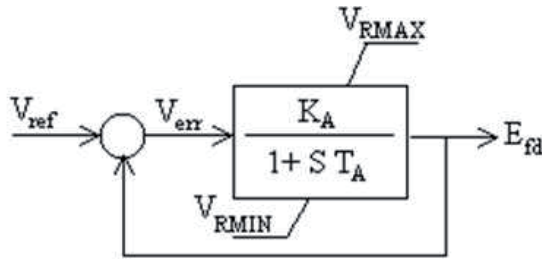
Fig. 3.19: AVR model
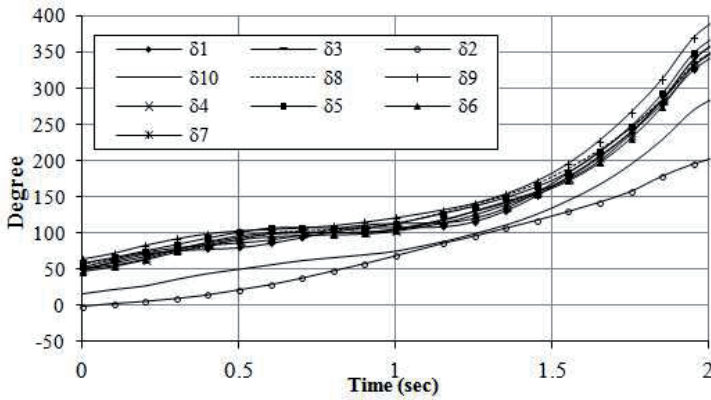
Fig. 3.20: Nonlinear response of NPCC system with generators represented by the transient model and equipped with AVR

Table 3.6: Correlation factor analysis for the nonlinear responses of the NPCC system with all generators represented by transient model

	$\delta2$	$\delta3$	$\delta4$	$\delta5$	$\delta6$	$\delta7$	$\delta8$	$\delta9$	$\delta10$
$\delta1$	0.9966	**0.9999**	0.9992	0.9994	0.9994	0.9995	0.9996	0.9995	0.9995
$\delta2$	–	0.9964	0.9955	0.9955	0.9959	0.9961	0.9977	0.9959	0.9981
$\delta3$	–	–	0.9992	0.9995	0.9994	0.9995	0.9995	0.9995	0.9995
$\delta4$	–	–	–	**0.9999**	**0.9999**	**0.9999**	0.9995	0.9999	0.9994
$\delta5$	–	–	–	–	**0.9999**	**0.9999**	0.9997	0.9998	0.9996
$\delta6$	–	–	–	–	–	**0.9999**	0.9996	0.9998	0.9995
$\delta7$	–	–	–	–	–	–	0.9997	0.9998	0.9996
$\delta8$	–	–	–	–	–	–	–	0.9996	0.9999
$\delta9$	–	–	–	–	–	–	–	–	0.9995

The results of Figs. 3.5, 3.18, and 3.20 as well as the correlation factor analysis shown in Tables 3.5, 3.6, and 3.7 ensures that the coherency grouping of generators is unaffected by either the generator model details or the consideration of the generator controls (represented here by an AVR).

The presented linearized model can also simulate other disturbances such as *sudden changes in the mechanical power input to generators* as described earlier. This will be demonstrated for the purpose of coherent groups identification by a numerical example.

Table 3.7: Correlation factor analysis for the nonlinear responses of the NPCC system with all generators represented by transient model and equipped with AVR

	δ2	δ3	δ4	δ5	δ6	δ7	δ8	δ9	δ10
δ1	0.9522	**0.9999**	0.9959	0.9971	0.9959	0.9974	0.9971	0.9984	0.9949
δ2	–	0.9527	0.9472	0.9955	0.9504	0.9491	0.9664	0.9476	0.9749
δ3	–	–	0.9961	0.9972	0.9971	0.9975	0.9972	0.9985	0.9952
δ4	–	–	–	**0.9999**	**0.9999**	**0.9999**	0.9969	0.9986	0.9945
δ5	–	–	–	–	**0.9999**	**0.9999**	0.9976	0.9993	0.9950
δ6	–	–	–	–	–	**0.9999**	0.9977	0.9990	0.9955
δ7	–	–	–	–	–	–	0.9978	0.9994	0.9953
δ8	–	–	–	–	–	–	–	0.9975	0.9991
δ9	–	–	–	–	–	–	–	–	0.9945

Fig. 3.21 and Fig. 3.22 shows the absolute angle response of all generators as subjected to 10% and 50% sudden drop in the mechanical input to generator 2. The consequent correlation factor analysis is shown in Tables 3.8 and 3.9 respectively. Fig. 3.23 shows the absolute angle response of all generators due to 10% sudden drop in mechanical input of generator 9 and correlation factor analysis is shown in Table 3.10. The presented results confirm clearly that the coherency grouping is neither dependent on the type of the disturbance used for identifying them nor its location. In addition, the results confirm that the coherency grouping is also independent of the severity of the disturbance. This a very important characteristics of coherency grouping, especially *when actual disturbance recording data are utilized for coherency identification; the location and the severity of the disturbance(s) are not an important factor for coherency identification purpose*.

Table 3.8: Correlation factors for 10% sudden drop in mechanical power input of G2

	δ2	δ3	δ4	δ5	δ6	δ7	δ8	δ9	δ10
δ1	0.9606	**0.9997**	0.9908	0.9952	0.9941	0.9945	0.9988	0.9936	0.9949
δ2	–	0.9539	0.9193	0.9322	0.9285	0.9299	0.9692	0.9266	0.9829
δ3	–	–	0.9939	0.9973	0.9965	0.9968	0.9976	0.9961	0.9923
δ4	–	–	–	**0.9993**	**0.9996**	**0.9995**	0.9841	0.9987	0.9741
δ5	–	–	–	–	**0.9999**	**0.9999**	0.9899	0.9988	0.9815
δ6	–	–	–	–	–	**0.9999**	0.9884	0.9988	0.9795
δ7	–	–	–	–	–	–	0.9891	0.9988	0.9803
δ8	–	–	–	–	–	–	–	0.9878	0.9975
δ9	–	–	–	–	–	–	–	–	0.9784

Table 3.9: Correlation factors for 50% sudden drop in mechanical power input of G2

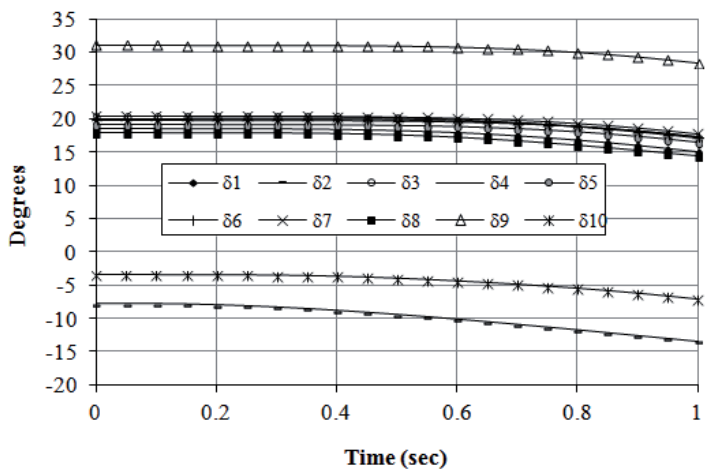|	δ2	δ3	δ4	δ5	δ6	δ7	δ8	δ9	δ10
δ1	0.9617	**0.9996**	0.9909	0.9952	0.9941	0.9945	0.9988	0.9935	0.9947
δ2	–	0.9551	0.9208	0.9338	0.9300	0.9314	0.9701	0.9280	0.9840
δ3	–	–	0.9940	0.9973	0.9965	0.9968	0.9975	0.9961	0.9920
δ4	–	–	–	**0.9993**	**0.9996**	**0.9995**	0.9839	0.9988	0.9734
δ5	–	–	–	–	**0.9999**	**0.9999**	0.9899	0.9988	0.9811
δ6	–	–	–	–	–	**0.9999**	0.9883	0.9988	0.9789
δ7	–	–	–	–	–	–	0.9889	0.9987	0.9797
δ8	–	–	–	–	–	–	–	0.9876	0.9973
δ9	–	–	–	–	–	–	–	–	0.9778

Fig. 3.21: Linearized absolute angle response for 10% sudden drop in mechanical input of G2
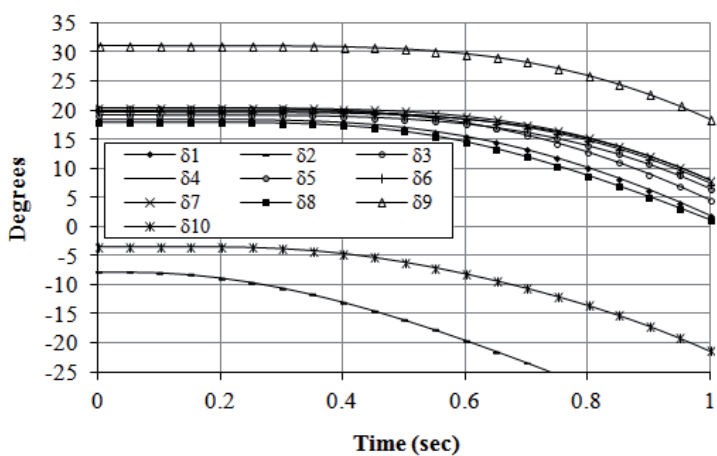

Fig. 3.22: Linearized absolute angle response for 50% sudden drop in mechanical input of G2
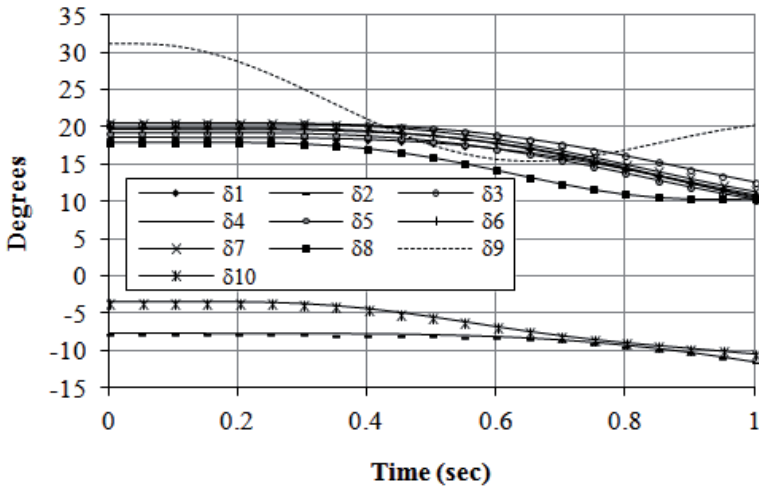
Fig. 3.23: Linearized absolute angle response for 10% sudden drop in mechanical input of G9

Table 3.10: Correlation factors for 10% sudden drop in mechanical power input of G9

	$\delta 2$	$\delta 3$	$\delta 4$	$\delta 5$	$\delta 6$	$\delta 7$	$\delta 8$	$\delta 9$	$\delta 10$
$\delta 1$	0.9888	**0.9999**	0.9988	0.9980	0.9988	0.9984	0.9415	0.5224	0.9513
$\delta 2$	–	0.9883	0.9884	0.9779	0.9806	0.9789	0.8821	0.4257	0.9001
$\delta 3$	–	–	0.9988	0.9982	0.9989	0.9985	0.9425	0.5244	0.9522
$\delta 4$	–	–	–	**0.9998**	**0.9998**	**0.9998**	0.9422	0.5229	0.9517
$\delta 5$	–	–	–	–	**0.9998**	**0.9999**	0.9606	0.5665	0.9682
$\delta 6$	–	–	–	–	–	**0.9999**	0.9565	0.5545	0.9642
$\delta 7$	–	–	–	–	–	–	0.9591	0.5612	0.9665
$\delta 8$	–	–	–	–	–	–	–	0.7282	0.9958
$\delta 9$	–	–	–	–	–	–	–	–	0.7391

3.3 COHERENCY-BASED NETWORK REDUCTION (STAGE II)

Network reduction is the second stage of three stages that are required for construction of coherency based electromechanical equivalence of electrical power systems. In this stage, based on coherency grouping, the system outside the study areas is divided to set of external areas (EA) connected to the study area by a number of interface buses as shown in Fig. 3.24.
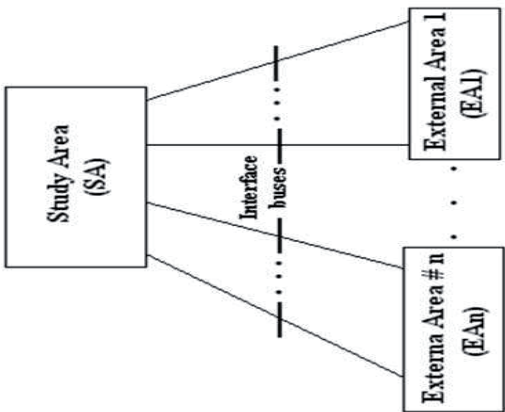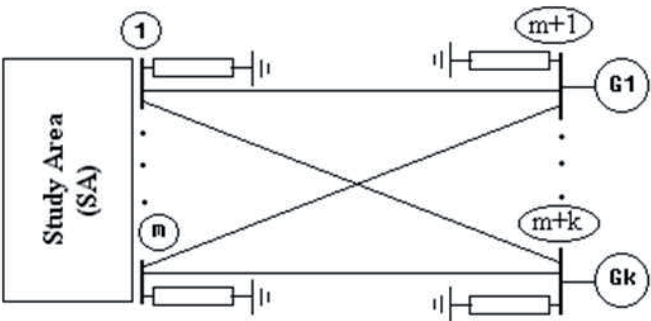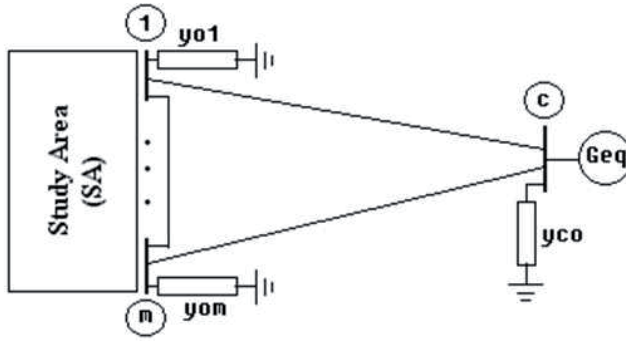

Fig. 3.24: Connections between the study area and the external areas

(a)

(b)

Fig. 3.25: Connection between a group of coherent generators and the study area; (a) physical interconnections with loads represented by constant impedance models; (b) network equivalence

For network reduction purpose, a single equivalent bus replaces terminal buses of each group of coherent generators in each external area. The generators of each coherent group then appear in parallel on the equivalent bus. The new lines connecting the equivalent bus and interface buses of the SA, the new lines connecting the interface buses, and the shunt admittance to ground at each of the equivalent bus and the interface buses for each external area shown in Fig. 3.25 are to be determined as described in this section. The network reduction is based on a reliable and simple technique that is adequately accurate as will be shown in the numerical examples. The parameters of the equivalent synchronous generator for each group of coherent generators will be determined in the dynamic aggregation, which is the third stage of the construction of an electromechanical equivalence.

3.3.1 PRELIMINARY CALCULATIONS

For each external area, a bus admittance matrix $Y_{BUS}{}^{EA}$ is formed representing the interconnections between the terminal buses in the external area and the interface buses. Equivalent admittance to ground model of loads in each of the external areas are calculated using equation (3.3). Modifying the proper diagonal elements in $Y_{BUS}{}^{EA}$ to include the loads equivalent admittance to ground forms a modified bus admittance matrix $Y_{MOD}{}^{EA}$. Area reduced admittance matrix Y^{RED_EA} is obtained by the same way described by equation (3.6). The Y^{RED_EA} is a square matrix of order $(m + k)$ with m is the number of interface buses and k is the number of coherent generator buses. The

corresponding equivalent circuit of the external area will take the form shown in Fig. 3.25(a).

3.3.2 *ADMITTANCE TO GROUND AND IMPEDANCE OF NEW LINES*

Fig. 3.25(a) demonstrates the interconnections between k coherent buses and m interface buses. The network reduction is shown in Fig. 3.25(b). Let c be an index for the equivalent common bus of a coherent group of generator and $Y_{ij}^{RED\_EA}$ be element (i, j) in the external area reduced admittance matrix Y^{RED_EA}. The admittance to ground on each of the interface buses are calculated using

$$y_{oi} = Y_{ii}^{RED\_EA} + \sum_{\substack{j=1 \\ j \neq i}}^{m+k} Y_{ij}^{RED\_EA} \qquad (3.35)$$

where $i = 1, 2... m$.

The admittance to ground on each of the common bus is calculated using

$$y_{co} = \sum_{i=m+1}^{m+k} (Y_{ii}^{RED\_EA} + \sum_{\substack{j=1 \\ j \neq i}}^{m+k} Y_{ij}^{RED\_EA}) \qquad (3.36)$$

The impedance $(R + jX)$ of the new lines is divided into two groups:

(i) New lines connecting the interface bus and the common equivalent bus. The impedance of these lines are calculated using

$$(R_{ic} + jX_{ic}) = 1/(-\sum_{j=m+1}^{m+k} Y_{ij}^{RED\_EA}) \qquad (3.37)$$

where $i = 1, 2... m$.

(ii) New lines connecting the interface buses. The impedance of these lines are calculated using

$$(R_{ij} + jX_{ij}) = 1/(-Y_{ij}^{RED\_EA}) \qquad (3.38)$$

59

where $i = 1, 2... m. j = 1, 2... m.$ And $j \neq i$.

3.3.3 COMMON BUS TERMINAL VOLTAGE

The common bus terminal voltage of a coherent group of generators is calculated as the mean value of the prefault steady state base-case load flow voltage of each generator in the coherent group. Hence,

$$V_c = \frac{1}{m} \sum_{i=m+1}^{m+k} V_{gi}^o \qquad (3.39)$$

The evaluation of the presented network equivalency technique will be provided through the overall electromechanical equivalence i.e. after the dynamic aggregation of coherent generators.

3.3.4 NETWORK REDUCTION FOR THE NPCC SYSTEM – CASE STUDY 2

In the first stage, based on coherency identification and grouping, the part of the NPCC system outside the study area is divided into two external areas as shown in Fig. 3.6. The proposed network reduction technique is applied to each EA to obtain the corresponding equivalent networks represented by admittances to ground at interface buses, the admittances to ground at common bus, and the new lines connecting these buses as shown in Fig. 3.26. The values of the parameters of these equivalent Network elements are shown in Table 3.11 and Table 3.12 for EA1 and EA2 respectively, with all values are in p.u on 100 MVA base.
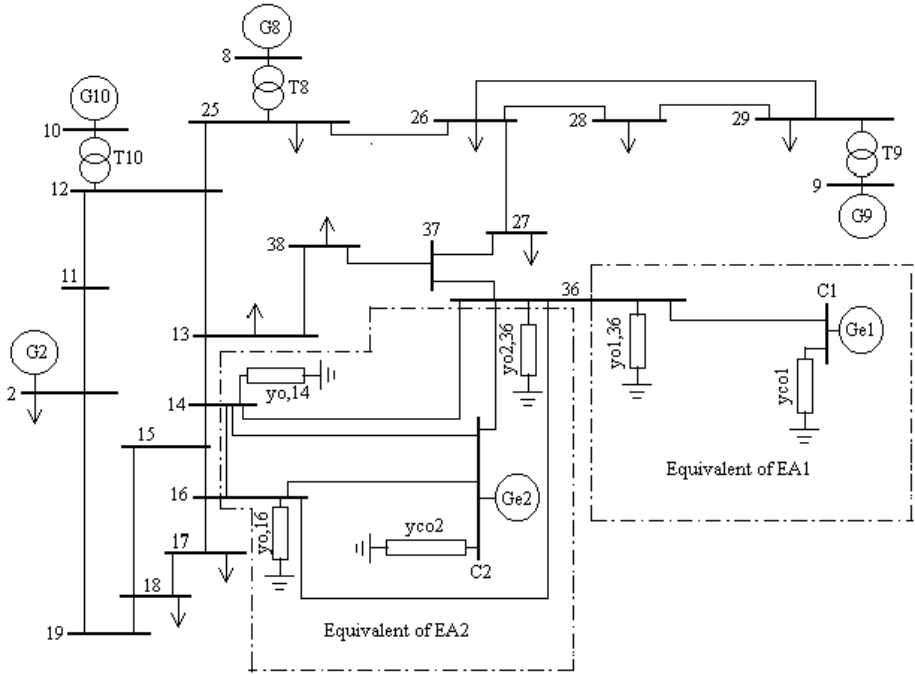
Fig. 3.26: Equivalent networks for EA1 and EA2 of the NPCC equivalent system

Table 3.11: Parameters of equivalent network of EA1

Lines			Admittances to ground
ID	R_{eq}	X_{eq}	
36-C1	0.0003	0.0138	yco1 = 7.9284 – j 1.8026 p.u
			yo1,36 = 7.0111 – j 1.4230 p.u

Table 3.12: Parameters of equivalent network of EA2

Lines			Admittances to ground
ID	R_{eq}	X_{eq}	
36-C2	0.0042	0.2834	yco2 = 0.2191-j0.2065 p.u
14-C2	0.0014	0.1160	yo2,36 = 2.6095-j1.0035 p.u
16-C2	0.0002	0.0158	yo,14 = 6.0711-j2.1633 p.u
36-14	0.0034	0.0634	yo,16 = 0.2396-j0.3017 p.u
36-16	0.0170	0.1701	
14-16	0.0068	0.0697	

3.4 DYNAMIC AGGREGATION OF COHERENT GENERATORS (STAGE III)

Dynamic aggregation of coherent generators is the third and final stage in the process of constructing power system electromechanical equivalence for use in transient stability and dynamic security studies. In this stage, the equivalent synchronous machine parameters and aggregate rotor dynamics of each coherent group will be determined. The classical synchronous machine model is assumed to represent each generator in a coherent group. The justifications of using the classical machine model are:

(i) The basic purpose of electromechanical equivalent is to reflect the approximate dynamic effect of external systems to disturbances in the study area.

(ii) The model is simple and does not require large computer memory and it is widely used in the analysis of multi-machines dynamics.

(iii)   An equivalent synchronous machine with much detailed representation may improve the accuracy of the equivalent, but this would defeat the purpose of the equivalency since it would lose simplicity with a doubtful gain in accuracy in estimating the transient stability of power systems.

(iv)   The accurate data of detailed synchronous machines and its control in large-scale power systems is very difficult to obtain. In addition, assuming values for these parameters is meaningless.

The proposed dynamic aggregation technique consists of two steps: (i) equivalent *rotor dynamics*, and (ii) *equivalent synchronous machine*.

3.4.1 EQUIVALENT ROTOR DYNAMICS

Since all generators in a coherent group are assumed to have identical angle and speed deviations with adequate tolerance, their acceleration equations may be added, resulting in the following equivalent equation for m coherent generators in a coherent group

$$(\sum_{i=1}^{m} M_i) \frac{\partial^2 \delta_i}{\partial t^2} = \sum_{i=1}^{m} P_{mi} - \sum_{i=1}^{m} P_{gi} - (\sum_{i=1}^{m} D_i) \omega_i \quad (3.40)$$

Based on equation (3.40), the equivalent p.u inertia constant, p.u damping, p.u mechanical input and p.u electrical power output, with all parameters calculated on the same basis, are

$$M_{eq} = \sum_{i=1}^{m} M_i \quad (3.41)$$

$$D_{eq} = \sum_{i=1}^{m} D_i \quad (3.42)$$

$$P_{meq} = \sum_{i=1}^{m} P_{mi} \quad (3.43)$$

$$P_{geq} = \sum_{i=1}^{m} P_{gi} \quad (3.44)$$

3.4.2 EQUIVALENT SYNCHRONOUS MACHINE

As discussed above, representing the equivalent generator by a classical model would be adequate for power system equivalency theory. The equivalent transient impedance of the equivalent synchronous machine is calculated by

$$1/(r_{eq} + jX'_{deq}) = 1/\sum_{i=1}^{m}(r_i + jX'_{di}) \quad (3.45)$$

An equivalent machine model can be simply modelled and simulated in any transient stability program with machine parameters defined by equations (3.41), (3.42), and (3.45). The common bus of a coherent group of generators is represented as PV-bus with power defined in (3.44) and bus voltage is defined in (3.39).

3.4.3 EVALUATION OF THE PRESENTED EQUIVALENCY–CASE STUDY 3

The parameters of the equivalent synchronous generators of coherent group1 and coherent group2 in the NPCC system shown in Fig. 3.26 are calculated using the

presented dynamic aggregation technique. The values of these parameters are shown in Table 3.13.

Table 3.13: Parameters of equivalent generators of group 1 and group 2

Parameters (p.u)	Equivalent of group 1	Equivalent of group 2
M_{eq} (sec)	115.8	66.1
D_{eq}	0.0	0.0
r_{eq}	0.0	0.0
X_{deq}	0.0127	0.0292
P_{geq}	23.5	12.0202
V_c	1.0306	0.9826

(All values on 100 MVA base)

Comparison between the dynamic response of the detailed NPCC system and its equivalent system is performed. The considered disturbance is a three-phase fault at bus 2 cleared after 3 cycles by removing line 2-19, which is the disturbance used in coherency identification, is simulated with all generators represented by their nonlinear classical model. A transient stability program is used for this purpose. The relative swing curves of generators in the study area of the original detailed system in comparison with its equivalent are shown in Fig. 3.27. Also the response of each group of coherent generators and their equivalent is shown in Fig. 3.28 and Fig 3.29 for group 1 and group 2 respectively. The comparison shows excellent agreement between each group and their equivalent. In addition, it is clear that the equivalent system response matches well with the original system response which proves the accuracy of the presented coherency-based electromechanical equivalence.

For the assurance of the validity of the presented equivalency technique, other disturbances are considered. Comparison between the dynamic response of the detailed NPCC system and its equivalent for fault at bus 29 cleared after 3 cycles by removing line 28-29 is performed with all generators represented by their nonlinear classical model. Fig. 3.30 shows the excellent agreement between the swing curves of generators in the study area of the original system and its equivalence. The response of each group of coherent generators and their equivalent is shown in Fig. 3.31 and Fig 3.32 for group 1 and group 2 respectively. The comparison shows excellent agreement between each group and their equivalent. It is clear that the equivalent system response matches well the original system response.
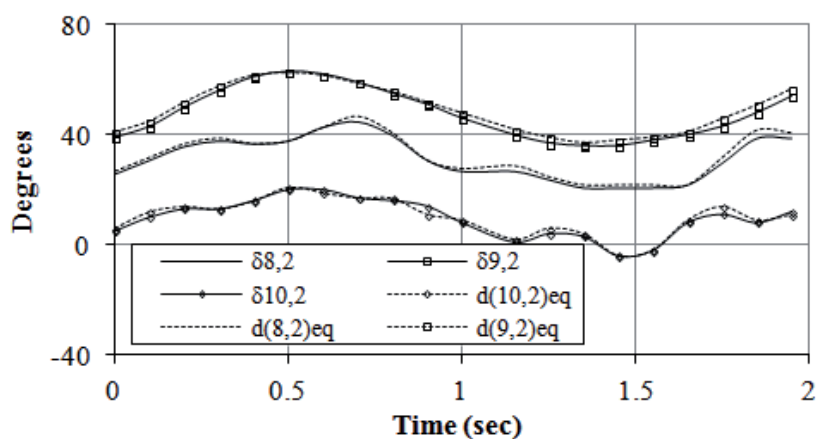
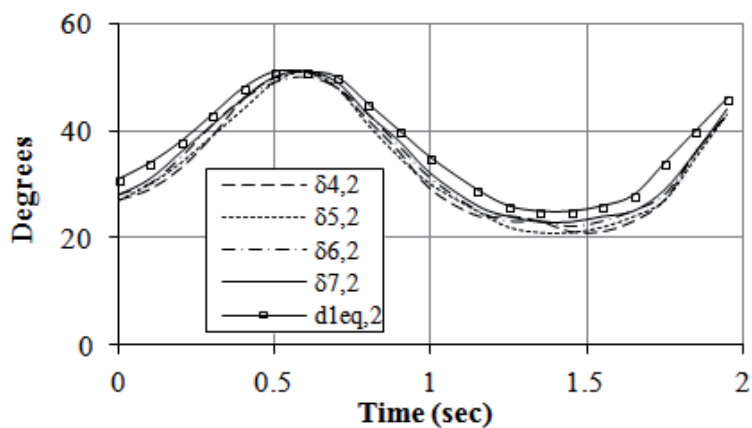Fig. 3.27: Comparison of swing curves in SA - fault at bus 2

Fig. 3.28: Swing curves of generators in group 1 and its equivalent generator - fault at bus 2
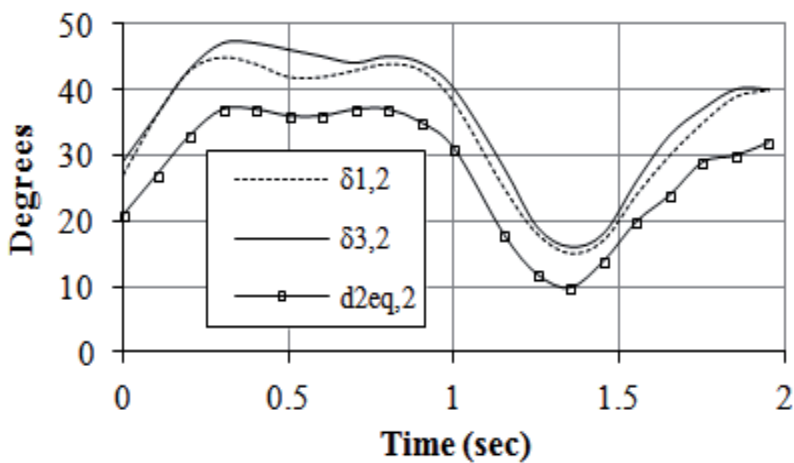
Fig. 3.29: Swing curves of generators in group 2 and its equivalent generator - fault at bus 2
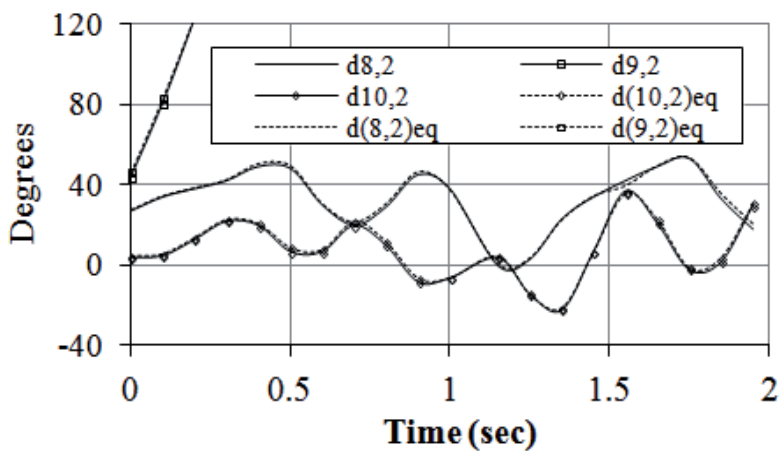
Fig. 3.30: Comparison of swing curves in SA - fault at bus 29

66
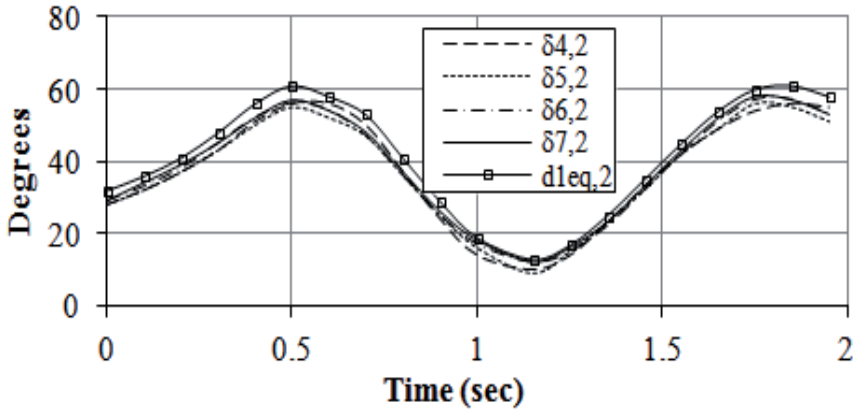
Fig. 3.31: Swing of generators in group 1 and its equivalent - fault at bus 29
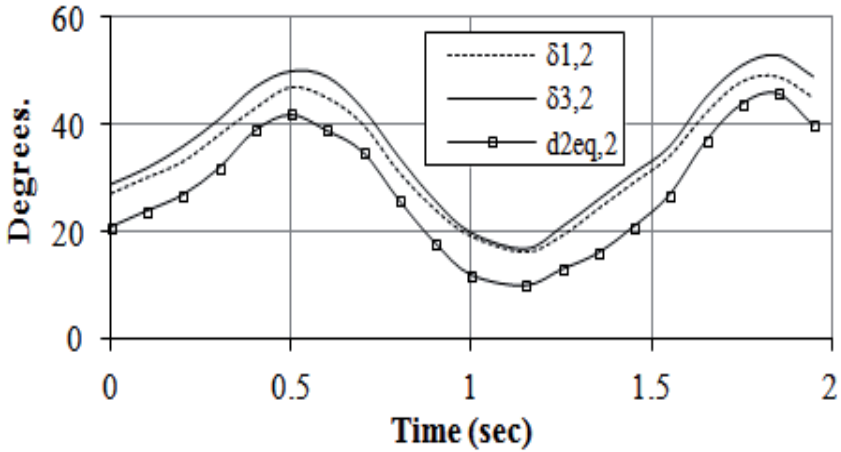
Fig. 3.31: Swing of generators in group 2 and its equivalent - fault at bus 29

3.5 COHERENCY-BASED ELECTROMECHANICAL EQUIVALENCE – CASE STUDY 4

In this case study, larger system in comparison with the NPCC system is considered. The objective is to show the superior capability of the coherency-based electromechanical equivalence is dynamic model reduction of large-scale power systems. In addition, this study provides more validation of the presented technique. The considered system is the 16 generator – 68 bus system of the GE report entitled 'Singular Perturbations, Coherency, and Aggregation of Dynamic Systems' [105]. The system data and load flow results are listed in Tables 3.14 to 3.16 while one-line

diagram of the system is shown in Fig. 3.32. The figure also shows the study area which contains three generators; G1, G8, and G9.

Table 3.14: Machine data of the 16 gen. – 68 bus system (on 100 MVA base)

Gen#	R_a	X_d	$X_d{'}$	$T_{do}{'}$	X_q	$X_q{'}$	$T_{qo}{'}$	H	D
1	0.0	0.1000	0.0310	10.20	0.069	0.0310	1.50	42.0	4.00
2	0.0	0.2950	0.0697	6.56	0.282	0.0697	1.50	30.2	9.75
3	0.0	0.2495	0.0531	5.70	0.237	0.0531	1.50	35.8	10.00
4	0.0	0.2620	0.0436	5.69	0.258	0.0436	1.50	28.6	10.00
5	0.0	0.3300	0.0660	5.40	0.310	0.0660	0.44	26.0	3.00
6	0.0	0.2540	0.0500	7.30	0.241	0.0500	0.40	34.8	10.00
7	0.0	0.2950	0.0490	5.66	0.292	0.0490	1.50	26.4	8.00
8	0.0	0.2900	0.0570	6.70	0.280	0.0570	0.41	24.3	9.00
9	0.0	0.2106	0.0570	4.79	0.205	0.0570	1.96	34.5	14.00
10	0.0	0.1690	0.0457	9.37	0.115	0.0000	0.00	31.0	5.56
11	0.0	0.1280	0.0180	4.10	0.123	0.0000	0.00	28.2	13.60
12	0.0	0.1010	0.0310	7.40	0.095	0.0000	0.00	92.3	13.50
13	0.0	0.0296	0.0055	2.90	0.286	0.0000	0.00	248.0	33.00
14	0.0	0.0180	0.0029	4.1	0.017	0.0000	0.00	300.0	100.00
15	0.0	0.0180	0.0029	4.1	0.017	0.0000	0.00	300.0	100.0
16	0.0	0.0356	0.0071	7.8	0.033	0.0000	0.00	225.0	50.0

Table 3.15: Line and transformer data of the 16 gen. – 68 bus system (on 100 MVA base)

Bus #		R	X	B	Tap
From	To				
1	2	0.0035	0.0411	0.0699	0.0
1	30	0.0008	0.0074	0.4800	0.0
2	3	0.0013	0.0151	0.2572	0.0
2	25	0.0070	0.0086	0.1460	0.0
2	53	0.0000	0.0181	0.0000	1.025
3	4	0.0013	0.0213	0.2214	0.0
3	18	0.0011	0.0133	0.2138	0.0
4	5	0.0008	0.0128	0.1342	0.0
4	14	0.0008	0.0129	0.1382	0.0
5	6	0.0002	0.0026	0.0434	0.0
5	8	0.0008	0.0112	0.1476	0.0
6	7	0.0006	0.0092	0.1130	0.0
6	11	0.0007	0.0082	0.1389	0.0
6	54	0.0000	0.0250	0.0000	1.070
7	8	0.0004	0.0046	0.0780	0.0
8	9	0.0023	0.0363	0.3804	0.0
9	30	0.0019	0.0183	0.2900	0.0
10	11	0.0004	0.0043	0.0729	0.0
10	13	0.0004	0.0043	0.0729	0.0
10	55	0.0000	0.0200	0.0000	1.070
12	11	0.0016	0.0435	0.0000	1.060
12	13	0.0016	0.0435	0.0000	1.060

13	14	0.0009	0.0101	0.1723	0.0
14	15	0.0018	0.0217	0.3660	0.0
15	16	0.0009	0.0094	0.1710	0.0
16	17	0.0007	0.0089	0.1342	0.0
16	19	0.0016	0.0195	0.3040	0.0
16	21	0.0008	0.0135	0.2548	0.0
16	24	0.0003	0.0059	0.0680	0.0
17	18	0.0007	0.0082	0.1319	0.0
17	27	0.0013	0.0173	0.3216	0.0
19	20	0.0007	0.0138	0.0000	1.06
19	56	0.0007	0.0142	0.0000	1.07
20	57	0.0009	0.0180	0.0000	1.009
21	22	0.0008	0.0140	0.2565	0.0
22	23	0.0006	0.0096	0.1846	0.0
22	28	0.0000	0.0143	0.0000	1.025
23	24	0.0022	0.0350	0.3610	0.0
23	59	0.0005	0.0272	0.0000	0.0
25	26	0.0032	0.0323	0.5310	0.0
25	60	0.0006	0.0232	0.0000	1.025
26	27	0.0014	0.0147	0.2396	0.0
26	28	0.0043	0.0474	0.7802	0.0
26	29	0.0057	0.0625	1.0290	0.0
28	29	0.0014	0.0151	0.2490	0.0
29	61	0.0008	0.0156	0.0000	1.025
9	36	0.0022	0.0196	0.3400	0.0
36	37	0.0005	0.0045	0.3200	0.0
34	36	0.0033	0.0111	1.4500	0.0
35	34	0.0001	0.0074	0.0000	0.946
33	34	0.0011	0.0157	0.2020	0.0
32	33	0.0008	0.0099	0.1680	0.0
30	31	0.0013	0.0187	0.3330	0.0
30	32	0.0024	0.0288	0.4880	0.0
1	31	0.0016	0.0163	0.2500	0.0
31	38	0.0011	0.0147	0.2470	0.0
33	38	0.0036	0.0444	0.6930	0.0
38	46	0.0022	0.0284	0.4300	0.0
46	49	0.0018	0.0274	0.2700	0.0
1	47	0.0013	0.0188	1.3100	0.0
47	48	0.0025	0.0268	0.4000	0.0
48	40	0.0020	0.0220	1.2800	0.0
35	45	0.0007	0.0175	0.3900	0.0
37	43	0.0005	0.0276	0.0000	0.0
43	44	0.0001	0.0011	0.0000	0.0

39	45	0.0000	0.0839	0.0000	0.0
45	51	0.0004	0.0105	0.7200	0.0
50	52	0.0012	0.0288	2.0600	0.0
50	51	0.0009	0.0221	1.6200	0.0
49	52	0.0076	0.1141	1.1600	0.0
52	42	0.0040	0.0600	2.2500	0.0
42	41	0.0040	0.0600	2.2500	0.0
41	40	0.0060	0.0840	3.1500	0.0
31	62	0.0000	0.0260	0.0000	1.04
32	63	0.0000	0.0130	0.0000	1.04
36	64	0.0000	0.0075	0.0000	1.04
37	65	0.0000	0.0033	0.0000	1.04
41	66	0.0000	0.0015	0.0000	1.00
42	67	0.0000	0.0015	0.0000	1.00
52	68	0.0000	0.0030	0.0000	1.00
1	27	0.032	0.32	0.41	0.0

Table 3.16: Load flow data of the 16 gen. – 68 bus system (on 100 MVA base)

Bus #	V	θ	P_G	Q_G	P_L	Q_L
1	1.0113	11.3748	0.0	0.0	2.5270	1.1856
2	1.0145	12.7902	0.0	0.0	0.0000	0.0000
3	0.9867	9.4023	0.0	0.0	3.2200	0.0200
4	0.9485	7.9774	0.0	0.0	5.0000	1.8400
5	0.9453	8.9247	0.0	0.0	0.0000	0.0000
6	0.9469	9.6960	0.0	0.0	0.0000	0.0000
7	0.9361	7.0566	0.0	0.0	2.3400	0.8400
8	0.9355	6.4103	0.0	0.0	5.2200	1.7700
9	0.9769	5.2973	0.0	0.0	1.0400	1.2500
10	0.9567	12.6041	0.0	0.0	0.0000	0.0000
11	0.9521	11.6162	0.0	0.0	0.0000	0.0000
12	0.9329	11.6566	0.0	0.0	0.0900	0.8800
13	0.9550	11.8581	0.0	0.0	0.0000	0.0000
14	0.9557	10.1395	0.0	0.0	0.0000	0.0000
15	0.9660	10.0850	0.0	0.0	3.2000	1.5300
16	0.9864	11.7987	0.0	0.0	3.2900	0.3200
17	0.9907	10.6343	0.0	0.0	0.0000	0.0000
18	0.9877	9.6989	0.0	0.0	1.5800	0.3000
19	0.9888	16.9840	0.0	0.0	0.0000	0.0000
20	0.9856	15.5510	0.0	0.0	6.8000	1.0300
21	0.9934	14.6299	0.0	0.0	2.7400	1.1500
22	1.0205	19.6010	0.0	0.0	0.0000	0.0000
23	1.0190	19.2783	0.0	0.0	2.4800	0.8500
24	0.9946	11.9821	0.0	0.0	3.0900	0.9200
25	1.0251	14.0365	0.0	0.0	2.2400	0.4700

Table 3.16: Load flow data (Cont.)

| Bus #	V	θ	P_G	Q_G	P_L	Q_L
26	1.0176	12.4118	0.0	0.0	1.3900	0.1700
27	1.0009	10.3774	0.0	0.0	2.8100	0.7600
28	1.0188	15.7431	0.0	0.0	2.0600	0.2800
29	1.0201	18.5368	0.0	0.0	2.8400	0.2700
30	1.0056	11.0560	0.0	0.0	0.0000	0.0000
31	1.0115	13.4427	0.0	0.0	0.0000	0.0000
32	1.0044	15.0366	0.0	0.0	0.0000	0.0000
33	1.0060	10.7555	0.0	0.0	1.1200	0.0000
34	1.0125	4.2345	0.0	0.0	0.0000	0.0000
35	1.0139	4.2554	0.0	0.0	0.0000	0.0000
36	0.9955	-0.4534	0.0	0.0	1.0200	-0.1946
37	0.9866	-6.8574	0.0	0.0	60.0000	3.0000
38	1.0108	13.0539	0.0	0.0	0.0000	0.0000
39	0.9782	-7.7357	0.0	0.0	2.6700	0.1260
40	1.0299	21.7878	0.0	0.0	0.6563	0.2353
41	0.9989	50.5653	0.0	0.0	10.0000	2.5000
42	0.9990	43.9908	0.0	0.0	11.5000	2.5000
43	0.9816	-7.1802	0.0	0.0	0.0000	0.0000
44	0.9814	-7.1923	0.0	0.0	2.6755	0.0484
45	1.0048	4.3284	0.0	0.0	2.0800	0.2100
46	0.9935	13.8655	0.0	0.0	1.5070	0.2850
47	1.0219	11.9268	0.0	0.0	2.0312	0.3259
48	1.0298	15.7245	0.0	0.0	2.4120	0.0220
49	0.9794	17.1011	0.0	0.0	1.6400	0.2900
50	0.9982	22.3745	0.0	0.0	1.0000	-1.4700
51	1.0075	8.6758	0.0	0.0	3.3700	-1.2200
52	0.9911	42.6675	0.0	0.0	24.7000	1.2300
53	1.0450	15.2365	2.5000	1.8143	0.0	0.0
54	0.9800	18.1387	5.4500	1.6983	0.0	0.0
55	0.9830	20.5494	6.5000	1.7421	0.0	0.0
56	0.9970	22.1845	6.3200	0.5475	0.0	0.0
57	1.0110	20.7144	5.0520	1.3970	0.0	0.0
58	1.0500	24.9613	7.0000	2.4948	0.0	0.0
59	1.0630	27.3086	5.6000	2.0083	0.0	0.0
60	1.0300	20.8380	5.4000	0.3999	0.0	0.0
61	1.0250	25.3746	8.0000	0.3888	0.0	0.0
62	1.0100	20.7536	5.0000	0.2625	0.0	0.0
63	1.0000	22.4735	10.0000	0.3137	0.0	0.0
64	1.0156	5.2943	13.5000	3.4035	0.0	0.0
65	1.0110	0.0000	36.0904	9.6285	0.0	0.0
66	1.0000	52.1013	17.8500	0.9853	0.0	0.0
67	1.0000	44.8511	10.0000	0.7527	0.0	0.0
68	1.0000	49.6220	40.0000	5.4071	0.0	0.0
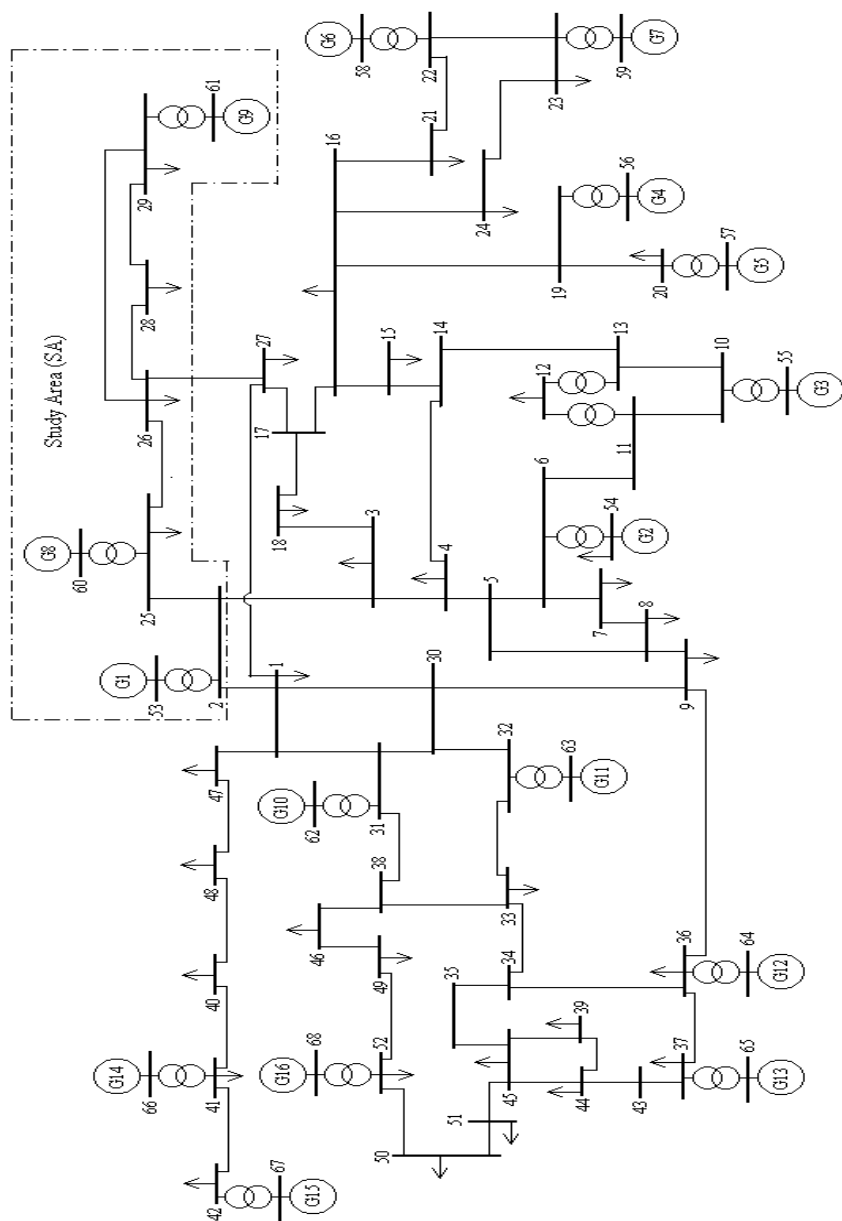
Fig. 3.32: The 16 generator – 68 bus system

For coherency grouping of generators outside the study area, a three-phase fault is applied at bus 29 and cleared after 3 cycles by removing line 28-29. The simulation is performed using the proposed linearized system model. The linearized response of the system is shown in Fig. 3.33. A minimum correlation factor of 0.999 is chosen for coherency identification. Therefore, high quality grouping is expected. Based on correlation factor analysis, three groups of coherent generators are identified.

(i) Group 1: G2, G3, G4, G5, G6, and G7,
(ii) Group 2: G10, G11, G12, and G13, and
(iii)   Group 3: G14 and G15.

The linearized response of each coherent group of generators is shown in Figs. 3.34 to 3.36 respectively. It is found that G16 in the external system is not coherent with any of these groups, hence it will be considered separately.
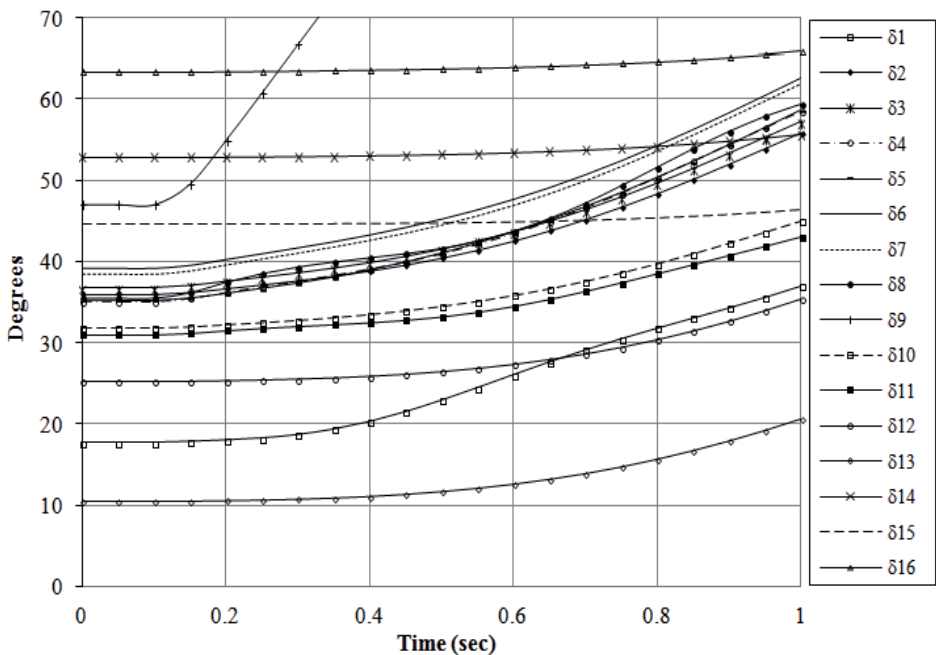
Fig. 3.33: The linearized absolute angle response of the 16 gen. – 68 bus system
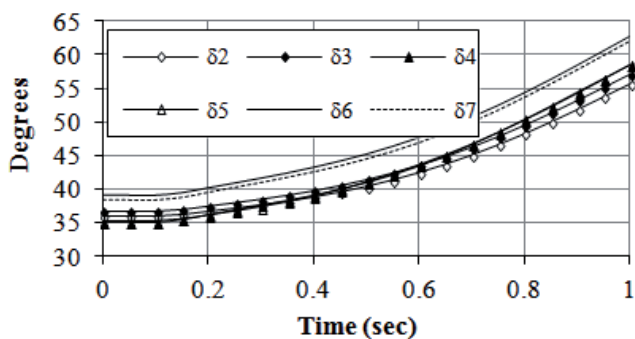
Fig. 3.34: Linearized response of the first coherent group
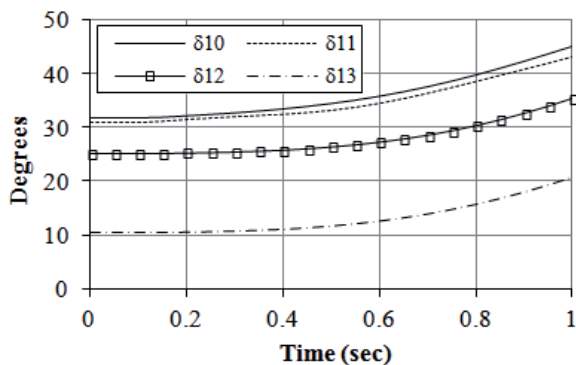
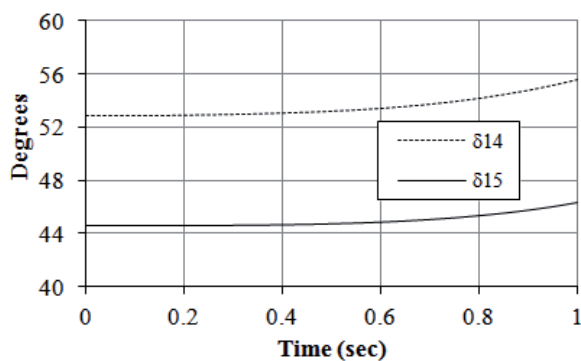Fig. 3.35: Linearized response of the second coherent group

Fig. 3.36: Linearized response of the third coherent group

Based on the coherency grouping, the external subsystem of the 16-generator system is divided into three external areas, namely EA1, EA2, and EA3 that include the three coherent groups of generators. In addition, G16 is considered as a separate external generator. This is shown in Fig. 3.37.

The presented network reduction and dynamic aggregation techniques are applied to each proposed external area in the 16-generator system. The parameters of the equivalent lines, equivalent admittances to the ground, and parameters of the equivalent synchronous machine for each coherent group of generators are shown in Tables 3.17, 3.18, and 3.19 for EA1, EA2, and EA3 respectively. All values are in p.u on 100 MVA base. Fig. 3.38 shows the proposed equivalent of the 16-generator system.

Table 3.17: Parameters of the equivalent of EA1 in the 16-generator system

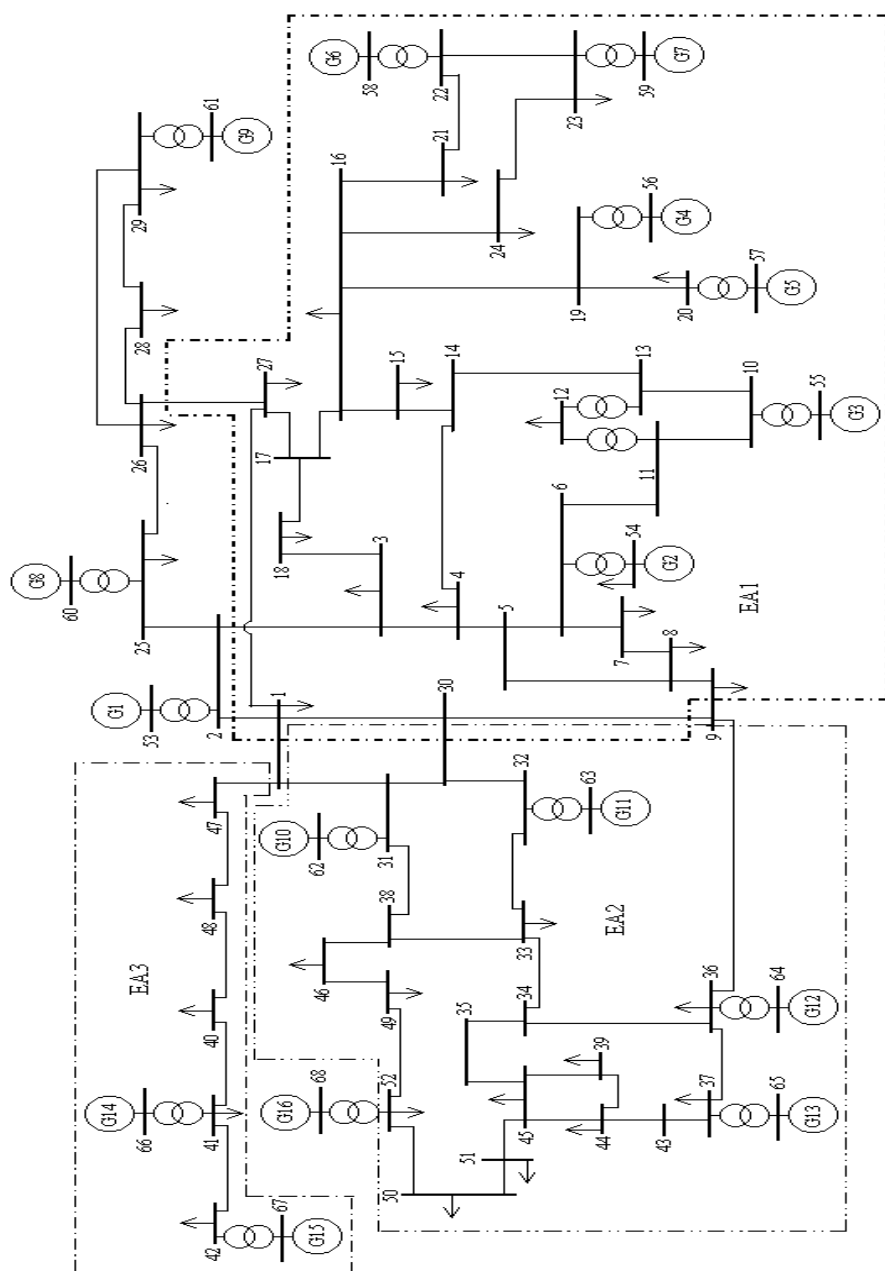| Equivalent synchronous machine (p.u)	Equivalent lines $R + j\,X$ (p.u)	Equivalent admittance to ground (p.u)
M_{eq} = 181.800 sec	C1-1 : 0.1439+j1.5637	yo1 = 2.6977-j0.4028
D_{eq} = 45.750	C1-2 : 0.0056+j0.0519	yo2 = 6.5269-j0.8628
r_{eq} = 0.0	C1-26: 0.0069+j0.0718	yo26 = 4.9354-j0.7291
X'_d = 0.009	C1-30: ∞	yo30 = 0.0+j0.3850
P_g = 35.9220	C1-9 : 0.0066+j0.0697	yo9 = 4.7660-j2.3877
V_c = 1.0140	1-2 : 0.0034+j0.0406	yoC1 = 26.2091-j7.5989
	1-26 : 0.0358+j0.4971	
	1-30 : 0.0008+j0.0074	
	1-9 : 3.6931+j26.6302	
	2-26 : 0.0034+j0.1571	
	2-30 : ∞	
	2-9 : 0.0342+j0.3547	
	26-30 : ∞	
	26-9 : 0.1753+j1.2219	
	30-9 : 0.0019+j0.0183	

Fig. 3.37: Coherent groups and external areas of the 16 gen. – 68 bus system

Table 3.18: Parameters of the equivalent of EA2 in the 16-generator system

Equivalent synchronous machine (p.u)	Equivalent lines $R + j\,X$ (p.u)	Equivalent admittance to ground (p.u)
M_{eq} = 399.5 sec D_{eq} = 65.66 r_{eq} = 0.0 X'_d = 0.0034 P_g = 64.5904 V_c = 1.0092	C2-1 : 0.0017+j0.0588 C2-52: 0.0443+j0.0948 C2-30: 0.0007+j0.0269 2 : 0.0178+j0.6108 0 : 0.0047+j0.0480 1-9 : ∞ 30-52: 0.0262+0.5371 52-9 : 0.6534+j1.6365 30-9 : ∞	yo1 = 0.7646+j0.5720 yo52 = 34.6369+j3.5207 yo30 = 1.1149+j1.1065 yo9 = 7.7142- j0.0368 yoC2= 62.9618- j11.3162

Table 3.19: Parameters of the equivalent of EA3 in the 16-generator system

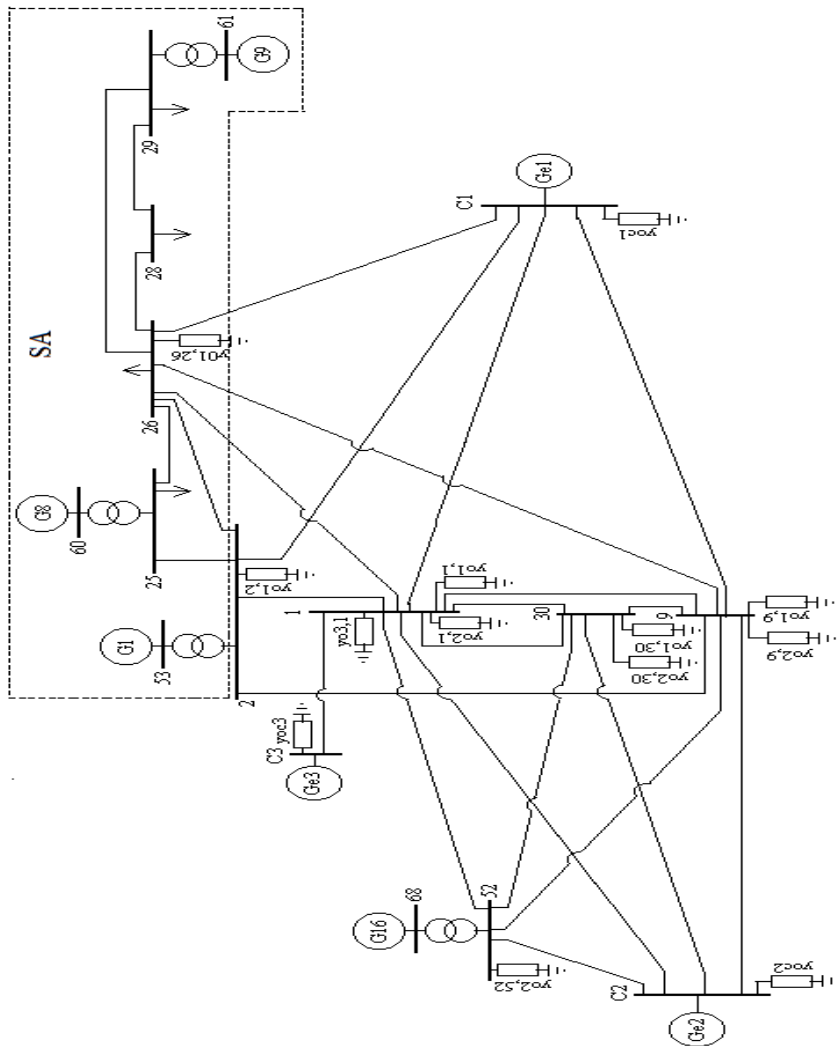| Equivalent synchronous machine (p.u)	Equivalent lines $R + j\,X$ (p.u)	Equivalent admittance to ground (p.u)
M_{eq} = 600 sec D_{eq} = 200 r_{eq} = 0.0 X'_d = 0.0014 P_g = 27.850 V_c = 1.00	C3-1: 0.0116+j0.1387	yo1 = 4.1972+j2.5684 yoC3 =22.8519- j0.4318

Fig. 3.38: Equivalence of the 16 gen. – 68 bus system

The validity of the determined equivalence is evaluated by comparing the dynamic response of the detailed system and its equivalent. A three-phase fault at bus 29 cleared after 3 cycles by removing line 28-29 is preformed for that purpose. All generators represented by their nonlinear classical model in a transient stability program. Fig. 3.39 shows the nonlinear response of all generators in the detailed 16-generator system. The correlation factor analysis confirms the coherency grouping as

obtained from by the linearized response. Fig. 3.40 shows a comparison between swing curves of retained generators considering the detailed system and its equivalent. In addition, the responses of each group of coherent generators and their equivalent are shown in Fig. 3.41, 3.42, and 3.43 for group 1, 2 and 3 respectively. The comparison shows excellent agreement between each group and their equivalent and it is clear that the equivalent system response matches well the original detailed system response.
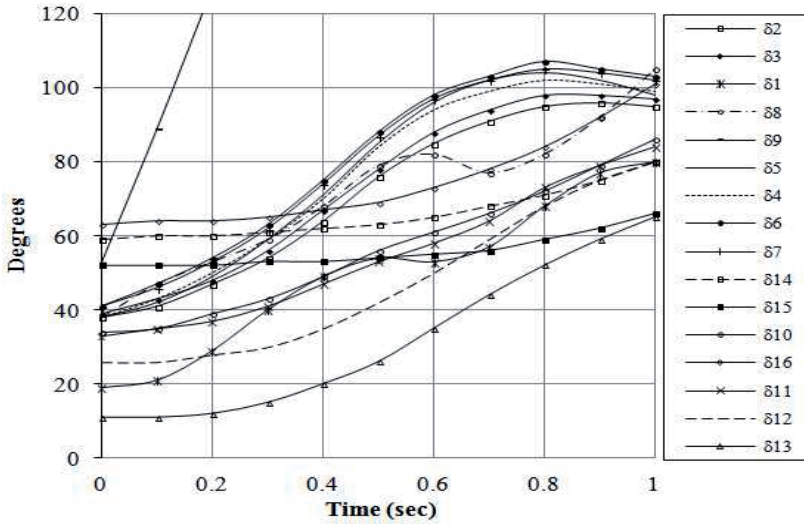

Fig. 3.39: Nonlinear response of the 16 gen. – 68 bus system for a fault at bus 29
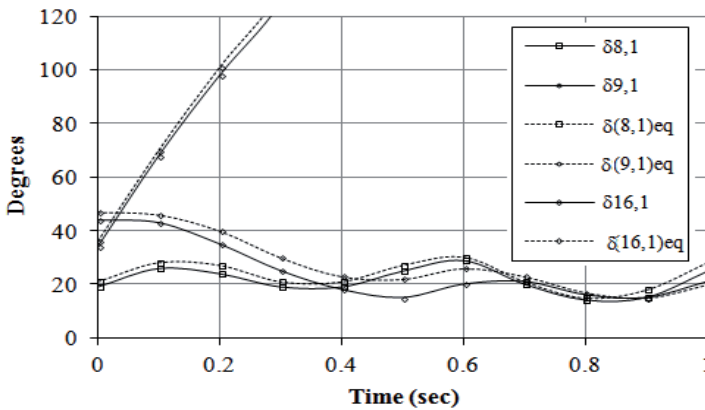
Fig. 3.40: Comparison between swing of generators in detailed system that retained in the equivalent
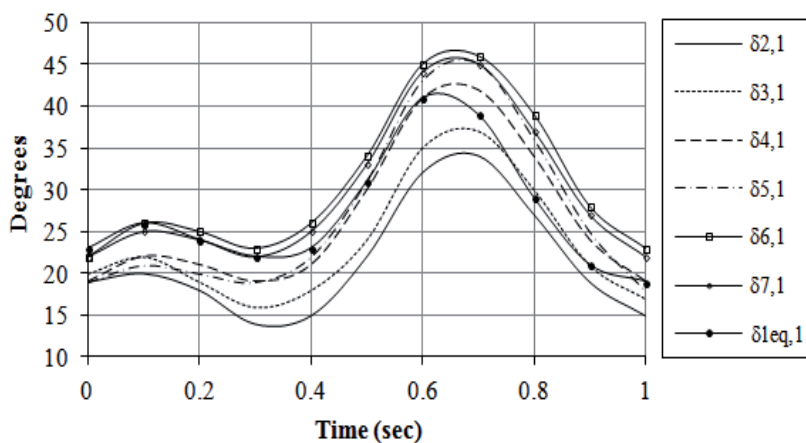
Fig. 3.41: Comparison of swing curves of group 1 and their equivalent
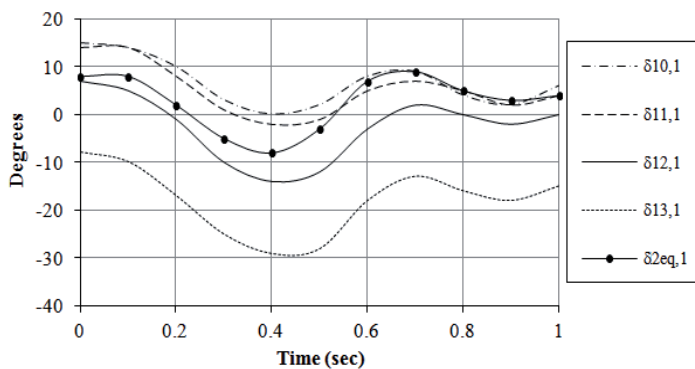

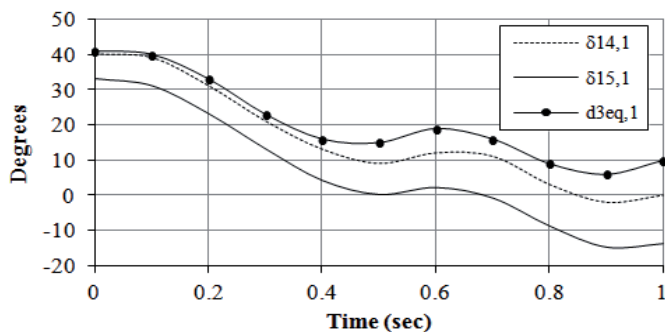Fig. 3.42: Comparison of swing curves of group 2 and their equivalent

Fig. 3.43: Comparison of swing curves of group 2 and their equivalent

82

3.6 THE CONCEPT OF REMOTE AREAS AND THEIR EQUIVALENCY TREATMENT

It is found in constructing the electrodynamic equivalent of the 16-generator system in the previous section that generator G16 in the external subsystem is not coherent with any group of external generators. This situation leads to the idea remote areas (RA) that may exist in large-scale power systems.

Generally, in constructing an electromechanical equivalent, a given power system is divided into two main parts: the study subsystem and external subsystem. According to the coherency grouping and the size of the external subsystem, this external subsystem can be subdivided into a set of external areas containing coherent groups of generators and a set of remote area that are connected to the external areas. This is illustrated in Fig. 3.44 for one external area and one remote area. It is assumed here that the generators comprising the remote areas are not necessary to be coherent. In addition, these generators are aggregated as one machine equivalence. These assumptions will be verified through a detailed case study.
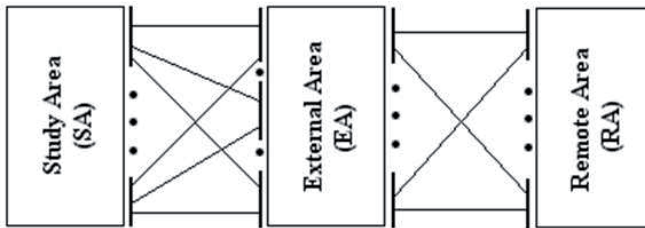

Fig. 3.44: Relation between various areas in a large-scale power system

4.6.1 TREATMENT OF REMOTE AREAS

An equivalent to RA is assumed to be determined by the same way as described in sections 3.4 and 3.6; however, the necessity of coherency of generators comprising an RA is excluded for producing the simplest possible electromechanical equivalence of generators in such areas. This is can be justified by considering the dynamics on the RA have minor impact on the SA. In addition, simulations will be used to evaluate these assumptions. According to the above assumption the application of the proposed electromechanical equivalent of power systems is extended to include very large systems with smaller computation time and cost.

4.6.2 VALIDATION OF EQUIVALENT OF RA IN LARGE-SCALE POWER SYSTEM – CASE STUDY 5

In this section the assumptions placed on the aggregation of RA generators are evaluated by linearized and non-linear simulations. The study system is constructed by integrating the IEEE WSCC 3 generator - 9 bus - system [104] and the GE 16-generator – 68 bus system [105] which is used in case study 4. The data of the nine-bus system and the operational settings are shown in Tables 3.20 to 3.22.

Table 3.20: Machine data of the WSCC system on 100 MVA base

Gen#	R_a	X_d	X_d'	T_{do}'	X_q	X_q'	T_{qo}'	H	D
17	0.0	0.2950	0.0697	6.56	0.2820	0.0697	1.50	24.0	8.0
19	0.0	0.8958	0.0198	6.00	0.8645	0.1969	0.54	6.0	2.0
18	0.0	0.3125	0.0813	5.89	0.2578	0.2500	0.60	3.0	1.0

Table 3.21: Line and transformer data of the WSCC system on 100 MVA base

Bus #		R	X	B	Tap
From	To				
52	75	0.0030	0.0300	1.4100	0.0
52	69	0.0300	0.3000	0.4100	0.0
69	70	0.0000	0.0057	0.0000	1.0
69	71	0.0100	0.0850	0.1760	0.0
69	77	0.0017	0.0092	0.1580	0.0
71	72	0.0032	0.0016	0.3060	0.0
72	73	0.0000	0.0062	0.0000	1.0
72	74	0.0008	0.0072	0.149	0.0
74	75	0.0011	0.0010	0.2090	0.0
75	76	0.0000	0.0058	0.0000	1.0
75	77	0.0039	0.0017	0.358	0.0

Table 3.22: Bus data of the WSCC system on 100 MVA base

Bus #	V	θ	P_G	Q_G	P_L	Q_L
69	-	-	0.000	-	0.00	0.00
70	1.040	-	0.716	-	0.00	0.00
71	-	-	0.000	-	1.25	0.50
72	-	-	0.000	-	0.00	0.00
73	1.025	-	1.630	-	0.00	0.00
74	-	-	0.000	-	1.00	1.35
75	-	-	0.000	-	0.00	0.00
76	1.025	-	0.850	-	0.00	0.00
77	-	-	0.000	-	0.90	0.30

- Values to be determined from the load flow study of the interconnected system

The WSCC system is considered to be connected to the GE 16-generator, 68-bus system of Fig. 3.32 at bus 52 as shown in Fig. 3.45. In this case, the WSCC generators and G16 are considered as a remote system with respect to the GE system excluding G16. This is because the two systems are *weakly interconnected* through the tie-lines 52-75 and 68-69. The connection of the WSCC system is made at bus 52 which is a bus contained in the external area of the NPCC system. Therefore, the selection of the WSCC generators and G16 to be considered as a remote area is clarified. Simulations will be used for evaluating these assumptions. The resulting power system has 19-generators and 77-buses. The linearized responses of the interconnected are shown in Fig. 3.46 for fault at bus 29 cleared after 3 cycles by removing line 28-29. The results and the correlation factor analysis show that the coherent grouping obtained in case study 4 remains unchanged as shown in Fig. 3.47 to 3.49. The response of generators in the RA is shown in Fig. 3.50 indicating that these generators are not coherent.
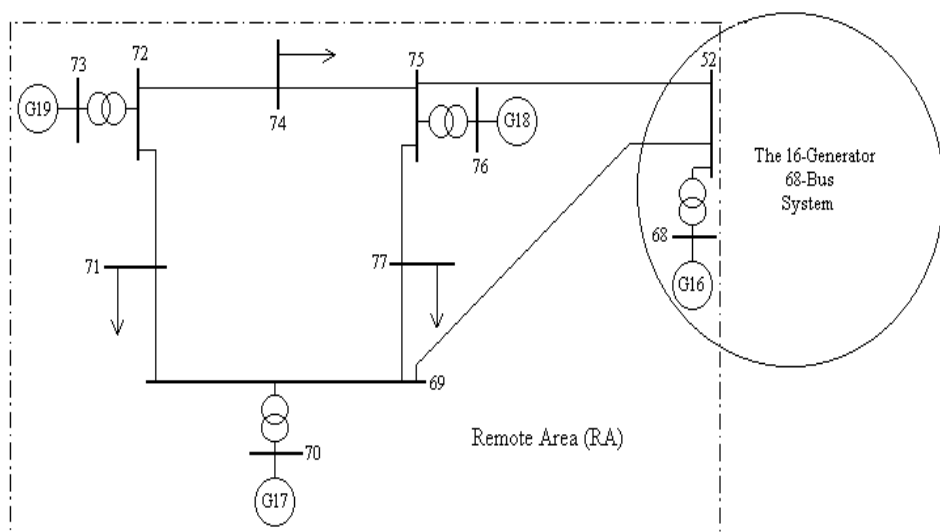
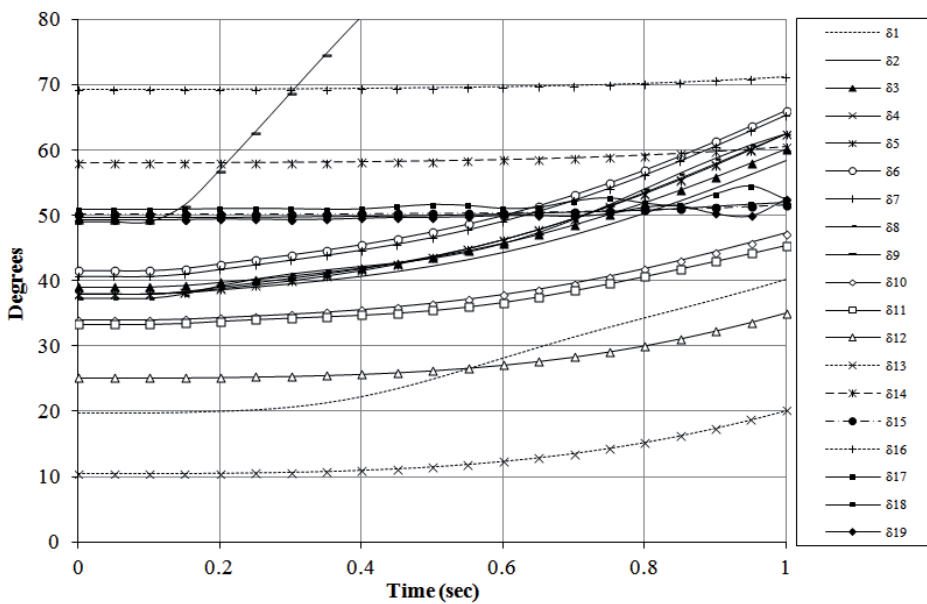Fig. 3.45: interconnecting the WSCC and the BPCC systems

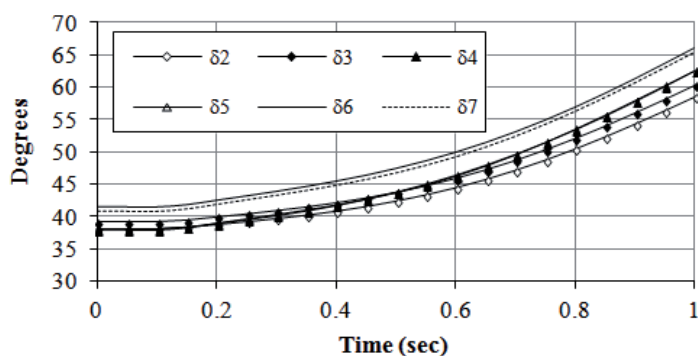Fig. 3.46: Linearized responses of the 19 generator system
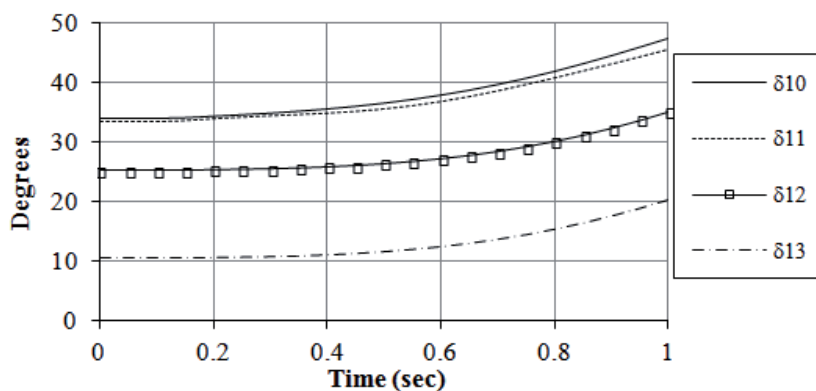
Fig. 3.47: Linearized response of group 1

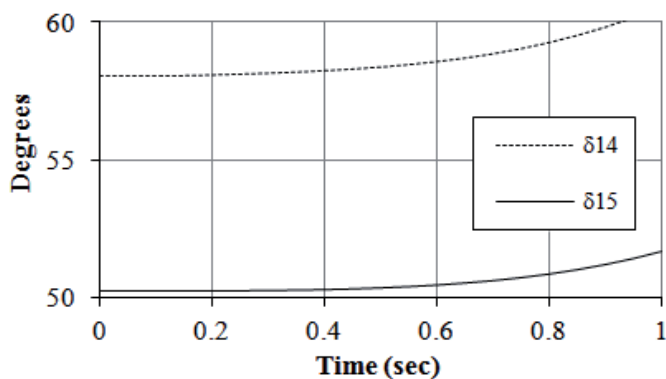Fig. 3.48: Linearized response of group 2

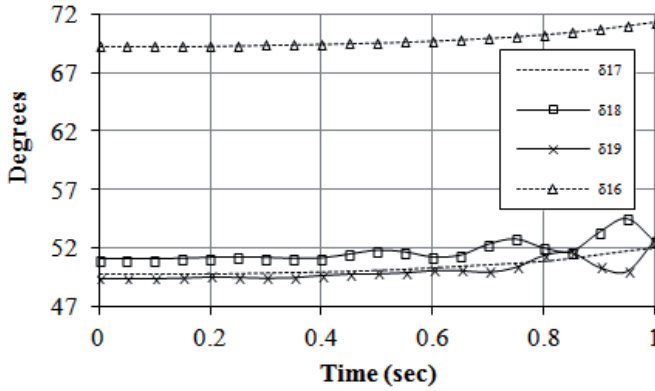Fig. 3.49: Linearized response of group 3

Fig. 3.50: Linearized response of RA generators

By applying the proposed network reduction and dynamic aggregation techniques, the parameters of the equivalent of the RA are shown in Fig. 3.51 and Table 3.23; all values are in p.u on 100 MVA base.
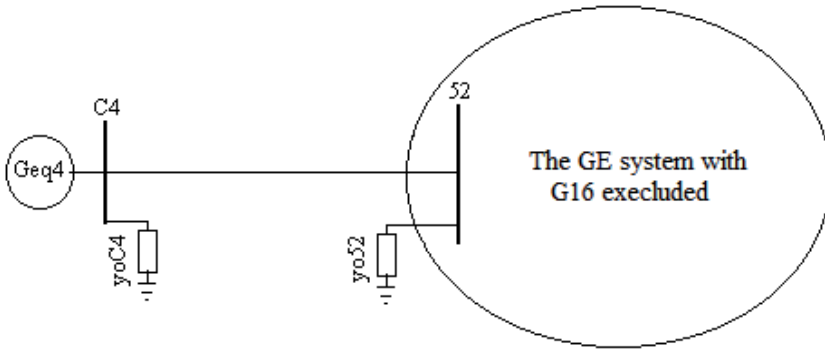

Fig. 3.51: Equivalence of the RA

Comparison between the dynamic response of the detailed system and its equivalent for fault at bus 29 cleared after 3 cycles by removing line 28-29 is simulated out with all generators represented by their nonlinear classical model. Fig. 3.52 shows the nonlinear response of all generators of the detailed 19-generator system confirming the coherency grouping. Fig. 3.53 shows a comparison between swing curves of generators in the SA for the detailed system and its equivalent. In addition, the response of each group of coherent generators and their equivalent is

shown in Fig. 3.54 to 3.56 for group 1, 2 and 3 respectively. The comparison shows excellent agreement between each group and their equivalent and it is clear that the equivalent system response matches well with the original system response. The response of generators in RA and their equivalent is shown in Fig. 3.57. It is expected that the response of the equivalent of RA generators will not match its detailed group, as they are not coherent; however, it is clear from the results that the introduction of the equivalent generator of RA generators does not hinder the accuracy of the electromechanical response of both the SA generators and the EA's generators.
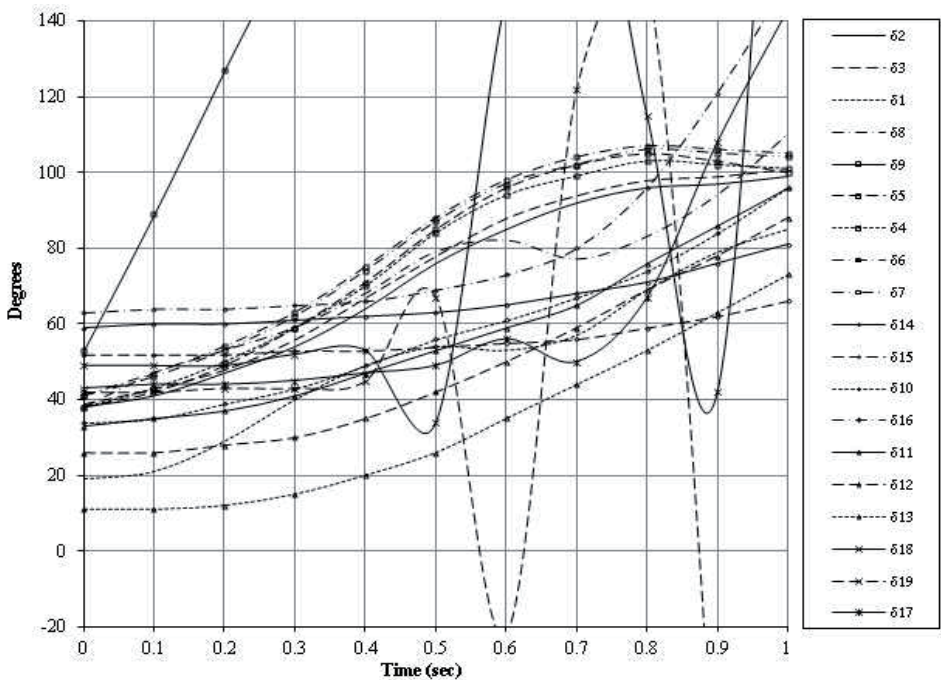

Fig. 3.52: Nonlinear response of the 19 generator system for a fault at bus 29

Table 3.23: Parameters of the equivalent of RA in the 19-generator system

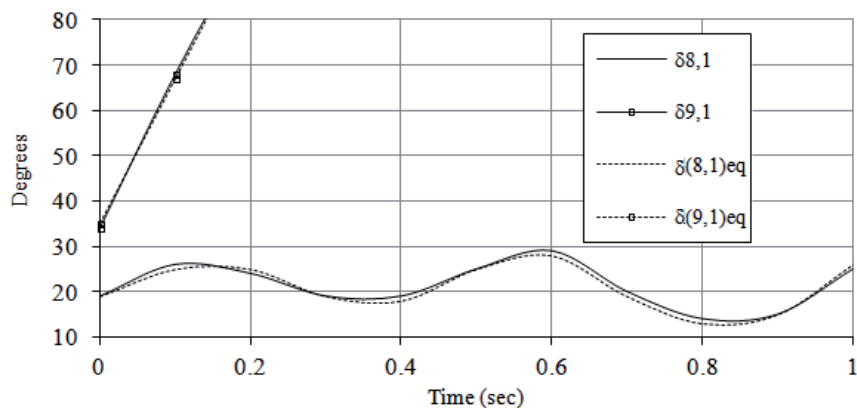| Equivalent synchronous machine (p.u)	Equivalent lines $R + j\,X$ (p.u)	Equivalent admittance to ground (p.u)
$M_{eq} = 258$ sec $D_{eq} = 61$ $r_{eq} = 0.0$ $X'_d = 0.0046$ $P_g = 43.196$ $V_{c4} = 1.015$	C4-52: 0.0034+j0.0282	yo52 = 25.409-j0.3524 yoC4 =2.8857+j1.3667

Fig. 3.53: Comparison of swing curves of the SA generators
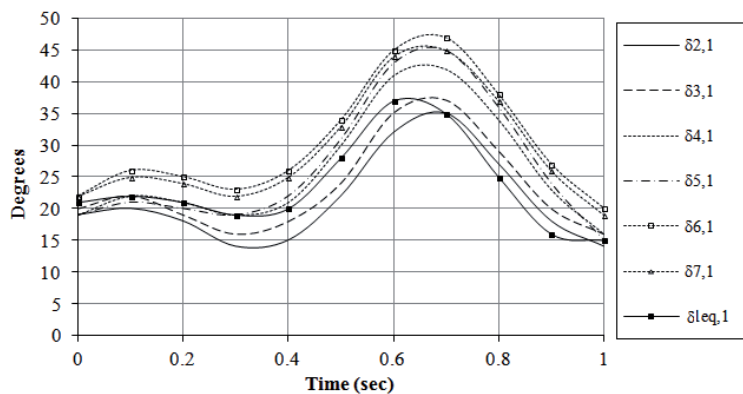

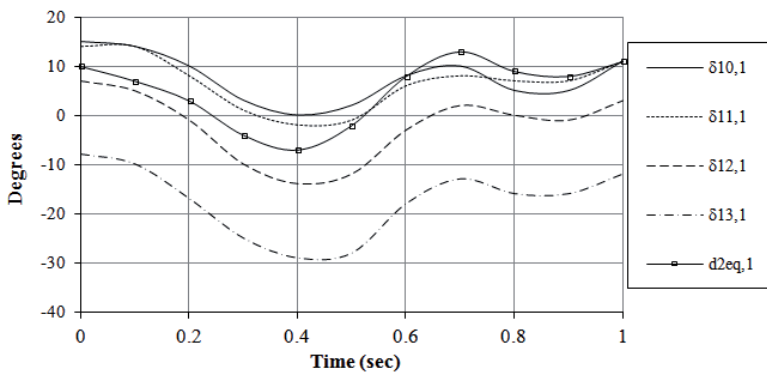Fig. 3.54: Comparison of swing curves of the EA1 generators

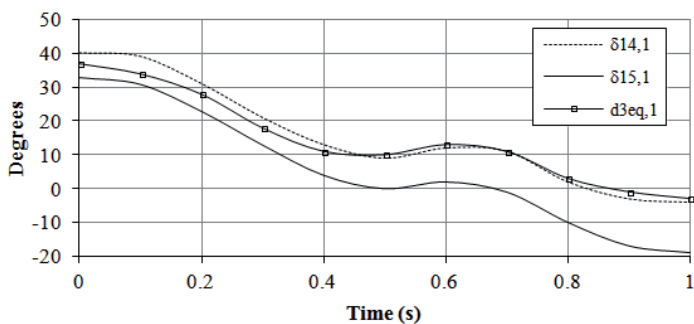Fig. 3.55: Comparison of swing curves of the EA2 generators

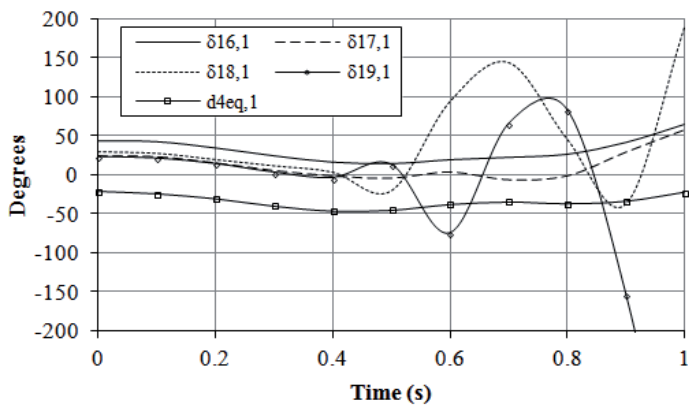Fig. 3.56: Comparison of swing curves of the EA3 generators

Fig. 3.57: Comparison of swing curves of the RA generators

3.7 RECENT AND FUTURE SECURITY REQUIREMENTS

This chapter describes the development and evaluation of accurate and simple techniques for coherency identification, network reduction, and dynamic aggregation of a coherent group of generators. In addition, the concept of remote areas is developed to enhance the contribution of the presented coherency-based electromechanical equivalent technique for simplifying the analysis of the transient stability of large-scale interconnected power systems. The evaluation is carried out by comparing the transient stability response of the detailed system and its equivalent for the power systems of different scales (up to 19-generator and 77-bus system). The comparison results show excellent agreements between the two responses. The sizes of the power systems under study after application of the proposed electromechanical reduction technique are greatly reduced as illustrated in Table 3.24.

Table 3.24: Power system size reduction by equivalent

Study system		NPCC	16 Gen - 68 Bus	19 Gen – 77 bus
Detailed System	No. of generators	10	16	19
	No. of buses	39	68	77
Reduced System	No. of generators	6	7	7
	No. of buses	23	15	16
	No. of SA generators*	4	3	3
	No. of SA buses*	21	11	11
	No. of EA's	2	3	3
	No. of generators in each EA	4, 2	6, 5, 2	6, 5, 2
	No. of RA's	-	1	1
	No. of generators in RA	-	1	4

* Common for detailed and reduced system.

Generally, the coherency-based electromechanical equivalence approach is accurate enough for significant model reduction of power systems. The reduced models are adequate for fast execution of dynamic security studies; however, its traditional form (such as that presented in this chapter) suffers from some drawbacks. These drawbacks are mainly associated, for example, with:

1) The *inherent uncertainties of the system parameters, actual topology, and operating conditions*. A situation that may reduce the harmony between the

actual system performance and the performance of the reduced models or even the performance of the detailed models. This is because the performance models are highly related to the accuracy of the input data for them. The data sets needed for executing a traditional coherency-based equivalence are mainly obtained from the data sets from the system databases.These data sets may suffer from inaccuracies, incomplete quantities, and deviations of the actual values with time, for example, due to aging of equipment. The actual topology of power systems is also uncertain. Occasionally some equipments are taken intentional out of service for maintenance purposes (e.g. scheduled maintenance). In addition, system faults cause unintentional and random outage of components due to the operation of protective devices or broken connections. Therefore, *one of the main accuracy issues of the traditional coherency-based equivalence is the uncertainty associated with the input data needed for coherency identification, network reduction, and dynamic aggregation*.

2) Another important issue is *the validity of the reduced model for long durations and for various operating conditions*. Even if the input data used in the construction of an electromechanical equivalence of a power system are accurate, the reduced model need to be updated frequently as the loading, topology, operational and control settings, and environmental conditions are time-dependent quantities. Consequently, from an accuracy point of view, the equivalence is valid only within a narrow range of changes around the original input data.

3) The necessity of updating the equivalence arises the issues associated with the *time needed for updating the system equivalence model and performing dynamic security analysis*. This is of special importance when the model is to be used for online security assessment.

4) Recent power systems are equipped with distributed generation resources as well as new technologies for energy production such as wind and solar energy sources. In addition, the penetration level (or the percentage of their contribution in the generation energy mix) increases and an increasing worldwide trend. Consequently, the dynamic behaviour of power system will be affected by these technologies and their consideration in the security analysis of power systems becomes an urgent need. Traditional equivalency techniques are mainly synthesized considering conventional synchronous machines as the power generation technologies. In addition, inclusion of the numerous new power generation technologies in the equivalence using traditional approaches is

expected to be complicated from a mathematical point of view as well as a conceptual point of view. Recalling that the appropriate minimization of dynamic order of the external and remote subsystems is the main target of electromechanical equivalence. In addition, for online applications, the speed of the equivalence construction is of major importance.

5) Another problem associated with variable generation resources (such as wind and solar) is that their output power is mainly dependent on stochastically distributed energy resources (e.g. the solar radiation and wind speeds are having highly random probability distributions or patterns). Although, the predictability of these energy resources is improving, their high randomness causes troubles in determining the exact operating point of variable generating technologies; a situation that complicates the security assessment as well as the deduction of appropriate corrective actions for system survival during disturbances. It is worthy to be mentioned here that the volatility in variable generation resources adds new causes of disturbances to the traditional system disturbances; faults, load changes, and fuel supply shortage.

The presented problems introduce a demand for finding new approaches for handling the dynamic security studies, and dynamic equivalency of power systems. The main required advances of new techniques are high-speed and flexibility. The high-speed is required for the on-line applications while the flexibility is required for the consideration of the vast number of new and renewable generating technologies. *Measuremt-based approaches for electromechanical equivalence and dynamic security studies present a key factor in significantly solving the mentioned problems. In upcoming volume of this book, measurement-based electromechanical equivalency will be presented considering conventional synchronous generators as well as new and renewable generating sources. The dynamic security and transient stability studies as well as corrective actions for online stability enforcement and restoration will also be considered in the second volume.*

B, b	Susceptance.
D	Damping constant.
$\underline{E}'$	Complex transient emf.
E'	Transient emf.
E'_q, E'_d	q- and d-axis transient emf.
E_r	Induction-motor rotor induced emf.
f_o	Synchronous frequency.
f	Frequency.
G, g	Conductance.
$\underline{I}_s, \underline{I}_g$	Complex stator current.
I_s, I_g	Stator current.
i_q, i_d	q- and d-axis current.
J	Jacobian matrix.
J_{ij}	Element (i, j) of the Jacobian matrix.
kVA	Kilo-volt-ampere rating of induction motor.
L	Inductance.
M	Inertia constant $= 2H$.
p	Time derivative operator.
P_m	Mechanical power.
P_e	Motor consumed active power.
P_s, Q_s	Static load active and reactive powers.
P_o, Q_o	Nominal active and reactive powers.
P, Q	Active and reactive powers.
P_G, P_g	Generator electrical power output.
P_L, Q_L	Load active and reactive powers.
R_s, R_r	Stator and rotor resistances of induction motor.
R_a, r	Stator resistance of synchronous machine.
S, s	Slip.
S_o, S_{cr}, S_{fl}	Operating, critical, and full load slips.
T'_o	O.C transient time constant of induction motor.
T_L	Mechanical load torque.
$t, \Delta t$	Time and time interval (or integration step size).
$\underline{V}_s, \underline{V}_g$	Complex stator voltage.

V_s, V_g	Stator voltage.
V_{so}, V_{go}	Stator prefault voltage.
V_q, v_d	q- and d-axis voltage.
V_L	Load bus voltage.
V_o	Normal bus voltage.
V_b	Interface bus voltage.
V	Bus voltage.
$X_d^{'}$	Synchronous machine transient reactance.
X_s, X_r	Stator and rotor leakage reactances of induction motor.
X_t	Total leakage reactance of induction motor.
X_m	Magnetizing reactance of induction motor.
X_{ss}, X_{rr}	Stator and rotor reactances of induction motor (leakage + magnetizing reactances)
$X^{'}$	Transient reactance of induction motor.
X_T	Transformer reactance.
Y, y	Admittance.
$\mathbf{Y_{BUS}}$	Bus admittance matrix.
Y_{ij}	Element (i, j) of the bus admittance matrix.
y_o	Admittance to ground model of static loads.
$Z^{'}$	Transient impedance of induction motor.
ω_o	Synchronous angular frequency.
ω_r, ω	Rotor angular frequency.
λ	Weighting coefficient.
ϕ	Power-factor angle.
Γ	Motor loading.
η	Full load efficiency.
Δ	Indicates that a variable represents a deviation from a specific prefault operating point.
θ	Phase angle of load bus voltage.
δ, d	Phase angle of generator internal voltage.
$\delta_{i,j}$	Power angle of generator #i relative to generator # j in detailed system with loads represented in details.
$d_{(i,j)eq}$	Power angle of generator #i relative to generator #j in the equivalent system with loads represented by static model.

$d_{ieq,j}$	Power angle of equivalent generator #i relative to generator #j in the equivalent system with loads represented by static model.
$\delta_{i,j\Sigma}$	Power angle of generator #i relative to generator #j in the equivalent system with (detailed/aggregate) dynamic loads.
$\delta_{\varepsilon\Sigma i}$	Power angle of equivalent generator #i in the equivalent system with (detailed/aggregate) dynamic loads.
ρ	Correlation factor.
σ	Standard deviation.
χ	Actual bus voltage to normal bus voltage ratio (V/V_o)
Ψ	Flux linkage.
cov	Covariance.

REFERENCES

[1] Hand MM, Baldwin S, DeMeo E, Reilly JM, Mai T, Arent D, Porro G, Meshek M, Sandor D, editors. Renewable electricity futures study NREL/TP-6A20-52409. Golden, CO: National Renewable Energy Laboratory; 2012.

[2] EPM 333: Economics of generation and operation. Available at: http://shimymb.tripod.com

[3] Maczulak A. Renewable energy: sources and methods. New York, USA: Facts On File, Inc.; 2010.

[4] Kreith F, Goswami DY, editors. Handbook of energy efficiency and renewable energy. USA: CRC Press; 2007.

[5] Wood AJ, Wollenberg BF. Power generation, operation, and control. Canada: John Wiley & Sons; 2012.

[6] Gul T, Stenzel T. Variability of wind power and other renewables: management options and strategies. International Energy Agency, Paris, France. 2005.

[7] Chowdhury S, Crossley P. Microgrids and active distribution networks: The Institution of Engineering and Technology; 2009.

[8] Patel MR. Wind and solar power systems: design, analysis, and operation: CRC press; 2005.

[9] Emmanuel I. Hydrogen-based Autonomous Power Systems. 2008.

[10] Iov F, Hansen AD, Sørensen PE, Cutululis NA. Mapping of grid faults and grid codes: Risø National Laboratory; 2007.

[11] Kumar P, Singh AK. Grid Codes: Goals and Challenges. Renewable Energy Integration: Springer; 2014. p. 17-39.

[12] Christiansen W, Johnsen DT. Analysis of requirements in selected Grid Codes. Prepared for Orsted-DTU Section of Electric Power Engineering, Technical University of Denmark (DTU). 2006.

[13] Tsili M, Papathanassiou S. A review of grid code technical requirements for wind farms. IET Renew Power Gener 2009;3(3):308–32.

[14] El-Shimy M. Modeling and analysis of reactive power in grid-connected onshore and offshore DFIG-based wind farms. Wind Energy 2014;7(2):279–95.

[15] El-Shimy M, Ghaly N, Abdelhamed M. Parametric study for stability analysis of grid-connected wind energy conversion technologies. In: 15th International middle-east power conference (MEPCON). Alex., Egypt: IEEE; 2010. p. 1–8.

[16]   EL-Shimy M, Ghaly B. Grid-connected wind energy conversion systems: transient response. In: Encyclopedia of energy engineering and Technology. 2nd ed., vol. IV. CRC Press, Taylor & Francis Group; 2014. p. 2162–83.

[17]   EL-Shimy M. Reactive Power Management and Control of Distant Large-Scale Grid-Connected Offshore Wind Power Farms. International Journal of Sustainable Energy (IJSE), 2012. Available online: Mar 20, 2012. Volume 32, Issue 5, pp. 449 - 465, 2013.

[18]   Wang Z, Ai Q, Xie D, Jiang C. A research on shading and LCOE of building integrated photovoltaic. In: Power and energy engineering conference (APPEEC), 2011 Asia–Pacific, March 25–28. Wuhan: IEEE; 2011. p. 1–4

[19]   EL-Shimy M. Viability analysis of PV power plants in Egypt. Renew Energy 2009;34(10):2187–96.

[20]   Branker K, Pathak M, Pearce JM. A review of solar photovoltaic levelized cost of electricity. Renew Sustain Energy Rev 2011;15(9):4470–82.

[21]   El-Shimy M. Analysis of levelized cost of energy (LCOE) and grid parity for utility-scale photovoltaic generation systems. MEPCON 2012 conference, Alexandria, Egypt, IEEE, December 23–25; 2012. p. 1–7.

[22]   El-Shimy M, Abdo T. PV technologies: History, technological advances, and characterization. In: Anwar S, editor. Encyclopedia of energy engineering and technology, vol. 2. Taylor & Francis Group; 2014. p. 1397–424.

[23]   Dobrotkova Z, Goodrich A, Mackay M, Philibert C, Simbolotti G, Wenhua X. Renewable energy technologies: cost analysis series. Volume 1 issue 4/5: Photovoltaic, International Renewable Energy Agency (IRENA); 2012.

[24]   Peng J, Lu L, Yang H. Review on life cycle assessment of energy payback and greenhouse gas emission of solar photovoltaic systems. Renew Sustain Energy Rev 2013;19:255–74.

[25]   Said M, EL-Shimy M, Abdelraheem M. Photovoltaics energy: Improved modeling and analysis of the levelized cost of energy (LCOE) and grid parity– Egypt case study. Sustainable Energy Technologies and Assessments. 2015;9:37-48.

[26]   Ackermann T, editor. Wind power in power systems. USA: Wiley Online Library; 2005.

[27]   El-Shimy M. Optimal site matching of wind turbine generator: case study of the Gulf of Suez region in Egypt. Renew Energy 2010;35(8):1870–8.

[28]   Venikov VA. Transient processes in electrical power systems. Moscow: Mir Publishers; 1977.

[29]   Machowski J, Bialek J, Bumby J. Power system dynamics: stability and control: John Wiley & Sons; 2011.

[30]   Padiyar, K R. *Power system dynamics*. BS publications, 2008.

[31]   Pavella M, Ernst D, Ruiz-Vega D. Transient stability of power systems: a unified approach to assessment and control: Springer Science & Business Media; 2000.

[32]   Eremia M, and Shahidehpour M, (eds). Handbook of Electrical Power System Dynamics: Modeling, Stability, and Control, John Wiley & Sons, Inc., Hoboken, NJ, USA. 2013.

[33]   El-Abiad A H. *Power Systems Analysis and Planning*. Hemisphere publishing Corporation, 1983

[34]   Jizhong Zhu, "Optimization Of Power System Operation", John Wiley & Sons, 2009

[35]   EL-Shimy M. Analysis of Levelized Cost of Energy (LCOE) and grid parity for utility-scale photovoltaic generation systems. 15th International Middle East Power Systems Conference (MEPCON'12), Dec. 23-25, 2012, Alexandria, Egypt, pp. 1- 7.

[36]   Kundur P, Paserba J, Ajjarapu V, Andersson G, Bose A, Canizares C, et al. Definition and classification of power system stability IEEE/CIGRE joint task force on stability terms and definitions. Power Systems, IEEE Transactions on. 2004;19(3):1387-401.

[37]   Fink LH, Carlsen K. Operating under stress and strain. IEEE Spectrum;(United States). 1978;15(3).

[38]   Dolezilek D, editor. Understanding, Predicting, and Enhancing The Power System Through Equipment Monitoring and Analysis. Conference Proceedings Second Annual WPDAC, Spokane, WA; 2000.

[39]   Apostolov A, Butt J. Distributed Recording of Abnormal Power System Conditions. 2002 Georgia Tech - Disturbance Analysis Conference; Atlanta, Georgia. 2002.

[40]   Abur A, Exposito AG. Power system state estimation: theory and implementation: CRC Press; 2004.

[41]   Advanced Concepts: FAQ. Available at: http://www.phasor-rtdms.com/phaserconcepts/phasor_adv_faq.html#Question7

[42]   Martin K, Benmouyal G, Adamiak M, Begovic M, Burnett Jr R, Carr K, et al. IEEE standard for synchrophasors for power systems. Power Delivery, IEEE Transactions on. 1998;13(1):73-7.

[43]   De La Ree J, Centeno V, Thorp JS, Phadke AG. Synchronized phasor measurement applications in power systems. Smart Grid, IEEE Transactions on. 2010;1(1):20-7.

[44]   Liscouski B, Elliot W. Final report on the august 14, 2003 blackout in the united states and canada: Causes and recommendations. A report to US Department of Energy. 2004;40(4).

[45]   Burnett Jr R, Butts M, Cease T, Centeno V, Michel G, Murphy R, et al. Synchronized phasor measurements of a power system event. Power Systems, IEEE Transactions on. 1994;9(3):1643-50.

[46]   Zhong Z, Xu C, Billian BJ, Zhang L, Tsai S, Conners RW, et al. Power system frequency monitoring network (FNET) implementation. Power Systems, IEEE Transactions on. 2005;20(4):1914-21.

[47]   Nuqui RF, Phadke AG. Phasor measurement unit placement techniques for complete and incomplete observability. Power Delivery, IEEE Transactions on. 2005;20(4):2381-8.

[48]   Jiang W, Vittal V, Heydt GT. A distributed state estimator utilizing synchronized phasor measurements. Power Systems, IEEE Transactions on. 2007;22(2):563-71.

[49]   Chakrabarti S, Kyriakides E. Optimal placement of phasor measurement units for power system observability. Power Systems, IEEE Transactions on. 2008;23(3):1433-40.

[50]   Korres GN, Manousakis NM. State estimation and bad data processing for systems including PMU and SCADA measurements. Electric Power Systems Research. 2011;81(7):1514-24

[51]   Ahmadi A, Alinejad-Beromi Y, Moradi M. Optimal PMU placement for power system observability using binary particle swarm optimization and considering measurement redundancy. Expert Systems with Applications. 2011;38(6):7263-9

[52]   Liu C-W, Chang C-S, Su M-C. Neuro-fuzzy networks for voltage security monitoring based on synchronized phasor measurements. Power Systems, IEEE Transactions on. 1998;13(2):326-32

[53]   Khatib AR, Nuqui RF, Ingram M, Phadke AG. Real-time estimation of security from voltage collapse using synchronized phasor measurements. Power Engineering Society General Meeting, 2004 IEEE: IEEE; 2004. p. 582-8.

[54]   Diao R, Sun K, Vittal V, O'Keefe RJ, Richardson MR, Bhatt N, et al. Decision tree-based online voltage security assessment using PMU measurements. Power Systems, IEEE Transactions on. 2009;24(2):832-9.

[55]   Rovnyak S, Liu C-W, Lu J, Ma W, Thorp J. Predicting future behavior of transient events rapidly enough to evaluate remedial control options in real-time. Power Systems, IEEE Transactions on. 1995;10(3):1195-203.

[56]   Bretas N, Phadke A. Real time instability prediction through adaptive time series coefficients. Power Engineering Society 1999 Winter Meeting, IEEE: IEEE; 1999. p. 731-6.

[57]   Liu C-W, Thorp JS. New methods for computing power system dynamic response for real-time transient stability prediction. Circuits and Systems I: Fundamental Theory and Applications, IEEE Transactions on. 2000;47(3):324-37.

[58]   Ota Y, Ukai H, Nakamura K, Fujita H. PMU based midterm stability evaluation of wide-area power system. Transmission and Distribution Conference and Exhibition 2002: Asia Pacific IEEE/PES: IEEE; 2002. p. 1676-80.

[59]   Varma RK, Gupta R, Auddy S. Damping of inter-area oscillation in power systems by static var compensator (SVC) using PMU-acquired remote bus voltage angles. International Journal of Emerging Electric Power Systems. 2007;8(4).

[60]   EL-Shimy M. Stability-based minimization of load shedding in weakly interconnected systems for real-time applications. International Journal of Electrical Power & Energy Systems. 2015;70:99-107.

[61]   Zhang C, Bo Z, Zhang B, Klimek A, Han M, Tan J. An integrated PMU and protection scheme for power systems. 2009 44th International Universities Power Engineering Conference (UPEC): IEEE; 2009.

[62]   Centeno V, De La Ree J, Phadke A, Michel G, Murphy R, Burnett Jr R. Adaptive out-of-step relaying using phasor measurement techniques. Computer Applications in Power, IEEE. 1993;6(4):12-7.

[63]   Centeno V, Phadke A, Edris A, Benton J, Gaudi M, Michel G. An adaptive out-of-step relay [for power system protection]. Power Delivery, IEEE Transactions on. 1997;12(1):61-71.

[64] Jiang J-A, Chen C-S, Fan P-L, Liu C-W, Chang R-S. A composite index to adaptively perform fault detection, classification, and direction discrimination for transmission lines. Power Engineering Society Winter Meeting, 2002 IEEE: IEEE; 2002. p. 912-7.

[65] Chen C-S, Liu C-W, Jiang J-A. A new adaptive PMU based protection scheme for transposed/untransposed parallel transmission lines. Power Delivery, IEEE Transactions on. 2002;17(2):395-404

[66] Jiang J-A, Yang J-Z, Lin Y-H, Liu C-W, Ma J-C. An adaptive PMU based fault detection/location technique for transmission lines. I. Theory and algorithms. Power Delivery, IEEE Transactions on. 2000;15(2):486-93.

[67] Laverty D, Morrow D, Best R, Crossley P. Differential ROCOF relay for loss-of-mains protection of renewable generation using phasor measurement over internet protocol. Integration of Wide-Scale Renewable Resources Into the Power Delivery System, 2009 CIGRE/IEEE PES Joint Symposium: IEEE; 2009. p. 1-.

[68] Snyder A, Mohammed A, Georges D, Margotin T, Hadjsdid N, Mili L. A robust damping controller for power systems using linear matrix inequalities. Power Engineering Society 1999 Winter Meeting, IEEE: IEEE; 1999. p. 519-24.

[69] Snyder AF, Ivanescu D, HadjSaid N, Georges D, Margotin T. Delayed-input wide-area stability control with synchronized phasor measurements and linear matrix inequalities. Power Engineering Society Summer Meeting, 2000 IEEE: IEEE; 2000. p. 1009-14

[70] Rovnyak S, Sheng Y. Using measurements and decision tree processing for response-based discrete-event control. Power Engineering Society Summer Meeting, 1999 IEEE: IEEE; 1999. p. 10-5.

[71] Mekki K, Hadjsaid N, Feuillet R, Georges D. Design of damping controllers using linear matrix inequalities techniques and distant signals to reduce control interactions. Power Industry Computer Applications, 2001 PICA 2001 Innovative Computing for Power-Electric Energy Meets the Market 22nd IEEE Power Engineering Society International Conference on: IEEE; 2001. p. 306-11

[72] Messina A, Vittal V, Ruiz-Vega D, Enriquez-Harper G. Interpretation and visualization of wide-area PMU measurements using Hilbert analysis. Power Systems, IEEE Transactions on. 2006;21(4):1763-71.

[73]   Liu Z, Ilic MD, editors. Toward PMU-based robust automatic voltage control (AVC) and automatic flow control (AFC). 2010 IEEE PES General Meeting, July; 2010.

[74]   Chow, Joe H. *Power system coherency and model reduction*. London: Springer, 2013.

[75]   Phadke AG, Thorp JS. Synchronized phasor measurements and their applications: Springer Science & Business Media; 2008.

[76]   Savulescu SC. Real-time stability assessment in modern power system control centers: John Wiley & Sons; 2009.

[77]   EL-Shimy M. Electromechanical System Equivalent and Dynamic Load Aggregation for Transient Stability of Electric Power System [PhD]. Cairo, Egypt: Ain Shams Univeristy; 2004.

[78]   Abuel-wafa AR, EL-Shimy M. Coherency-Based Electromechanical Equivalents for use in Power System Stability Studies. Scientific Bulletin - Faculty of Engineering - Ain Shams University. 2003;38(3):475 – 87.

[79]   Abuel-wafa AR, EL-Shimy M. Treatment of large-scale Power Systems in Transient Stability Studies. Scientific Bulletin - Faculty of Engineering - Ain Shams University. 2003;48(4):675 – 87

[80]   Abuel-wafa AR, EL-Shimy M. An Enhanced Technique for Transient Stability Analysis of large-scale Power Systems. Scientific Bulletin - Faculty of Engineering - Ain Shams Uni. 2003;38(3):475 – 87

[81]   Kundur P, Balu NJ, Lauby MG. Power system stability and control: McGraw-hill New York; 1994.

[82]   Xue Y, Van Custem T, Ribbens-Pavella M. Extended equal area criterion justifications, generalizations, applications. IEEE Transactions on Power Systems. 1989;4(1):44-52.

[83]   Xue Y, Pavella M. Extended equal-area criterion: an analytical ultra-fast method for transient stability assessment and preventive control of power systems. International Journal of Electrical Power & Energy Systems. 1989;11(2):131-49

[84]   Dong Y, Pota H. Transient stability margin prediction using equal-area criterion. IEE Proceedings C (Generation, Transmission and Distribution). 1993;140(2):96-104

[85]   Chang H-C, Wang M-H. Another version of the extended equal area criterion approach to transient stability analysis of the Taipower system. Electric Power Systems Research. 1992;25(2):111-20

[86]   Chiodo E, Lauria D. Transient stability evaluation of multimachine power systems: a probabilistic approach based upon the extended equal area criterion. Generation, Transmission and Distribution, IEE Proceedings-. 1994;141(6):545-53.

[87]   Choo YC, Kashem MA, Negnevitsky M. Transient Stability Assessment of a small power system subjected to large disturbances.   Australasian Universities Power Engineering Conference (AUPEC)2006. p. 1-5

[88]   John J G.Power System Analysis. McGraw Hill, Inc., 1994

[89]   Heydt GT. Computer Analysis Methods for Power Systems. Macmillan Co., 1986.

[90]   Homer E, Bruce R. A Study of Stability Equivalent. IEEE, PAS-88, (3), Mach 1969.

[91]   Rahimi A, Stanton KN, Salmon DM. Dynamic Aggregation and the Calculation of Transient Stability Incides. Power Apparatus and Systems, IEEE Transactions on. 1972(1):118-22

[92]   Turner A, Undrill J. Construction of power systems electromechanical equivalents by modal analysis. IEEE Trans Power Apparatus and Systems. 1971

[93]   Undrill J, Casazza J, Gulachenski E, Kirchrnayer L. Electromechanical Equivalent for Use in Power System Stability Studies. Power Apparatus and Systems, IEEE Transactions on. 1971(5):2060-71.

[94]   Okubo S, Suzuki H, Uemura K. Modal analysis for power system dynamic stability. Power Apparatus and Systems, IEEE Transactions on. 1978(4):1313-8.

[95]   Price W, Gulachenski E, Kundur P, Lange F, Loehr G, Roth B, et al. Testing of the modal dynamic equivalents technique. Power Apparatus and Systems, IEEE Transactions on. 1978(4):1366-72

[96]   Price WW, Ewart DN, Gulachenski EM, Silva RF. Dynamic equivalents from on-line measurements. Power Apparatus and Systems, IEEE Transactions on. 1975;94(4):1349-57.

[97]   Podmore R. Identification of coherent generators for dynamic equivalents. IEEE Transactions on Power Apparatus and Systems. 1978:1344-54.

[98]   Germond AJ, Podmore R. DYNAMIC AGGREGATION OF GENERATING UNIT MODELS. No. LRE-ARTICLE-1978-003. 1978.

[99]   Mathews JH. Numerical methods for mathematics, science and engineering: Prentice-Hall; 1992.

[100]   Dommel HW. Digital Computer Solution of Electromagnetic Transients in Single-and Multiphase. Networks IEEE. 1969;88(4):388-99.

[101]   Kent MH, Schmus WR, Mccrackin FA, Wheeler LM. Dynamic modeling of loads in stability studies. Power Apparatus and Systems, IEEE Transactions on. 1969(5):756-63.

[102]   Machowski J, Bumby JR. Power system dynamics and stability: John Wiley & Sons; 1997.

[103]   Rogers G, Manno J, Alden R. An aggregated motor model for industrial plants. IEEE Trans Power Apparat Syst PAS-103 (April (4)). 1984.

[104]   Anderson PM, Fouad AA. Power system control and stability: John Wiley & Sons; 2008.

[105]   Chow JH, Avramovic B, Kokotovic P, Winkelman J. Singular perturbations, coherency and aggregation of dynamic systems. Report, Electric Utility Systems Engineering Department, General Electric Company, Schenectady. 1981.